



Division of Intramural Research

Fourteenth Annual NHLBI DIR Research Festival



Photo courtesy of NIH Almanac

Friday, April 29, 2016
Natcher Conference Center
Bethesda, MD

2015 – 2016 NHLBI DIR Fellows Advisory Committee

Adrienne Campbell
Cardiovascular Pulmonary
Branch

Beverley Dancy
Systems Biology Center

Teegan Dellibovi-Ragheb
Cell Biology and Physiology
Center

Elizabeth Gordon
Cardiovascular-Pulmonary
Branch

Scott Gordon
Cardiovascular-Pulmonary
Branch

Thirupugal Govindarajan
Genetics and Developmental
Biology Center

Kang Le
Cardiovascular-Pulmonary
Branch

Lo Lai
Biochemistry and Biophysics
Center

Sayantane Niyogi
Cell Biology and Physiology
Center

Rajiv Ramasawmy
Cardiovascular-Pulmonary
Branch

Ankit Saxena
Hematology Branch

Agila Somasundaram
Biochemistry and
Biophysics Center

Sreya Tarafdar
Biochemistry and
Biophysics Center

Javier Traba Dominguez
Center for Molecular
Medicine

Adam Trexler
Biochemistry and
Biophysics Center

Ling Yang
Center of Molecular
Medicine

Special thanks to the Foundation for Advanced Education in Sciences (FAES) and NHLBI Principal Investigators for providing lunch and refreshments for the Research Festival.



Robert Adelstein
Bernard Brooks
Haiming Cao
Julie Donaldson
Cynthia Dunbar
Herbert Geller
Robert Hogg
Christopher Hourigan
Paul Hwang
Jennifer Lee

Rodney Levine
Stewart Levine
Chengyu Liu
Nehal Mehta
Joel Moss
Yosuke Mukoyama
Elizabeth Murphy
Keir Neuman
Richard Pastor
Tiffany Powell-Wiley

Rolf Swenson
Justin Taraska
Swee Lay Thein
John Tisdale
Nico Tjandra
Clare Waterman
Han Wen
Adrian Wiestner
Hong Xu

NHLBI DIR Office of Education

Herbert Geller, Director
Dami Kim, Program Coordinator
Jackie Lee, Program Coordinator

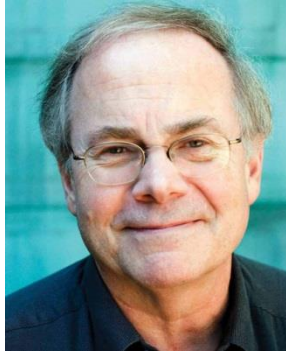
NHLBI Office of the Scientific Director

NHLBI Cores and Offices

Fourteenth Annual NHLBI DIR Research Festival

Friday, April 29, 2016

8:00 – 8:30	Arrival, Registration, Check-In	<i>Atrium</i>
8:30 – 8:40	Introduction and Welcome Elizabeth Gordon, Ph.D., Chair Fellows Advisory Committee, NHLBI	<i>Auditorium</i>
8:40 – 10:30	Morning Pitch Session <i>Session Chairs: Rajiv Ramasawmy, Ph.D. and Javier Traba, Ph.D.</i>	<i>Auditorium</i>
10:30 – 10:40	BREAK	
10:40 – 11:40	Keynote Speaker Gregory Petsko, D.Phil – “ <i>Post Doc, Ergo Doc?</i> <i>Revisiting the Postdoctoral Experience in the 21st Century</i> ”	<i>Auditorium</i>
11:40 – 11:50	Introduction to the Office of Education Herbert M. Geller, Ph.D., Director, Office of Education, NHLBI	<i>Auditorium</i>
11:50 – 12:00	Group Picture	<i>Auditorium</i>
12:00 – 12:30	Lunch	<i>Conf. Rooms F & G</i>
12:30 – 1:45	Poster Session I – #1-16, 17-86	<i>Atrium & Balcony</i>
1:45 – 3:25	Afternoon Pitch Session <i>Session Chairs: Scott Gordon, Ph.D. and Sreya Tarafdar, Ph.D.</i>	<i>Auditorium</i>
3:25 – 4:40	Poster Session II – #1-16, 87-158	<i>Atrium & Balcony</i>
4:40 – 5:00	Awards Ceremony & Closing Remarks Robert S. Balaban, Ph.D., Scientific Director, NHLBI Best Pitch Awards – Postbaccalaureate and Postdoctoral Fellows Best Poster Awards – Postbaccalaureate, Predoctoral, Postdoctoral Fellows, and Staff Scientist Outstanding Fellow Award Outstanding Mentoring Awards – PI and Staff Scientist	<i>Auditorium</i>
5:00 –	Networking Hour Rock Bottom Restaurant & Brewery – Bethesda, MD	



Gregory Petsko, D. Phil

Arthur J. Mahon Professor of Neuroscience, Brain and Mind Research Institute, Weill Cornell Medical College
Professor of Neuroscience, Neurobiology and Neuroscience, Weill Cornell Medical College

NHLBI Research Festival 2016 Keynote Speaker

"Post Doc, Ergo Doc? Revisiting the Postdoctoral Experience in the 21st Century"

Dr. Gregory Petsko is the Arthur J. Mahon Professor of Neurology and Neuroscience at Weill Cornell Medical College and Director of the Helen and Robert Appel Alzheimer's Disease Research Institute. He also holds appointments as Professor of Biomedical Engineering at Cornell University, Adjunct Professor of Neurology at Harvard Medical School, and Tauber Professor of Biochemistry and Chemistry, Emeritus, at Brandeis University. He received his B.A. from Princeton University and his D. Phil. from Oxford University, which he attended as a Rhodes Scholar.

Dr. Petsko's research focuses on finding a treatment or preventive therapy for one or more of the major neurodegenerative diseases: Alzheimer's disease, Parkinson's disease, Frontotemporal dementia, Lewy Body Dementia, Multiple Systems Atrophy, Progressive Supranuclear Palsy, and Amyotrophic Lateral Sclerosis. Dr. Petsko's awards include Sachar Award, McKnight Endowment Fund for Neuroscience Award and Alexander von Humboldt Senior Scientist Award. He has been elected to the National Academy of Sciences, the Institute of Medicine, the American Academy of Arts and Sciences, and the American Philosophical Society. Dr. Petsko has an honorary Doctor of Laws from Dalhousie University. He is former President of the American Society for Biochemistry and Molecular Biology, and is currently President of the International Union of Biochemistry and Molecular Biology.

Dr. Petsko's public lectures on the aging of the population and its effects for human health have fascinated a wide audience on the Internet (one of his TED talks, for example, has been downloaded over 600,000 times). For the past twelve years, he has also written a widely-read and much reprinted column on science and society, the first ten years of which have just appeared in book form. One of his greatest accomplishments is the more than 100 graduate students and postdocs he has helped to train, a list that includes five Howard Hughes Investigators, two members of the National Academy of Sciences, and the second woman ever to head a Max-Planck Institute in Germany.

Directions for Pitch Presenters

1. Two Session Chairs will help those who are giving pitches queue up and keep track of time.
2. The allowed pitch time per person is three minutes total. You will be escorted off the stage if you surpass three minutes.
3. Please introduce yourself and give your pitch number at the start of your pitch. You should be on the stage ready to talk as the person before you is still speaking in order to minimize delays.

Pitch Judging

We invite all audience members to judge the pitches for the “Best Pitch” Award. Please rate each pitch on a scale of 1-10, where 1 is the lowest and 10 is the highest, based on how clear and effective each presenter was in convincing you to visit their poster later. There is a separate web page for each session as listed below.

Morning Pitch Session Schedule

URL: <http://nhlbioc.polladdy.com/s/morning-pitch-session>



Order	Time	Poster #	Name	Title
1	8:45AM	17	Helena Mora-Jensen	The Combination Of ACP-196 And ACP-319 Leads To Increased Survival In The TCL1-192 CLL Mouse Model
2	8:48AM	21	Ryan McGlinchey	Cysteine Cathepsins Are Essential In Lysosomal Degradation Of α -Synuclein
3	8:51AM	22	Wenfei Jin	Genome-Wide Detection Of DNase I Hypersensitive Sites In Single Cells And FFPE Tissue Samples
4	8:54AM	23	Xiangbo Ruan	Regulation Of Hepatic Gluconeogenesis By Human Long Non-Coding RNAs
5	8:57AM	24	Madeleine Strickland	An Addition To The Toolkit Of NMR Spectroscopy For Large Proteins And Complexes: Lanthanide-Induced Pseudocontact Shifts
6	9:00AM	25	Inhye Ahn	Correlation Of Clinical And Mutational Markers Of Disease Progression In Chronic Lymphocytic Leukemia Treated With Ibrutinib
7	9:03AM	26	Zhanghan Wu	Two Distinct Actin Networks Mediate Traction Oscillations To Confer Mechanosensitivity Of Focal Adhesions
8	9:06AM	28	Andrea Stoehr	Proteomic Profiling Reveals That 3-Dimensional Engineered Heart Tissue Culture Promotes Maturation And Aerobic Respiration Of Human Induced Pluripotent Stem Cell-Derived Cardiomyocytes
9	9:09AM	29	Pinar Gurel	The Role Of Actin Structural Plasticity In Mechanosensation
10	9:12AM	31	Jose Martina	Novel Role Of TFEB And TFE3 In Cellular Response To ER Stress
11	9:15AM	32	Claudio Anselmi	Mechanism Of Activation Of The TRPV1 Channel By A Double-Knot Tarantula Toxin
12	9:18AM	34	Chase Brisbois	Apolipoprotein C-III Nanodiscs Studied By Site-Specific Tryptophan Fluorescence
13	9:21AM	38	Patali Cheruku	The Thrombopoietin Receptor Agonist Eltrombopag Has DNA Repair Activity In Human Hematopoietic Stem And Progenitor Cells

Order	Time	Poster #	Name	Title
14	9:24AM	39	Barbara Medvar	Bayesian Analysis Of E3 Ubiquitin Ligase/AQP2 Interactions In The Renal Collecting Duct
15	9:27AM	42	Jessica Flynn	Structural Features of α -Synuclein Revealed by Raman Spectroscopy
16	9:30AM	44	Anna Lopata	Artificial Actin-Binding Proteins With Novel Multifunctional Properties
17	9:33AM	47	Todd Schoborg	Centrosome-Pole Cohesion Requires Abnormal Spindle And Calmodulin To Ensure Proper Centrosome Inheritance In Neural Stem Cells But Is Dispensable For Brain Size
18	9:36AM	48	Alejandro Morales Martinez	Micro-CT Scouting For Transmission Electron Microscopy Of Human Tissue Specimens
19	9:39AM	50	Keval Patel	The Transmission Of The Proton Motive Force Along I-Band Segments Of The Mitochondrial Reticulum
20	9:42AM	52	Andrea Knab	Dramatic Radiation Dose Reduction Over 7 Years Of Experience For Coronary CT
21	9:45AM	53	Jessica Tang	Identification And Characterization Of Novel A Gene That Regulates Mitochondrial DNA Replication
22	9:48AM	58	Elizabeth Gordon	Defining Roles For Apolipoprotein A-1 And Apolipoprotein E In Modifying Asthmatic Airway Inflammation
23	9:51AM	59	Ling Yang	Integrative Transcriptome Analyses Of Metabolic Responses In Mice Define Pivotal Lncrna Metabolic Regulators
24	9:54AM	62	Colleen Skau	An FMN2-Mediated Perinuclear Actin/Adhesion System Protects Against DNA Damage During Confined Cell Migration
25	9:57AM	65	Randi Parks	Regulation Of The Permeability Transition Pore Is Altered In Mice Lacking The Mitochondrial Calcium Uniporter
26	10:00AM	67	Debbie Figueroa	Development Of A Human Circulating Fibrocyte Model To Assess The Effect Of The 5A Apolipoprotein A-I Mimetic Peptide In Idiopathic Pulmonary Fibrosis
27	10:03AM	63	Yangtengyu Liu	Generation of Rhesus Monkey iPSC-Derived Endothelial Cells
28	10:06AM	68	Julia Liu	MICU1 Serves As A Molecular Gatekeeper To Prevent In Vivo Mitochondrial Calcium Overload
29	10:09AM	71	Elizabeth Carstens	Circumventing Trogocytosis Through A Complement Based Retargeting Strategy In Lymphoid Malignancy
30	10:12AM	74	Scott Gordon	A High Density Lipoprotein Proteome Index Correlates With Atherosclerosis Severity In Humans.
31	10:15AM	75	Fabrizio Marinelli	Molecular Mechanisms Of Coupled Transport In Secondary Transporters: Lessons From A Na ⁺ /Ca ²⁺ Exchanger
32	10:18AM	78	Luigi Alvarado	High Throughput Single-Cell RNA Sequencing of iPSC-Derived Hematopoietic Stem Cells: One Drop Closer to Treatments of Inherited Bone Marrow Failure Syndromes
33	10:21AM	79	Komudi Singh	Exploring The Role Of Parkin In Astrocyte Mediated Neurotropic Function
34	10:24AM	80	Beverley Dancy	The Mitochondrial Interactome By Crosslinking Mass Spectrometry: Evidence For Supercomplexes In Intact Mitochondria



Afternoon Pitch Session Schedule

URL: <http://nhlbioe.polladdy.com/s/afternoon-pitch-ratings>

Order	Time	Poster #	Name	Title
1	1:50PM	158	Yi Zhang	The Mitochondrial Outer Membrane Protein MDI Promotes Local Protein Synthesis And mtDNA Replication
2	1:53PM	155	Thaddeus Davenport	Examination Of Antigen-Induced Endocytic Structures In B Lymphocytes By Fluorescence Microscopy
3	1:56PM	87	Daniela Malide	Imaging Adipose Tissue Across Scales Of Resolution: From Two-Photon To Super-Resolution Microscopy
4	1:59PM	88	Fan Zhang	A Drosophila Model Demonstrates Mitochondrial Regulation of Stem Cell Homeostasis
5	2:02PM	89	Marianita Santiana	Investigations Into Rotavirus And Norovirus Replication, Assembly And Exit
6	2:05PM	90	Javier Traba	Fasting Regulates NLRP3 Inflammasome Activation In Humans By Modulating Mitochondrial Integrity
7	2:08PM	93	Lingdi Wang	Mitochondrial Nutrient Sensing, Foxo1 Stability And The Retrograde Control Of Gluconeogenesis
8	2:11PM	94	Juan Jesus Haro Mora	Improvement Of Definitive Erythroid Cell Production From Human ES Cells Using Serum-Free ES-Sac Generation
9	2:14PM	98	Nikolaos Angelis	Regulatory Role Of MYB On Fetal Hemoglobin Expression
10	2:17PM	99	Adam Trexler	The Lipid Landscape At Single Sites Of Exocytosis
11	2:20PM	101	Brittany MacTaggart	Using Whole-Exome Sequencing To Identify Genetic Variants In Patients Diagnosed With Pentagony Of Cantrell
12	2:23PM	102	Koyeli Banerjee	Structural Insight Into Interaction Of Fibrin And Very Low Density Lipoprotein Receptor
13	2:26PM	103	Diana Melo	Spectrum Of Cardiovascular Involvement In Erdheim-Chester Disease Evaluated By Cardiac Computed Tomography
14	2:29PM	106	Zhihong Yang	Dietary Marine Long-Chain Monounsaturated Fatty Acid (LCMUFA) Attenuates The Development Of Atherosclerosis Via PPAR Signaling Pathway In Mouse Models
15	2:32PM	108	Ezibobiara Umejiego	Roflumilast Effect On Aquaporin-2 Phosphorylation And Trafficking In Rat Renal Inner Medullary Collecting Duct
16	2:35PM	110	Maria Mills	Single Molecule Measurements Of DNA Decatenation By The Topoisomerase III-Recq Helicase Complex
17	2:38PM	112	Thomas Baird	Identification And Characterization Of Novel Members Of The Nonsense-Mediated mRNA Decay Pathway
18	2:41PM	115	Donovan Ruth	On The Robustness Of SAC Silencing In Closed Mitosis
19	2:44PM	118	Matthew Mulé	Comprehensive Residual Disease Assessment Improves AML Relapse Risk Stratification In Autologous Hematopoietic Cell Transplantation

Order	Time	Poster #	Name	Title
20	2:47PM	119	Yvonne Baumer	Cholesterol Crystals In Atherogenesis And Beyond?
21	2:50PM	121	Kiyoshi Isobe	Use Of CRISPR-Phosphoproteomics To Investigate Role Of Myosin Light Chain Kinase In Vasopressin Signaling
22	2:53PM	122	Caitlin Mencia	Low Concentration Xyloside Treatment Alters GAG Profile And Morphology In Neural Cells
23	2:56PM	124	Wai Lim Ku	Genome-Wide Identification Of H2A.Z-Interacting Proteins By Bppi-Seq
24	2:59PM	125	Eman Dadashian	Ibrutinib Acts As A Dual B-Cell Receptor And Toll-Like Receptor Inhibitor In Chronic Lymphocytic Leukemia
25	3:02PM	126	Maile Hollinger	Sirolimus-Induced Preservation Of Bone Marrow Hematopoietic Stem And Progenitor Cells In Immune And Nonimmune Mediated Mouse Models Of Bone Marrow Failure
26	3:05PM	127	Dipannita Dutta	A Membrane Trafficking Screen To Identify Clathrin-Independent Endocytosis Machinery
27	3:08PM	128	Lucas Axiotakis	Modular LIM Domains Mediate Actin Cytoskeletal Strain Recognition
28	3:11PM	140	Leah Yingling	Lower Technology Fluency Is Not A Barrier To User Adoption Of A Mobile Health (mHealth) Wrist-Worn Physical Activity (PA) Monitor System: Observations From The Washington, D.C. Cardiovascular (CV) Health And Needs Assessment
29	3:14PM	150	Zong-Heng Wang	Drosophila Clueless Is Involved In Parkin-Dependent Mitophagy By Promoting VCP-Mediated Marf Degradation
30	3:17PM	151	Joseph Lerman	Improvement In Psoriasis Skin Disease Severity Is Associated With Reduction Of Coronary Plaque Burden
31	3:20PM	153	Iris Garcia-Pak	Maturation Of Induced Pluripotent Stem Cell Derived Cardiomyocytes Via Co-Culture With Supporting Cells Of The Developing Heart

NHLBI Cores and Offices

Animal MRI Core

Stasia A. Anderson, Ph.D., Director

Building 10, Room B1D49C; E-mail: andersos1@nhlbi.nih.gov

Phone: (301) 402-0908

Web: <https://www.nhlbi.nih.gov/research/intramural/researchers/core/animal-mri-core>

The AMRI Core performs magnetic resonance imaging of small animal models in the NHLBI. We perform and interpret magnetic resonance imaging studies and work with investigators on the best approaches for the research model and goals. Training in MRI and data analysis is available and interested fellows may learn to perform MRI studies. Examples of imaging studies in the AMRI Core are:

- Cardiac imaging for heart function and size
- High resolution imaging of myocardium for identification of infarct and scars
- Imaging blood vessels; angiography and vessel wall imaging
- Atherosclerotic plaque imaging
- Perfusion of skeletal muscle or tumors
- Whole body imaging for identification of non-cardiac defects in mouse models
- High resolution microimaging of embryos and fixed tissue

Core imaging studies are performed in the NIH Mouse Imaging Facility (MIF). Through the MIF, it is possible to incorporate additional imaging modalities such as computed tomography, ultrasound and bioluminescence as needed.

Animal Surgery & Resources (ASR) Core

Randall R. Clevenger, B.S., LATG, 14E Surgical Facility Manager,

Building 14E, Room 106B; E-mail: rc85n@nih.gov

Phone: (301) 496-0405, Fax: (301) 402-0170

Joni Taylor, B.S., LATG, Large Animal Resources Manager

Building 10, Room B1D416; E-mail: jt100s@nih.gov

Phone: (301) 496-0823

Timothy Hunt, B.S., LATG, CRC Surgery Manager

Building 14E, Room 106B; Email: th118w@nih.gov

Phone: (301) 402-0913, Fax: (301) 402-0170

James “Buster” Hawkins, DVM, MS, DACLAM

Animal Program Director

Building 14E, Room 105C; E-mail: hawkinsj@nih.gov

Phone: (301) 451-6743, Fax: (301) 480-7576

Main phone: 301-496-5927

Web: <http://www.nhlbi.nih.gov/research/intramural/researchers/core/animal-surgery-and-resources-core>

The Animal Surgery & Resources (ASR) Core provides veterinary medical care and technical services for NHLBI research animals used in both basic and preclinical research. These support services include: anesthesia, veterinary medical care, surgery, surgical support, training in surgical and microsurgical techniques, post-operative care, purchasing (large animals), and health monitoring. In addition, ASR provides technical services such as blood & tissue collection, and tail vein injections.

The ASR staff also provides NHLBI investigators with collaborative research support services such as developing animal models and new surgical procedures, assistance with research design, as well as animal protocol development and execution. Our surgical support equipment includes anesthesia machines with mechanical ventilation for species ranging from rodents to nonhuman primates, radiography, digital fluoroscopy, Faxitron, ultrasound, laser Doppler, and operating microscopes.

ASR supports a wide range of animal models for DIR investigators. Some of the animal models we provide surgical support for include xenotransplantation (involving baboons and genetically engineered pigs), stem cell models (rats, mice and pigs) myocardial infarction with and without reperfusion (rats, mice, rabbits, dogs, and nonhuman primates), hind limb ischemia (rats, mice, rabbits), gene vector delivery to liver (mice, rabbits), plethysmography (mice) and support for MRI and other imaging procedures. We can also perform cardiac function testing on rats and mice including invasive blood pressure, left ventricular pressure, and pressure-volume loops. Surgical and perioperative support services are provided in the Building 14E Surgical Facility, the B-2 level of the CRC and the NMR Center. We provide support services to all NHLBI animals housed in NIH facilities.

Our goal is to facilitate getting the research accomplished expeditiously using the best, most humane methods. We will work with each investigator in developing their respective animal model and then either train them in all procedures to enable them to work independently, perform the procedures for them, or work in concert to expedite the animal data generated.

Biochemistry Facility

Duck-Yeon Lee, Ph.D., Director

Building 50, Room 3120 & 3121; E-mail: leedy@nhlbi.nih.gov

Phone: (301) 435-8369, Fax: (301) 451-5459

Web: <http://www.nhlbi.nih.gov/research/intramural/researchers/core/biochemistry-facility>

The mission of the Biochemistry Facility is to provide services and consultation with expertise in biochemical enzyme/protein purification and assay to NHLBI researchers. The Facility currently features 1) ESI-LC/MS spectrometers to measure accurate mass of intact protein and small organic compounds, 2) HPLCs equipped with radiochemical and fluorescence detector that allow a purification of protein labeled with radioisotope or fluorescence probe, 3) Atomic absorption spectrometer to measure metal content, and 4) Amino acid analysis.

Bioinformatics Core Facility (opening May 2016)

Mehdi Pirooznia, M.D., M.Sc., Ph.D., Director

Building 10, Room 7N218A

The Bioinformatics Core facilitates, amplifies, and accelerates biological and medical research and discovery through the application of the latest bioinformatics methods and technologies. This mission is achieved by delivering high quality and comprehensive support for experimental design, analysis and visualization in a timely fashion. The core is responsive to research scientists' needs and effectively evolve with advances in the field.

The core services include but are not limited to the following:

- Statistical analysis including basic statistical analysis, advanced statistical analysis (e.g., linear and generalized mixed model analysis, longitudinal modeling), and custom statistical methods (e.g., tailored to specific research projects)
- Omics Analysis including: Transcriptomics (Microarray and RNA-seq), Genomics (Genome, exome and targeted DNA-seq), Epigenomics (Methyl-seq, ChIP-seq, etc.), Proteomics, and Metabolomics

- Gene/Target/Disease Analysis: Functional annotation at variant, gene, and geneset level, Interaction analysis, and Pathway enrichment analysis
- Ad-hoc consultation: Advise on experimental designs, data management and analysis
- Computing resource development and maintenance, including Bioinformatics Software Development, Systems Toolkits Development, customized biological databases and Web Services development
- Training: Personalized training to match user's specific requirements and group training and workshops

Biophysics Core Facility

Grzegorz (Greg) Piszczek, Ph.D., Director

Building 50, Room 3124; E-mail: piszczek@nih.gov

Phone: (301) 435 8082; Fax: (301) 496-0599

Web: <http://www.nhlbi.nih.gov/research/intramural/researchers/core/biophysics-core>

The mission of the Biophysics Core Facility is to provide state of the art equipment and training to assist investigators within the NHLBI in studies of macromolecular interactions, dynamics and stability. The Biophysics Core Facility currently has resources to study oligomeric state of biomolecular assemblies, perform measurements of affinity, stoichiometry, kinetics and thermodynamics of interactions between proteins, DNA, RNA and their cognate ligands. Biophysical characterization capabilities include measurements of molecular weight, shape, and conformation of biological macromolecules. Oligomeric state of biomolecules as well as their hydrodynamic size and shape, can be studied using both analytical ultracentrifugation (Beckman XLI-Proteomelab) and light scattering techniques (Dynamic Light Scattering; DLS and Multi Angle Static Light Scattering; SEC-MALS).

Most physical or chemical processes have an associated heat effect that can be used as basis for a number of analytical techniques. Microcalorimetry is now the biophysical method of choice for label-free analysis of biomolecular interactions and stability. The Biophysics Facility has several Isothermal Titration and Differential Scanning Calorimeters (ITC and DSC) that can be applied in these studies. Surface Plasmon Resonance (SPR) is a complimentary method for studying macromolecular interactions that can also provide information on binding kinetics and the Biophysics Core is equipped with the Biacore 3000 and ForteBio Octet RED 96 systems. Molecular interactions can also be studied by microscale thermophoresis (MST) using the Nanotemper Monolith NT.115 instrument. Additionally, Facility users can take advantage of several optical spectroscopy methods, including steady-state and time resolved fluorescence, fluorescence anisotropy and circular dichroism (CD).

DNA Sequencing and Genomics Core Facility

Jun Zhu, Ph.D., Acting Director

Building 10, Room 5N107; E-mail: zhuj4@nhlbi.nih.gov

Phone: (301) 443-7927

Yoshiyuki Wakabayashi, Ph.D., Deputy Director

Building 10, Room 5N107; E-mail: yoshiyuki.wakabayashi@nih.gov

Phone: (301) 451-6090

Web: <http://www.nhlbi.nih.gov/research/intramural/researchers/core/dna-sequencing-and-genomics-core/>

The DNA Sequencing Core and Genomics core (DSGC) strives to provide the state-of-art next generation sequencing (NGS) services to NHLBI investigators in a cost-effect manner. Equipped with Illumina sequencers (Miseq and Hiseq), the core supports diverse NGS applications, including not but limited to genome/exome sequencing, RNAseq, ChIP-seq and small RNA sequencing.

Our integrated services consist of experimental design and consultation, library QA/QC, data acquisition and preliminary data analysis. In addition, the DGSC also offers trainings on library preparation for a wide range of NGS applications. Additional assistance will also be provided in a collaborative manner for projects that require extensive protocol optimization and software development.

Echocardiography Laboratory

Vandana Sachdev, M.D., Director

Building 10-CRC, Room 5-1436, E-mail: vs74y@nih.gov

Phone: (301) 496-3015

Cynthia L. Brenneman, R.N., R.C.S., Lab Manager

Building 10-CRC, Room 5-1436, E-mail: cb179i@nih.gov

Phone: (301) 451-3799

Web: <http://www.nhlbi.nih.gov/research/intramural/researchers/core/echocardiography-laboratory>

The Echocardiography Laboratory performs comprehensive cardiac imaging for NHLBI and all institutes at the Clinical Research Center. They collaborate in prospective and retrospective cardiovascular phenotyping studies and implement new technologies as necessary for detailed assessment of ventricular systolic and diastolic function, valvular abnormalities, and structural heart disease.

Representative research applications include:

- 3D imaging for structural cardiac defects
- Strain imaging for ventricular function
- Contrast imaging for left ventricular size, function, and evaluation of intracardiac abnormalities
- Contrast perfusion imaging of myocardium and skeletal muscle for the evaluation of microvascular flow
- Protocol-specific imaging of patients with mitral regurgitation to evaluate newer methods for quantitation of regurgitation severity

Electron Microscopy Core Facility

Christopher Bleck, Ph.D., Director

Building 14E, Room 111B

Phone: (301) 496-4711, E-mail: christopher.bleck@nih.gov

Erin Stempinski, Scientific Support Staff

Building 14E, Room 104A, E-mail: erin.stempinski@nih.gov

Phone: (301) 496-6448

Camron Keshavarz

Building 14E, Room 104

Phone: (301) 402-1229, Email: camron.keshavarz@nih.gov

Web: <http://www.nhlbi.nih.gov/research/intramural/researchers/core/electron-microscopy-core>

The NHLBI Electron Microscopy (EM) Core staff works with investigators and fellows to provide high-resolution transmission and scanning electron microscopy images of a variety of their samples including tissue, cell pellets, tissue culture, and inorganic material. In addition to conventional processing techniques for electron microscopy, we also provide microwave processing, negative staining, on-section gold immunolabeling, freeze fracture, platinum replicas, correlative light and electron microscopy, and other project-specific techniques. Potential clients can contact us to set up an initial consultation so that we can better understand the needs of your project. We will work with you when you submit a sample request to establish a projected cost and date when the EM Core will receive

and process the samples. We encourage fellows to get training on any part of the sample processing and imaging to streamline future projects.

Flow Cytometry Core Facility

J. Philip McCoy, Jr., Ph.D., Director

Building 10, Room 8C104, E-mail: mccoyjp@mail.nih.gov

Phone: (301) 451-8824, Fax: (301) 480-4774

Web: <http://www.nhlbi.nih.gov/research/intramural/researchers/core/flow-cytometry-core>

The mission of the NHLBI Flow Cytometry Core Facility is to provide investigators at the NHLBI access to state-of-the-art flow cytometry, including cell sorting, high dimensional cell analysis, cytokine quantification, and imaging flow cytometry. This is done by having cytometers and software available in the core facility and by providing consultation to investigators. Investigators are responsible for specimen preparation and staining. The staff of the flow cytometry laboratory will gladly assist you in designing your experiments and in developing optimal preparation and staining procedures. For analytical experiments, data will be provided as either hard copies or on appropriate media as listmode files. Software and computer workstations are available for "offline" analysis of these files. For sorting experiments, each investigator is responsible for bringing appropriate media and test tubes. In addition to cell sorting and analytical cytometry, the core facility also provides multiplex bead array expertise for analysis of extracellular cytokines, and imaging flow cytometry where the staining patterns of fluorochromes can be visualized.

iPSC Core

Jizhong Zou, Ph.D., Director

Building 10, Room 5N214

Phone: (301) 594-4717; E-mail: zouj2@nhlbi.nih.gov

Web: <http://intranet.nhlbi.nih.gov/content/ipsc>

The mission of induced Pluripotent Stem Cells (iPSC) Core is to accelerate stem cell research in the NHLBI by providing investigators consultation, technical services and training in human pluripotent stem cell technology. The major services that iPSC Core currently provides include (1) generation of human iPSCs from fibroblast cells, CD34+ hematopoietic stem/progenitor cells, and peripheral blood mononuclear cells (PBMCs) using non-integration methods; (2) CRISPR/Cas9 mediated human iPSC gene knockout, gene correction, and AAVS1 safe harbor transgene knockin; (3) human iPSC-cardiomyocyte (CM) differentiation. The Core also provides control iPSC lines and validated iPSC culture reagents. In addition to providing services and consultations to NIH researchers, the Core staff collaborates with investigators to work on custom and exploratory projects. Research conducted by the Core seeks to better understand the mechanisms underlying pluripotent stem cell self-renewal and differentiation to optimize culture conditions and operating procedures.

Imaging Probe Development Center

Rolf Swenson, Ph.D., Director

Building 9800, Room 3042, E-mail: rolf.swenson@nih.gov

Phone: (301) 217-7626

Web: <http://www.nhlbi.nih.gov/research/intramural/researchers/programs/imaging-probe-development-center/>

The Imaging Probe Development Center (IPDC) was founded with the goal of providing the fundamental synthetic chemistry support needed to advance molecular imaging technologies for the interdisciplinary NIH research community. The IPDC laboratories are located in Rockville, Maryland, with state-of-the-art equipment and the new PET facility at the NIH main campus. The IPDC has a rolling solicitation system, and NIH scientists are welcome to contact us and submit a proposal requesting synthesis of a particular probe in which they are interested. Probes can be intended for all types of imaging modalities, such as optical fluorescence, PET/SPECT, and MRI. IPDC scientists can synthesize requested probes that are completely novel or that are published in literature but

commercially unavailable. We look for automation solutions to improve capabilities and throughput. We have produced molecular imaging probes ranging from low-molecular-weight entities to high-molecular-weight conjugates, including fluorescent dyes and their analogs, lanthanide complexes, fluorogenic enzyme substrates, caged dyes that become fluorescent upon irradiation, radio- and fluorescent-labeled peptides, proteins and antibodies, gold and iron oxide nanoparticles, dendrimers, and liposomes. Recent efforts have included hyperpolarized MRI probes, tools for super-resolution spectroscopy, and PET probes derived from tyrosine kinase inhibitors. Examples of some of our recent projects will be provided.

Light Microscopy Core Facility

Christian A. Combs, Ph.D., Director

Building 10, Room 6N-309; E-mail: combsc@nhlbi.nih.gov

Phone: (301) 496-3236; Mobile: 301-768-2568

Daniela A. Malide, M.D., Ph.D., Facility Manager

Building 10, Room 6N-309; E-mail: dmalide@nhlbi.nih.gov

Phone: (301) 402-4719, Fax: (301) 480-1477

Xufeng Wu, Ph.D., Deputy Director

Building 50, Room 2318; E-mail: wux@nhlbi.nih.gov

Phone: (301) 402-4187, Fax: (301) 402-1519

Web: <http://www.nhlbi.nih.gov/research/intramural/researchers/core/light-microscopy-core/>

We are a state-of-the-art microscopy facility that has served the needs of the NHLBI DIR since 2000. We have helped to publish more than 250 papers in this period and have helped researchers from all of the NHLBI Centers and Branches. The mission of this facility is to provide state of the art equipment, training, experimental design, and image processing capabilities to assist researchers in experiments involving light microscopy. We have twenty two microscopes in six locations in Bldgs. 10 and 50. These microscopes provide a wide array of techniques including wide-field fluorescence and transmitted light imaging, confocal, two-photon, total internal reflection fluorescence microscopy (TIRF), and super-resolution microscopy (STED/SIM/STORM). While we primarily serve the needs of NHLBI DIR researchers, a few of our microscopes are available to other NIH researchers. In addition to the microscopes, we also have a broad array of image processing software for quantification of image intensities, morphological analysis, co-localization analysis, particle tracking, 3D volume reconstruction, etc. Our poster will highlight in a general way the various capabilities, techniques, microscopes available in the facility.

Murine Phenotyping Core

Danielle Springer, VMD, DACLAM, Director

Building 14E, Room 107A; E-mail: springerd@nhlbi.nih.gov

Phone: (301) 594-6171; Fax: (301) 480-7576

Web: <http://www.nhlbi.nih.gov/research/intramural/researchers/core/murine-phenotyping-core>

The Murine Phenotyping Core's central mission is development of a comprehensive in-depth knowledge of murine phenotyping methodologies in order to assist investigators with design, research applications, experimental methodologies, data acquisition and interpretation of murine cardiovascular, metabolic, neuromuscular and pulmonary platforms. We seek to provide investigators with high quality scientific and technical support as well as centralized access to state of the art murine phenotyping equipment for the characterization of genetically engineered mouse models. We are currently developing Standard Operating Procedures for our specialized equipment in order to provide high quality, reproducible and reliable data.

We provide consultation on appropriate methodologies to acquire cardiovascular, metabolic, neuromuscular, or pulmonary data from your mouse model. The lab assists with experimental design, data collection and acquisition, and data analysis. As most platforms require technical expertise, well developed standard operating procedures, and consistent and refined technique we recommend using our laboratory to collect your data for you. We also are happy to train any interested NHLBI scientist on any SOP, technical skill, equipment operation, etc. that you would like to acquire knowledge on.

NHLBI Safety Committee

Ilsa I. Rovira, M.S., Chair

Building 10-CRC, Room 5-3288; E-mail: rovirai@nih.gov

Phone: (301) 594-2466

Véronique A. Bonhomme, Health Sciences Safety Specialist

Building 13, Room 3K03; Email: veronique.bonhomme@nih.gov

Phone: (301) 496-2346

The NHLBI Safety Committee was formed to promote a safer working environment by encouraging more staff involvement, improved communication of common safety hazards and a more proactive attitude to safety issues. The members were chosen from laboratory areas to benefit from their collective experience. We intend to gather more practical input of common safety problems. We strive to become a resource for all staff regarding safety questions that come up regularly in laboratories and welcome input from the community to improve safety practices in the Institute.

Office of Biostatistics Research (OBR)

Nancy L. Geller, Ph.D., Director

Rockledge 2, Room 9202; E-mail: gellern@nhlbi.nih.gov

Phone: (301) 435-0434

The OBR collaborates in the planning, design, implementation, monitoring and analyses of studies funded by NHLBI. OBR also provides statistical consultation to any NHLBI investigator who requests advice. OBR has expertise in study design and collaborates in data management and analysis of many studies sponsored by the NHLBI DIR. OBR's primary responsibility is to provide objective, statistically sound, and medically relevant solutions to problems that are presented. When a question raised requires new methodology, the OBR is expected to obtain a new and valid statistical solution. OBR has a broad research mission and the professional staff is often asked to serve on in-house administrative committees as well as advisory committees for other Institutes within NIH and other agencies within DHHS.

Office of Technology Transfer and Development (OTTAD)

Alan H. Deutch, Ph.D., Director

Building 31, Room 4A29F; E-mail: deutch@nhlbi.nih.gov

Phone: (301) 402-5579; Fax: (301) 594-3080

Brian Bailey, Ph.D., Technology Development Specialist

Building 31, Room 4A29; E-mail: bbailey@nhlbi.nih.gov

Phone: (301) 402-5579; Fax: (301) 594-3080

The OTTAD provides a complete array of services to support the National Heart, Lung, and Blood Institute's technology development activities. To ensure that these activities comply with Federal statutes, regulations and the policies of the National Institutes of Health, a large part of OTTAD's responsibilities includes the day-to-day

negotiations of transactional agreements between the NHLBI and outside parties, including universities, pharmaceutical and biotechnology companies. These agreements provide for:

- The exchange of research materials under the Simple Letter of Agreement (SLA) or the Material Transfer Agreement (MTA);
- Collaborative research conducted under cooperative research and development agreements (CRADAs);
- Clinical studies of the safety and efficacy of new pharmaceuticals under clinical trial agreements (CTAs); and
- Exchange of confidential information under confidential disclosure agreements (CDAs)

The OTTAD also reviews employee invention reports, and provides instructions to the NIH's Office of Technology Transfer (OTT) concerning filing of domestic and foreign patent applications. The OTTAD participates in the marketing of NHLBI technologies as well as provides educational presentations and brochures related to technology transfer for NHLBI scientists. Additionally, the OTTAD advises NHLBI scientists on patent rights, policies, and procedures related to technology transfer. The NHLBI OTTAD staff participates in meetings, discussions and conferences, as appropriate, to stay apprised of and monitor the scientists' needs.

Pathology Core Facility

Zu-Xi Yu, M.D., Ph.D., Core Director

Building 10, Room 5N315; E-mail: yuz@mail.nih.gov

Phone: (301)496-5035, Fax: (301) 480-6560

Web: <http://www.nhlbi.nih.gov/research/intramural/researchers/core/pathology-core>

The Pathology Core provides morphologic services for the studies of experimental pathology (animal models) and optimizes the uses of supplies and equipment for histology to all NHLBI DIR scientists. Services include standard histological and tissue preparation, embedding, sectioning and routine histology staining; frozen tissue section, immunohistochemistry and diagnostic pathology. Ongoing interaction of Pathology Core personnel with each investigator facilitates communication regarding histology products, morphologic findings, histopathological interpretation, and new technical developments, thus increasing the efficiency of the research projects. Staff members are well-trained, extremely experienced technicians, and the laboratory has a wide repertoire of specialized techniques. The research pathology and immunohistochemistry are subsequently operating using standard operating procedures based on good lab practice guidelines.

Proteomics Core Facility

Marjan Gucek, Ph.D., Director

Building 10, Room 8C103C; E-mail: Marjan.Gucek@nih.gov

Phone: (301) 594-1060, Fax: (301) 402-2113

Web: <http://www.nhlbi.nih.gov/research/intramural/researchers/core/proteomics-core>

We provide investigators at the NHLBI access to mass spectrometry and gel based proteomics for identification and quantitation of proteins and their posttranslational modifications (PTM). We have state-of-the-art equipment, including an Orbitrap Fusion instrument.

Our workflows for relative protein quantitation are based on DIGE, label-free, SILAC and TMT approaches. We can also help investigators identify and quantify protein posttranslational modifications, including phosphorylation, nitrosylation, acetylation, ubiquitination, succinylation, etc. We provide training in proper sample preparation and lead the researchers through mass spectrometric analysis to data searching and interpretation. Users have access to a variety of proteomics software platforms (Mascot, Proteome Discoverer, Sequest, Scaffold) for re-searching the data or viewing the results.

In addition to helping the NHLBI investigators, we develop new approaches for PTM characterization and absolute protein quantitation.

Systems Biology Core

Xujing Wang, Ph.D., Director

Building 10, Room 7N220 & 7N224, E-mail: xujing.wang@nih.gov

Phone: (301) 451-2862, Fax: (301) 480-7576

Web: <http://www.nhlbi.nih.gov/research/intramural/researchers/core/bioinformatics-and-systems-biology>

The Systems Biology (BISB) Core aims to assist PIs overcome the technical challenges in utilizing bioinformatics and systems biology techniques. In addition, the core is interested in collaborating with PIs to incorporate systems biology approaches synergistically and develop transformative and translational research. Our Core currently maintains a Linux server that contains 12 computational nodes of ~600 cores and 250TB storage.

Some examples of services that we provide include: the Analysis of high throughput sequencing, microarray, proteomic data; Experimental design assistance for OMICS studies; Integrated analysis of transcriptome, miRNA, epigenome and proteomics data; Functional Genomics analysis of data including pathway and functional enrichment analysis; Systems biology analysis of data to identify potential therapeutic targets or biomarkers; Development of predictors for diagnosis and prognosis of disease; Data and text mining from Public databases and literature; Personalized consulting; Customized data analysis and interpretation.

Transgenic Core

Chengyu Liu, Ph.D., Director

Building 50, Room 3305; E-mail: Liuc2@mail.nih.gov

Phone: (301) 435-5034; Fax: (301) 435-4819

Web: <http://www.nhlbi.nih.gov/research/intramural/researchers/core/transgenic-core>

The Transgenic Core's main mission is to keep up with the latest advancements in genome engineering technologies and to provide state-of-the-art services to assist NIH scientists in generating genetically engineered animal models. In the past several years, the Core has successfully used the ZFN, TALEN, and CRISPR methods to generate gene-targeted mouse lines. The revolutionary CRISPR technology has enabled the Core to simultaneously target multiple genomic loci and achieve gene knockout in difficult mouse strains, such as immunocompromised mice. Besides developing these new technologies, the Core is continuing to provide a variety of services using the classical mouse genetic and reproductive methodologies, such as producing transgenic lines using the pronuclear microinjection method, generating knockout mice using ES cell-mediated homologous recombination and blastocyst microinjection, cryopreserving and resurrecting mouse lines. The Core has imported the TARGATT mouse line, which enables the insertion of a single copy transgene into a predefined genomic locus. In addition, the core also offers services for injecting stem cells or differentiated cells into immunocompromised mice for testing their ability to form teratomas or evaluating their differentiation capabilities.



Poster Titles and Session Assignments

Please mount your poster upon arrival so it may be viewed for the entire Festival.

Cores and Offices will present during both poster sessions.

For research poster session assignments, see below:

Poster Session I (12:30-1:45PM): #1-16, 17-86

Poster Session II (3:35-4:50PM): #1-16, 87-158

Core and Office Posters

1. **The Animal MRI Core.** S. Anderson; Animal MRI Core.
2. **Animal Surgery & Resources (ASR) Core.** R.R. Clevenger, J. Taylor, T. Hunt, J. Hawkins; Animal Surgery & Resources (ASR) Core.
3. **Biochemistry Facility.** D. Y. Lee; Biochemistry Facility.
4. **Biophysics Core Facility.** G. Piszczek; Biophysics Core.
5. **DNA Sequencing and Genomics Core Facility.** J. Zhu, Y. Wakabayashi; DNA Sequencing and Genomics Core Facility.
6. **Electron Microscopy Core Facility.** C. Bleck, E. Stempinski, C. Keshavarz. Electron Microscopy Core.
7. **induced Pluripotent Stem Cells (iPSC) Core.** J. Beers, Y. Lin, K. Linask, J. Zou; iPSC Core.
8. **The Imaging Probe Development Center.** B. Blackman, F. Bhattacharyya, C. Mushti, A. Opina, N. Raju, D. Sail, Z. Shi, O. Vaslatiy, C. Woodroffe, H. Wu, X. Zhang, R. Swenson; Imaging Probe Development Center.
9. **Light Microscopy Core.** D. Malide, X. Wu, C.A. Combs. Light Microscopy Core.
10. **Murine Phenotyping Core.** A. Noguchi, M. Allen, D. Springer, Murine Phenotyping Core.
11. **NHLBI Safety Committee.** I. Rovira, V. Bonhomme; NHLBI Safety Committee.
12. **Office of Biostatistics Research.** N. Geller; Office of Biostatistics Research.
13. **Office of Technology Transfer and Development.** B. Bailey, A. Deutch; Office of Technology Transfer and Development.
14. **Pathology Core.** D. Tang, X. Qu, Z.X. Yu, Pathology Core.
15. **Systems Biology Core.** Y. Chen, S. Gao, P.S. Krishnan, I. Tunc, N. Wolanyk, X. Zhang, X. Wang; Systems Biology Core.
16. **Transgenic Core.** Y. Du, W. Xie, Y. Zhan, C. Liu; Transgenic Core.

Research Posters

17. **The Combination of ACP-196 and ACP-319 Leads to Increased Survival in the TCL1-192 CLL Mouse Model.** H. Mora-Jensen¹, C.U. Niemann^{1,3}, M. Gulrajani², F. Krantz², T. Covey², B.J. Lannutti², A. Wiestner¹, S.E.M. Herman¹; ¹Laboratory of Lymphoid Malignancies, NHLBI, ²Acerta Pharma, Redwood City, CA, ³Department of Hematology, Copenhagen University Hospital, Denmark.
18. **Myosin II Facilitates Ligand Discrimination During T Cell Activation.** J. Hong, S. Murugesan, J. Hammer; Molecular Cell Biology Section.
19. **Effects of Heterologous Expression of Human Cyclic Nucleotide Phosphodiesterase 3A (hPDE3A) on Redox Regulation in Yeast.** D.K. Rhee, J.C. Lim, S.C. Hockman, F. Ahmad, D.H. Woo, Y.W. Chung, S. Liu, A.L. Hockman, V.C. Manganiello; Laboratory of Translational Research.
20. **Brg Cancer Mutations Disrupt Direct Interaction with PRC1 to Enhance Polycomb Activity.** B.Z. Stanton, C. Hodges, W.L. Ku, K. Zhao, G.R. Crabtree; Systems Biology Center, NHLBI & Stanford School of Medicine.
21. **Cysteine Cathepsins Are Essential in Lysosomal Degradation of α -Synuclein.** R.P. McGlinchey, J.C. Lee; Laboratory of Molecular Biophysics.

22. **Genome-wide Detection of DNase I Hypersensitive Sites in Single Cells and FFPE Tissue Samples.** W. Jin, Q. Tang, M. Wan, K. Cui, Y. Zhang, G. Ren, B. Ni, J. Sklar, T.M. Przytycka, R. Childs, D. Levens, K. Zhao; Laboratory of Epigenome Biology.
23. **Regulation of Hepatic Gluconeogenesis by Human Long non-coding RNAs.** X. Ruan, P. Li, H. Cao; Laboratory of Obesity and Metabolic Diseases.
24. **An Addition to the Toolkit of NMR Spectroscopy for Large Proteins and Complexes: Lanthanide-induced Pseudocontact Shifts.** M. Strickland, C.D. Schwieters, A.M. Stanley, G. Wang, A.C.L. Opina, S. Buchanan, A. Peterkofsky, O. Vaslatiy, N. Tjandra; Laboratory of Structural Biology.
25. **Correlation Of Clinical And Mutational Markers Of Disease Progression In Chronic Lymphocytic Leukemia Treated With Ibrutinib.** I. Ahn¹, A. Albitar², C. Underbayev³, S. Herman³, S. Soto³, X. Tian⁴, M. Stetler-Stevenson⁵, I. Maric⁶, M. Farooqui³, M. Albitar², A. Wiestner³; ¹Medical Oncology Service, NCI, ²NeoGenomics Laboratories, Irvine, CA, ³Hematology Branch, NHLBI, ⁴Office of Biostatistics Research, NHLBI, ⁵Laboratory of Pathology, Center for Cancer Research, NCI, ⁶Department of Laboratory Medicine, Clinical Center, NIH.
26. **Two Distinct Actin Networks Mediate Traction Oscillations To Confer Mechanosensitivity Of Focal Adhesions.** Z. Wu, S.V. Plotnikov, C.M. Waterman, J. Liu; 1. Theoretical Cellular Physics Section, LMB, BBC, NHLBI 2. Laboratory of Cell and Tissue Morphodynamics, CBPC, NHLBI, 3. Department of Cell and Systems Biology, University of Toronto.
27. **Improved Differentiation of Mouse Embryonic Stem Cells into Purkinje Neurons.** C. J. Alexander, J. A. Hammer; Laboratory of Cell Biology.
28. **Proteomic Profiling Reveals that 3-dimensional Engineered Heart Tissue Culture Promotes Maturation and Aerobic Respiration of Human Induced Pluripotent Stem Cell-derived Cardiomyocytes.** A. Stoehr¹, B. Ulmer², I. Mannhardt², S. Patel³, M. Gucek³, T. Eschenhagen², A. Hansen², E. Murphy¹; ¹Systems Biology Center, NHLBI, ²Dep. of Exp. Pharmacology and Toxicology, CVRC, DZHK, UKE, Hamburg, Germany, ³Proteomics Core Facility, NHLBI
29. **The Role of Actin Structural Plasticity in Mechanosensation.** P.S. Gurel, Y. Takagi, J. E. Bird, J.R. Sellers, G.M. Alushin; Cell Biology and Physiology Center.
30. **Characterization of GB1 using H/D Fractionation.** P. Shukla¹, P. Bryan², Y. Chen², J. Orban², N.Tjandra^{1*}; ¹Laboratory of Structural Biophysics, NHLBI, ²Institute for Bioscience and Biotechnology Research, University of Maryland.
31. **Novel Role of TFEB and TFE3 in Cellular Response to ER Stress.** J.A. Martina, H.I. Diab, O.A. Brady, R. Puertollano; Protein Trafficking and Organelle Biology Group.
32. **Mechanism of Activation of the TRPV1 Channel by a Double-Knot Tarantula Toxin.** C. Anselmi¹, C. Bae^{2,3}, A. Jara-Oseguera², J. I. Kim³, K. J. Swartz², J. D. Faraldo-Gómez¹; ¹Theoretical Molecular Biophysics Section NHLBI, ²NINDS, ³Gwangju Institute of Science and Technology, Republic of Korea.
33. **CoSync: an R package for Co-Synchronization Network Analysis of Pseudo-temporally Ordered Single Cell Data.** Y. Chen, S. Gao, N. Wolanyk, X. Wang; Systems Biology Core.
34. **Apolipoprotein C-III Nanodiscs Studied by Site-Specific Tryptophan Fluorescence.** C. Brisbois, J. Lee; Laboratory of Molecular Biophysics.
35. **High-Resolution Structural Insight Into The Myosin VI-F-Actin Interface.** L.Y. Kim¹, P.S. Gurel¹, T. Omabegho², Z. Bryant^{2,3}, G.M. Alushin¹; ¹Cell Biology and Physiology Center, NHLBI, ²Department of Bioengineering and ³Department of Structural Biology, Stanford University.
36. **Identifying Clusters of Genes Driving Complex Disease Progression.** N. Wolanyk, X. Wang, M. Hessner, S. Gao; Systems Biology Core.
37. **The Disruptive State Of The Membrane Active Antimicrobial Peptide Piscidin 1 Investigated By Multi- μ S All-Atom Simulations And Solid-State NMR: Surface Defects Are Favored Over Stable Pores.** B.S. Perrin, Jr., R. Fu, M.L. Cotten, R.W. Pastor; Laboratory of Computational Biology.

38. **The Thrombopoietin Receptor Agonist Eltrombopag Has DNA Repair Activity in Human Hematopoietic Stem and Progenitor Cells.** P.S. Cheruku, A. Cash, A. Larochelle; Regenerative Therapies for Inherited Blood Disorders.
39. **Bayesian Analysis of E3 Ubiquitin Ligase/AQP2 Interactions in the Renal Collecting Duct.** B. Medvar^{1,2}, A. Sarkar², M.A. Knepper¹; ¹Epithelial Systems Biology Laboratory, ²Vitreous State Laboratory, The Catholic University of America.
40. **Global Organization of a Protein Binding Site Network.** J. Lee, J. Konc, D. Janežič, B.R. Brooks; Laboratory of Computational Biology.
41. **Brownian Ratchet Mechanism of Plasmid Segregation.** L. Hu, J. Liu; Biochemistry and Biophysics Center.
42. **Structural Features of α -Synuclein Revealed by Raman Spectroscopy.** J.D. Flynn, J. C. Lee; Laboratory of Molecular Biophysics.
43. **Characterization of a Murine Model of Psoriasis and its Association to Cardiometabolic Dysfunction.** Q. Ng, A. Sorokin, Y. Baumer, M. Playford, H. Teague, A. Noguchi, M. Winge, P. Marinkovich, N. Mehta; Section of Inflammation and Cardiometabolic Disease.
44. **Artificial Actin-Binding Proteins With Novel Multifunctional Properties.** A. Lopata, C. Tiede, D.C. Tomlinson, J.R. Sellers, P.J. Knight, M. Peckham; Laboratory Of Molecular Physiology.
45. **Autologous Stem Cell Transplantation In Immunoglobulin Light Chain Amyloidosis With Factor X Deficiency.** S. Cordes, M. Gertz, K.K. Buadi, Y. Lin, M.Q. Lacy, P. Kapoor, S.K. Kumar, A. McCurdy, A. Dispenzieri, D. Dingli, S. Hayman, W.J. Hogan, R.K. Pruthi.; Department of Hematology, Mayo Clinic, Rochester, MN.
46. **High-Resolution Maps Of Chromatin Interaction Reveal CTCF As A Facilitator Of Enhancer-Promoter Interaction To Maintain Robustness Of Gene Expression.** G. Ren, W. Jin, K. Cui, J. Rodrigez, D.R. Larson, K. Zhao; Systems Biology Center.
47. **Centrosome-Pole Cohesion Requires Abnormal Spindle And Calmodulin To Ensure Proper Centrosome Inheritance In Neural Stem Cells But Is Dispensable For Brain Size.** T. Schoborg, A. Zajac, C. Fagerstrom, R.X. Guillen, N.M. Rusan; Laboratory of Molecular Machines & Tissue Architecture.
48. **Micro-CT Scouting For Transmission Electron Microscopy Of Human Tissue Specimens.** A.G. Morales, E.S. Stempinski, X. Xiao, A. Patel, A. Panna, K.N. Olivier, P.J. Mcshane, C. Obinson, A.J. George, D.R. Donahue, P. Chen, H. Wen; Laboratory of Imaging Physics.
49. **Novel Role of TRPML2 in the Regulation of the Innate Immune Response.** Y. Hua, L. Sun, S. Vergarajauregui, H. Diab, R. Puertollano; Laboratory of Cell Biology.
50. **The transmission of the proton motive force along I-Band segments of the mitochondrial reticulum.** K.D. Patel, B. Glancy, R.S. Balaban; Laboratory of Cardiac Energetics.
51. **The Impact of Aging of Hematopoietic Stem and Progenitor Cells (HSPCs) in Non-Human Primates as Interrogated by Genetic Barcode Clonal Tracking** K. Yu, C. Wu, D. Espinoza, I. Yabe, S. Panch, S. Hong, S. Koelle, R. Lu, A. Bonifacino, A. Krouse, M. Metzger, R. E. Donahue, C.E. Dunbar; Molecular Hematopoiesis Section.
52. **Dramatic Radiation Dose Reduction over 7 Years of Experience for Coronary CT Angiography.** A. Knab, D. Melo, J. Yu, D.W. Groves, E.A. Nelson, K. Bronson, M. Stagliano, S. Rollison, A.D. Choi, S.M. Shanbhag, M.Y. Chen; Advanced Cardiovascular Imaging Group.
53. **Identification and Characterization of a Novel Gene that Regulates Mitochondrial DNA Replication.** J. Tang, Y. Zhang, K. Delaney, H. Xu; Laboratory of Molecular Genetics.
54. **Self-reported Depression and Anxiety Associate with Vascular Inflammation and Coronary Heart Disease Beyond Traditional Cardiovascular Risk Factors in Psoriasis.** T.M. Abera, A.A. Joshi, J.B. Lerman, J.A. Rodante, J.I. Silverman, T.Z. Aridi, M.Y. Chen, M.P. Playford, N.N. Mehta; Section of Inflammation and Cardiometabolic Diseases.

55. **Virtual Neighborhood-Built-Environment Quality Audits Provide Insights into Neighborhood Walkability: The Washington, DC Cardiovascular Health and Needs Assessment.** J. Adu-Brimpong¹, N. Coffey², C. Ayers³, D. Berrigan⁴, L. Yingling¹, S. L. Thomas¹, V. Mitchell¹, T. M. Powell-Wiley¹; ¹Social Determinants of Cardiovascular Risk and Obesity, NHLBI. ²Global and Community Health Department at George Mason University School of Public Health. ³Donald W. Reynolds Cardiovascular Clinical Research Center at University of Texas Southwestern Medical Center. ⁴Division of Cancer Control and Population Sciences at National Cancer Institute.
56. **Use of Mobile Health (mHealth) Technology to Identify Targets for Improving Cardiovascular (CV) Health For Women in a Resource-limited Community: Observations from the Washington, D.C. CV Health and Needs Assessment.** S. Thomas, L. Yingling, G. Wallen, A. Todaro-Brooks, M. Peters-Lawrence, J. Henry, J. Saybe, J. Adu-Brimpong, V. Mitchell, D. Sampson, T. Johnson, K. Wiley, Jr., A. Graham, L. Graham, A. Johnson, T. Powell-Wiley; Social Determinants of Cardiovascular Risk and Obesity Group.
57. **RNA-seq Reveals Markers for the Two Major Cell Types in the Mouse Renal Collecting Duct.** L.H. Chen, J.W. Lee, C.L. Chou, S.M. Wall, D. Brown, M.A. Knepper; Epithelial Systems Biology Laboratory.
58. **Defining Roles for Apolipoprotein A-1 and Apolipoprotein E in Modifying Asthmatic Airway Inflammation.** E.M. Gordon, H. Xu, S.J. Levine; Laboratory of Asthma and Lung Inflammation.
59. **Integrative Transcriptome Analyses of Metabolic Responses in Mice Define Pivotal lncRNA Metabolic Regulators.** L. Yang, P. Li, W. Yang, X. Ruan, Y. Zhao, K. Kieseewetter, H. Luo, J. Zhu, H. Cao; Laboratory of Obesity and Metabolic Diseases.
60. **Standard 3D Printed Phantom Used For Calibration In Micro Stereo Radiography And Far-Field Phase Contrast Imaging.** A. George, P. Chen, H. Wen; Laboratory of Imaging Physics.
61. **Curvature Preference in Professional Phagocytes: A Mechanochemical Modeling Approach.** S. Kale, J. Liu; Theoretical Cellular Physics.
62. **An FMN2-Mediated Perinuclear Actin/Adhesion System Protects Against DNA Damage During Confined Cell Migration.** C.T. Skau, P.S. Gurel, H. Racine-Thiam, A. Tubbs, M.A. Baird, M.W. Davidson, M. Piel, G.M. Alushin, A. Nussenzweig, C.M. Waterman. Laboratory of Cell and Tissue Morphodynamics.
63. **Generation of Rhesus Monkey iPSC-derived Endothelial Cells.** Y. Liu¹, Z. Yu¹, Y. Huang¹, H. Liu¹, Y. Lin², J. Zou², H. San³, C. Dunbar⁴, G. Chen¹, M. Boehm¹; ¹Laboratory of Cardiovascular Regenerative Medicine, ²IPS Core, ³Animal Program, ⁴Hematology Branch.
64. **Microtubule Affinity-Regulating Kinase, MARK2 Regulates Directed Cell Migration Through Modulation Of Myosin Activity.** A. Pasapera, R.N. Fischer, C.M. Waterman; Laboratory of Cell and Tissue Morphodynamics.
65. **Regulation Of The Permeability Transition Pore Is Altered In Mice Lacking The Mitochondrial Calcium Uniporter.** R.J. Parks, S. Menazza, A.M. Aponte, T. Finkel, E. Murphy; Laboratory of Cardiac Physiology.
66. **Having Fun With Shapes: α -Synuclein Lipid Tubules, Ribbons And Discs.** Z. Jiang, J.C. Lee; Laboratory of Molecular Biophysics.
67. **Development of a Human Circulating Fibrocyte Model to Assess the Effect of the 5A Apolipoprotein A-I Mimetic Peptide in Idiopathic Pulmonary Fibrosis.** D.M. Figueroa, S. Levine; Laboratory of Asthma and Lung Inflammation.
68. **MICU1 Serves as a Molecular Gatekeeper to Prevent *in vivo* Mitochondrial Calcium Overload.** J.C. Liu, J. Liu, K.M. Holmström, S. Menazza, R.J. Parks, M.M. Fergusson, Z.X. Yu, D.A. Springer, C.H. Halsey, C. Liu, E. Murphy, T. Finkel; Laboratory of Molecular Biology.
69. **Actin Retrograde Flow Orients and Aligns Activated Integrins in Focal Adhesions.** V. Swaminathan, C.M. Waterman; Laboratory of Cell and Tissue Morphodynamics.
70. **Substrate Topology Regulates Actomyosin Morphodynamics.** R.S. Fischer, X. Sun, J. Fourkas, W. Losert, C.M. Waterman; Laboratory of Cell and Tissue Morphodynamics.

71. **Circumventing Trogocytosis Through A Complement Based Retargeting Strategy In Lymphoid Malignancy.** E.J. Carstens¹, M. Skarzynski¹, V. Butera¹, M.A. Lindorfer², I. Ahn¹, I. Maric¹, M. Stetler-Stevenson¹, E.M. Cook², B. Vire¹, J. Valdez¹, Susan Soto¹, M.Z.H. Farooqui¹, C. Rader^{3,4}, R.P. Taylor², A. Wiestner¹; ¹Laboratory of Lymphoid Malignancies, NHLBI, ²University of Virginia School of Medicine, ³Scripps Res. Inst., ⁴NCI
72. **Rab22 And Arf6 Control T Cell Conjugate Formation Through Regulation Of The Clathrin-Independent Endosomal System.** D. Johnson^{1,2}, J. Wilson², J. Donaldson¹; ¹Cell Biology and Physiology Center, NHLBI, ²Cellular and Molecular Medicine, University of Arizona.
73. **Identification and Characterization of Novel Members of the Nonsense-Mediated mRNA Decay Pathway.** T.D. Baird, J.R. Hogg; Laboratory of Ribonucleoprotein Biochemistry.
74. **A High Density Lipoprotein Proteome Index Correlates with Atherosclerosis Severity in Humans.** S.M. Gordon, X. Wang, D. Sviridov, M. Chen, A.T. Remaley. Lipoprotein Metabolism Section.
75. **Molecular Mechanisms Of Coupled Transport In Secondary Transporters: Lessons From A Na⁺/Ca²⁺ Exchanger.** F. Marinelli, J. Liao, C. Lee, Y. Huang, Y. Jiang, J. D. Faraldo-Gómez; Theoretical Molecular Biophysics Section.
76. **Improving the Lennard-Jones Parameters of Ions in CHARMM.** M. Pourmousa, R.M. Venable, R.W. Pastor; Laboratory of Computational Biology.
77. **Effect of Overexpression of LCAT and ApoA-I on Atherosclerosis and Lipoprotein Metabolism in Mice.** A. Zarzour, A. Ossoli, B. Vaisman, S. Gordon, M. Amar, L. Calabresi, A. Remaley; Lipoprotein Metabolism Section.
78. **High Throughput Single-cell RNA Sequencing of iPSC-Derived Hematopoietic Stem Cells: One Drop Closer to Treatments of Inherited Bone Marrow Failure Syndromes.** L. Alvarado, G. Chen, I. Asokan, K. Johnson, JP. Ruiz, Y. Wakabayashi, J. Zhu, J. Zhou, M. Boehm, A. Larochelle; Laboratory of Regenerative Therapies for Inherited Blood Disorders.
79. **Exploring The Role Of Parkin In Astrocyte Mediated Neurotropic Function.** K. Singh, M. Sack; Laboratory of Mitochondrial Biology and Metabolism.
80. **The Mitochondrial Interactome by Crosslinking Mass Spectrometry: Evidence for Supercomplexes in Intact Mitochondria.** B.M. Dancy, R.S. Balaban; Laboratory of Cardiac Energetics.
81. **Pulsatile Contractions are an Intrinsic Property of MyosinIIa in Adherent Cells.** M.A. Baird, R. S. Fischer, A. Wang, R.S. Adelstein, C.M. Waterman; Cell Biology and Physiology Center.
82. **Nonmuscle Myosin II-A Plays a Role in Spermatid Elongation.** C.B. Lerma Cervantes¹, M.A. Conti¹, K. Tokuhira², Y. Zhang¹, M.J. Kelley³, R.S. Adelstein¹; ¹Laboratory of Molecular Cardiology, NHLBI, ²Laboratory of Cellular and Developmental Biology, NIDDK, ³Division of Medical Oncology, Duke University.
83. **Formin-Generated Actomyosin Arcs Propel T Cell Receptor Microcluster Movement At The Immunological Synapse.** S. Murugesan, J. Hong, J. Yi, D. Li, J. Beach, L. Shao, E. Betzig, X. Wu, J.A. Hammer; Cell Biology and Physiology Center.
84. **Investigating the Mesoscale Structure and Dynamics of Dense-Core Vesicle Docking Machinery.** J. Cierniecki, A. Trexler, K. Sochacki, J. Taraska; Laboratory of Cellular and Molecular Imaging.
85. **Actin Dynamics and Non-Muscle Myosin 2 Monomer Availability Drive Localized Filament Expansion.** J. R. Beach, K. Bruun, K. Remmert, D. Li, L. Shao, E. Betzig, J. A. Hammer; Cell Biology and Physiology Center
86. **Intercellular Transmission Of Enteroviral Populations With Vesicles.** Y.H. Chen¹, P.M. Takvorian², A. Cali², E.S. Stempinski³, G. Altan-Bonnet⁴, N. Altan-Bonnet¹; ¹Laboratory of Host-Pathogen Dynamics, NHLBI, ²Rutgers University, ³Electron Microscopy Core Facility, NHLBI, ⁴NCI
87. **Imaging Adipose Tissue Across Scales of Resolution: From Two-photon To Super-resolution Microscopy.** D. Malide; Light Microscopy Facility.
88. **A *Drosophila* Model Demonstrates Mitochondrial Regulation of Stem Cell Homeostasis.** F. Zhang, K. Zhou, H. Xu; Laboratory of Molecular Genetics.

89. **Investigations into Rotavirus and Norovirus Replication, Assembly and Exit.** M. Santiana, W.L. Du, Y. Mutsafi Ben Halevy, S. Sosnovtsev, J. Patton, K. Green, N. Altan-Bonnet; Laboratory of Host-Pathogen Dynamics.
90. **Fasting Regulates NLRP3 Inflammasome Activation In Humans By Modulating Mitochondrial Integrity.** J. Traba, S.S. Geiger, M. Kwarteng-Siaw, T.C. Okoli, J. Li, K. Han, M. Pelletier, A.A. Sauve, D. Gius, R.M. Siegel, M.N. Sack; Cardiovascular and Pulmonary Branch.
91. **Host Cell Pathways Hijacked for Coronavirus Transmission.** T.A. Dellibovi-Ragheb, M.C. Hagemeyer, P.M. Takvorian, A. Cali, N. Altan-Bonnet; Laboratory of Host-Pathogen Dynamics.
92. **Macrophage Deposition of Cholesterol into the Extracellular Matrix.** X.T. Jin¹, D. Sviridov², Y. Liu¹, B. Vaisman², L. Addadi³, A.T. Remaley², H.S. Kruth¹; ¹Experimental Atherosclerosis Section, ²Lipoprotein Metabolism Section, ³Department of Structural Biology, Weizmann Institute of Science, Israel.
93. **Mitochondrial Nutrient Sensing, FoxO1 Stability and the Retrograde Control of Gluconeogenesis.** L. Wang, I. Scott, L. Zhu, M. Sack. Cardiovascular and Pulmonary Branch.
94. **Improvement Of Definitive Erythroid Cell Production From Human ES Cells Using Serum-Free ES-Sac Generation.** J.J. Haro-Mora, N. Uchida, A. Fujita, J. Tisdale; Molecular & Clinical Hematology Branch.
95. **Multiplex Cytokine Profiling as Monitor and Prognosis Tool in Sickle Cell Disease Progression to Crisis.** E.A. Barbu, L. Mendelsohn, A. Ikeda, H. Ackerman, S.L. Thein; Sickle Cell Group.
96. **CD16A Based Universal Chimeric Antigen Receptors Enhanced ADCC Mediated by NK Cells.** L. Chen, D. Chinnasamy, R. Childs; Laboratory of Transplantation Immunotherapy.
97. **Investigating Protein Dynamics at Sites of Exocytosis in Live Cells.** A. Somasundaram, J. W. Taraska; Laboratory of Cellular and Molecular Imaging.
98. **Regulatory Role Of MYB On Fetal Hemoglobin Expression.** N. Angelis, X. Wang, L. Mendelsohn, S. L. Thein; Sickle Cell Branch.
99. **Imaging The Lipid Landscape At Single Sites Of Exocytosis.** A.J. Trexler, J.W. Taraska; Laboratory of Molecular and Cellular Imaging.
100. **A Simple CRISPR Tool For Off-Target Analysis.** I.Tunc, S.Hong, X.Wang, C.E. Dunbar; Systems Biology Core, Hematology Branch.
101. **Using Whole-Exome Sequencing To Identify Genetic Variants In Patients Diagnosed With Pentagony Of Cantrell.** B. MacTaggart, C. Bowen, M. Markowitz, J. Chong, M.J. Bamshad, X. Ma, R.S. Adelstein; Laboratory of Molecular Cardiology, NHLBI, University of Washington Centers for Mendelian Genomics.
102. **Structural Insight into Interaction of Fibrin and Very Low Density Lipoprotein Receptor.** K. Banerjee¹, S. Yakovlev², L. Medved², N. Tjandra¹; ¹Laboratory of Structural Biophysics, NHLBI, ²University of Maryland School of Medicine.
103. **Spectrum of Cardiovascular Involvement in Erdheim-Chester Disease Evaluated by Cardiac Computed Tomography.** D. Melo, A. Knab, S.M. Shanbhag, W.A. Gahl, J.I. Estrada-Veras, M.Y. Chen; Advanced Cardiovascular Imaging Group.
104. **Drosophila Methionine Sulfoxide Reductase A Cannot Act As An Oxidase.** S. Tarafdar¹, N.M. Rusan², R.L. Levine¹; ¹Laboratory of Biochemistry, ²Cell Biology and Physiology Center.
105. **Genomic Sequencing of Cell-free DNA in Sickle Cell Disease.** L. Tumburu, L. Li, Y. Wakabayashi, I. Tunc, X. Wang, J. Zhu, S.L. Thein; Sickle Cell Branch.
106. **Dietary Marine Long-Chain Monounsaturated Fatty Acid (LCMUFA) Attenuates The Development Of Atherosclerosis Via PPAR Signaling Pathway In Mouse Models.** Z.H. Yang¹, M. Bando², H. Miyahara³, J. Takeo³, B. Vaisman¹, M. Pryor¹, H. Sakaue², M. Sata², A. Remaley¹; ¹Lipoprotein Metabolism Section, Cardio-Pulmonary Branch, NHLBI, ²Institute of Biomedical sciences, Tokushima University Graduate School, ³Central Research Laboratory, Nippon Suisan Kaisha.
107. **Automated Tracking And Analysis Of Sleep-Like Behavior In Drosophila Larvae.** C. Kim¹, Q. Gaudry², S.T. Harbison¹; ¹Laboratory of System Genetics, NHLBI, ²Dept. of Biology, University of Maryland, College Park, MD.

108. **Roflumilat Effect on Aquaporin-2 Phosphorylation and Trafficking in Rat Renal Inner Medullary Collecting Duct.** E. Umejiego, C-L Chou, M.A. Knepper; Epithelial Systems Biology Laboratory.
109. **Functional Regulation of TIP150-Cortex Interaction with cortactin Mediating Directional Cell Migration.** G. Adams, X. Peng, D. Cao, Z. Wang, X. Yao, (C. Waterman); Laboratory of Cell Biology and Tissue Morphodynamics.
110. **Single Molecule Measurements of DNA Decatenation by the Topoisomerase III-RecQ Helicase Complex.** M. Mills, K.C. Neuman; Laboratory of Single Molecule Biophysics.
111. **Spatiotemporal regulation of adhesions disassembly at the G2/M transition of the cell cycle.** H.R. Thiam, C.M. Waterman; Laboratory of Cell and Tissue Morphodynamics.
112. **Identification and Characterization of Novel Members of the Nonsense-Mediated mRNA Decay Pathway.** T.D. Baird, J.R. Hogg; Laboratory of Ribonucleoprotein Biochemistry.
113. **Local Hypoxia Controls Neuro-Vascular Patterning Through CXCL12 And VEGF-A In The Developing Skin.** W. Li, Y. Mukouyama; Laboratory of Stem Cell and Neuro-Vascular Biology.
114. **Rapamycin Stimulates Regulatory T Cells In A Mouse Model Of Immune-Mediated Bone Marrow Failure.** Z. Lin, W. Sun, M. Hollinger, J. Chen, X. Feng, N.S. Young; Hematology Branch.
115. **On the Robustness of SAC Silencing in Closed Mitosis.** D. Ruth, J. Liu; Theoretical Cellular Physics.
116. **Elucidating the Properties of Prenylated Ras Isoforms in Biological Membranes.** M. Chakrabarti, R. W. Pastor; Laboratory of Computational Biology.
117. **Fluorescent Cell Barcoding: Optimization and Troubleshooting for Multiplexing Flow Cytometry Phenotyping and Signaling Profiling.** V. Giudice, X. Feng, S. Kajigaya, N. Young, A. Biancotto; Hematology Branch.
118. **Comprehensive Residual Disease Assessment Improves AML Relapse Risk Stratification In Autologous Hematopoietic Cell Transplantation.** M.P. Mulé¹, G.N. Mannis², B.L. Wood³, J.P. Radich³, J. Hwang², N.R. Ramos¹, C. Andreadis², L. Damon², A.C. Logan², T.G. Martin², C.S. Hourigan¹; ¹Myeloid Malignancies Section, NHLBI, ²Department of Medicine, Division of Hematology and Blood and Marrow Transplantation, University of California, San Francisco, ³Fred Hutchinson Cancer Research Center, Seattle, WA.
119. **Cholesterol Crystals In Atherogenesis And Beyond?** Y. Baumer, S. McCurdy, T. Weatherby-Carvalho, S. Halherr, P. Halbherr, N. Yamazaki, N. Mehta, W. Boisvert; Section of Inflammation and Cardiometabolic Diseases, NHLBI, University of Hawaii, John A Burns School of Medicine, Center for Cardiovascular Research.
120. **Positional Changes Of Pericentrin Are Related To PCM Activity At The Centrosome.** K. Plevock, B. Galletta, C. Fagerstrom, K. Slep, N. Rusan. Laboratory of Molecular Machines and Tissue Architecture.
121. **Use of CRISPR-Phosphoproteomics to Investigate Role of Myosin Light Chain Kinase in Vasopressin Signaling.** K. Isobe, V. Raghuram, C.-R. Yang, P. Sandoval, C.L. Chou, M.A. Knepper; Epithelial Systems Biology Laboratory, Systems Biology Center.
122. **Low Concentration Xyloside Treatment Alters GAG Profile and Morphology in Neural Cells.** C. Mencia, C. Agbaegbu, H. Katagiri, H. Geller; Developmental Neurobiology Group.
123. **Cathepsin L as a Synuclease: Degradation Mechanisms of α -Synuclein Amyloid Fibrils.** G.A. Dominah, R.P. McGlinchey, J.C. Lee; Laboratory of Molecular Biophysics.
124. **Genome-wide identification of H2A.Z-interacting proteins by bPPI-seq.** W. Ku, Y. Zhang, K. Cui, W. Jin, Q. Tang, W. Lv, B. Ni, K. Zhao; Laboratory of Epigenome Biology.
125. **Ibrutinib Acts As A Dual B-Cell Receptor And Toll-Like Receptor Inhibitor In Chronic Lymphocytic Leukemia.** E. Dadashian, S.E.M. Herman, E. McAuley, D. Wong, C. Sun, D. Liu, A. Wiestner; Laboratory of Lymphoid Malignancies.
126. **Sirolimus-Induced Preservation Of Bone Marrow Hematopoietic Stem And Progenitor Cells In Immune And Nonimmune Mediated Mouse Models Of Bone Marrow Failure.** M.K. Hollinger; Cell Biology Section.
127. **A Membrane Trafficking Screen To Identify Clathrin-Independent Endocytosis Machinery.** D. Dutta*, J. Wayt*, J. Donaldson; Cell Biology and Physiology Center.

128. **Modular LIM domains Mediate Actin Cytoskeletal Strain Recognition.** L. Axiotakis, R. Cail, G. Alushin; Cell Biology and Physiology Center.
129. **Disruption in Arterial Branching Leads to Defective Hair Follicle Development.** J.Y. Choi, W. Li, Y.S. Mukouyama; Laboratory of Stem Cell and Neuro-Vascular Biology.
130. **Tissue-Resident Macrophage Progenitors Differentiate into Pericytes through TGF- β Signaling in Developing Skin Vasculature.** T. Yamazaki¹, A. Nalbandian¹, Y. Uchida¹, W. Li¹, T.D. Arnold², Y. Kubota³, M. Ema⁴, Y. Mukouyama¹; ¹Laboratory of Stem Cell and Neuro-Vascular Biology, NHLBI, ²Department of Pediatrics, Physiology, and Program in Neuroscience, University of California, San Francisco, ³Center for Integrated Medical Research, School of Medicine, Keio University, ⁴Department of Stem Cells and Human Disease Models Research Center for Animal Life Science, Shiga University of Medical Science.
131. **Amoeba Host Model for Evaluation of *Mycobacterium abscessus* Clinical Isolates Virulence.** J.L. Da Silva, J. Nguyen, K. Fennelly, A. Zelazny, K. Olivier; Microbiology Service.
132. **KMT2D Controls Regulatory T Cell Development By Modulating Histone H3 Lysine K4 Methylation At Foxp3 Locus.** K. Placek, K. Cui, G. Hu, K. Zhao; Systems Biology Center.
134. **Rapamycin Augments Regulatory T cell Expansion through Interaction with CD3-CD45R- Cells.** W. Sun, K. Keyvanfar, Z. Lin, J. Chen, X. Feng, N. Young; Hematology Branch.
135. **Microfluidic Models of the Microvasculature for Red Blood Cell Metrology in Sickle Cell Disease.** J. Betz^{1,2}, D. LaVan¹, H. Ackerman²; ¹Sickle Cell Branch, NHLBI, ²NIST.
136. **α M β 2 Integrins Mediate The Formation Of A Focal Adhesion-Like Cytoskeleton And Signaling Platform During Phagocytosis.** V. Jaumouill , T.-L. Liu, E. Betzig, C.M. Waterman; Laboratory of Cell and Tissue Morphodynamics.
137. **Mechanism of LCAT Activation by Compound A.** L. Freeman, S. Demosky, M. Konaklieva, R. Kuskovsky, S. Gordon, A. Ossoli, R. Shamburek, A. Aponte, M. Gucek, J. Tesmer, R. Levine, A. Remaley; Lipoprotein Metabolism Section.
138. **Molecular Mechanisms Underlying Arterio-Venous Alignment In The Skin.** Y. Uchida, Y. Mukouyama; Laboratory of Stem Cell and Neuro-Vascular Biology.
139. **Erk Regulation Of Actin Capping And Bundling By Eps8 Promotes Cortex Tension And Leader Bleb-Based Migration.** J.S. Logue^{1,2}, A.X. Cartagena-Rivera², M.A. Baird¹, M.W. Davidson³, R.S. Chadwick², C.M. Waterman¹; ¹Laboratory of Cell and Tissue Morphodynamics, NHLBI, ²NIDCD, ³National High Magnetic Field Laboratory and Department of Biological Science, The Florida State University.
140. **Lower Technology Fluency is Not A Barrier to User Adoption of a Mobile Health (mHealth) Wrist-worn Physical Activity (PA) Monitor System: Observations from the Washington, D.C. Cardiovascular (CV) Health and Needs Assessment.** L.R. Yingling¹, V. Mitchell¹, C. Ayers², M. Peters-Lawrence³, G.R. Wallen⁴, A.T. Brooks⁴, J. Adu-Brimpong, S. Thomas¹, J.S. Henry⁵, J. Saygbe¹, D.M. Sampson⁶, A.A. Johnson⁷, A.P. Graham⁷, L.A. Graham⁷, K.L. Wiley⁸, T.M. Powell-Wiley¹; ¹Social Determinants of Cardiovascular Risk and Obesity, NHLBI, ²Donald W. Reynolds Cardiovascular Clinical Research Center at the University of Texas Southwestern Medical Center, Dallas, TX, ³Clinical Center, NIH; ⁴Office of the Clinical Director, NHLBI; ⁵Office of the National Coordinator for Health Information Technology, Washington, D.C.; ⁶Office of Behavioral and Social Sciences Research, Office of the Director, NIH; ⁷College of Nursing and Allied Health Sciences, Howard University, Washington, D.C.; ⁸Division of Genomic Medicine, NHGRI.
141. **Effects of Ion and Local Lipid Composition on the Physicochemical Properties of PIP₂-Monolayers.** K. Han, R.M. Venable, R.W. Pastor; Laboratory of Computational Biology.
142. **Is Endothelial Alpha-Globin Predominantly Expressed By The Hba-A1 Or Hba-A2 Locus In Mice?** L. Pecker, J. Butcher, G. Isakson, H. Ackerman; Sickle Cell Disease Branch.
143. **A New Strategy for Fetal Hemoglobin Induction with Lentiviral-Mediated Knockdown of *POGZ*; evidence in a human erythroleukemia cell line.** B. Gudmundsdottir, N. Uchida, J.F. Tisdale; Molecular and Clinical Hematology Branch.

144. **Myosin 18A Localizes With Myosin II At Cell: Cell Junctions In Epithelial Cells And Tissues.** K. Remmert¹, J. Beach¹, N. Porat-Shliom², R. Weigert², J. Hammer¹; ¹Laboratory of Cell Biology, NHLBI, ²Intracellular Membrane Trafficking Unit; Oral and Pharyngeal Cancer Branch; NIDCR.
145. **Receptor Associated Protein (RAP) Abrogates House Dust Mite-induced Experimental Asthma by Attenuating Dendritic Cell Function.** A. Mishra¹, P.K. Dagur², J.P. McCoy², K.J. Keeran³, G.Z. Nugent³, K.R. Jeffries³, X. Qu⁴, Z.X. Yu⁴, S.J. Levine¹; ¹Laboratory of Asthma and Lung Inflammation, ²Flow Cytometry Core Facility, ³Animal Surgery and Resources Core Facility, ⁴Pathology Core Facility.
146. **A New Energy Potential for Solvent Paramagnetic Relaxation Enhancements (sPRE) in XPLOR-NIH.** H. Kooshapur¹, N. Tjandra¹, C. Schwieters²; ¹Laboratory of Molecular Biophysics, NHLBI, ²Division of Computational Bioscience, Center for Information Technology, NIH.
147. **Biophysical Assays To Detect The Interaction Between Alpha Globin And Enos.** D. Ma, H. Ackerman; Sick Cell Branch.
148. **Recognition Of A Bacterial Alarmone Through Long-Distance Association Of Two Riboswitch Domains.** C.P. Jones, A.R. Ferré-D'Amaré; Laboratory of Ribonucleoprotein Biochemistry.
149. **A New Mechanism of Selective mtDNA Inheritance Regulated by TFAM.** Z. Chen, H. Xu; Laboratory of Molecular Genetics.
150. **Drosophila Clueless is Involved in Parkin-Dependent Mitophagy by Promoting VCP-Mediated Marf Degradation.** Z.H. Wang, C. Clark, E. Geisbrecht; Kansas State University and University of Missouri-Kansas City.
151. **Improvement In Psoriasis Skin Disease Severity Is Associated With Reduction Of Coronary Plaque Burden.** J.B. Lerman, A.A. Joshi, J. Rodante, T. Aberra, M.T. Kabbany, T. Salahuddin, Q. Ng, J. Silverman, M.Y. Chen, D.A. Bluemke, N.N. Mehta; Section of Inflammation and Cardiometabolic Diseases.
152. **Conformational Heterogeneity of Inactive Bax?** A. Barnes, P. Shukla, J.L. Baber, M.-P. Strub, N. Tjandra; Laboratory of Molecular Biophysics.
153. **Maturation of Induced Pluripotent Stem Cell Derived Cardiomyocytes via Co-Culture with Supporting Cells of the Developing Heart.** I.H. Garcia-Pak¹, W. Li¹, H. Uosaki², E. Tampakakis², J. Zou³, Y. Lin³, C. Kwon², Y. Mukoyama¹; ¹Laboratory of Stem Cell and Neuro-Vascular Biology, NHLBI, ²Division of Cardiology, The Johns Hopkins University School of Medicine, ³iPSC Core Facility, NHLBI.
154. **Generating HERV-E Envelope Antigen-Specific CD8+ T Cells Utilizing Overlapping Peptide Libraries To Identify Tcrs For The Immunotherapy Of Metastatic Clear Cell Renal Cell Carcinoma.** S. Doh, E. Cherkasova, R.W. Childs; Laboratory of Transplantation Immunotherapy.
155. **Examination of Antigen-Induced Endocytic Structures in B Lymphocytes by Fluorescence Microscopy.** T.M. Davenport, A. Dickey, K. Sochacki, J. Taraska; Laboratory of Molecular Biophysics.
156. **Optimization of Detection of Chondroitin Sulfate on Western Blots with Antibody CS-56.** H. Nagase, Y. Katagiri, C.A. Mencia, C. Agbaegbu, H.M. Geller; Developmental Neurobiology Group.
157. **Improving Free Energy Calculations With Non-Boltzmann Bennett Reweighing Using QM And MM.** F.C. Pickard IV, G. Koenig, B.R. Brooks; Laboratory of Computational Biology.
158. **The Mitochondrial Outer Membrane Protein MDI Promotes Local Protein Synthesis And mtDNA Replication.** Y. Zhang, Y. Chen, M. Gucek, H. Xu; Laboratory of Molecular Genetics.

Abstracts in Order of First Author

Self-reported Depression and Anxiety Associate with Vascular Inflammation and Coronary Heart Disease Beyond Traditional Cardiovascular Risk Factors in Psoriasis. T.M. Aberra, A.A. Joshi, J.B. Lerman, J.A. Rodante, J.I. Silverman, T.Z. Aridi, M.Y. Chen, M.P. Playford, N.N. Mehta; Section of Inflammation and Cardiometabolic Diseases.

Psoriasis is a chronic inflammatory skin disease associated with increased aortic vascular inflammation, measured by 18-fluorodeoxyglucose positron emission tomography/computed tomography (FDG PET/CT), and an increased risk of myocardial infarction. Patients with psoriasis are also more likely to suffer from comorbid depression and anxiety. Whether these comorbidities accelerate the development of subclinical atherosclerosis in psoriasis is unknown.

Patients were selected from within a larger psoriasis cohort. Those who reported a history of depression and/or anxiety (n=40) on survey were matched by age and gender to patients who reported no history of psychiatric illness (n=40). Target-to-background ratio from FDG PET/CT was used to assess aortic vascular inflammation and coronary CT angiography scans were analyzed to determine coronary plaque burden. Multivariable linear regression was performed to understand the effect of self-reported depression or anxiety on vascular inflammation and coronary plaque burden after adjustment for Framingham risk (standardized β reported).

In unadjusted analyses, vascular inflammation and coronary plaque burden were significantly increased in patients with self-reported depression and/or anxiety as compared to patients with psoriasis alone. After adjustment for Framingham Risk Score, vascular inflammation ($\beta=0.23$, $p=0.026$), total coronary plaque burden ($\beta=0.14$, $p=0.047$), and non-calcified coronary plaque burden ($\beta=0.14$, $p=0.046$) were associated with self-reported depression and/or anxiety.

Self-reported depression and anxiety in psoriasis are associated with increased vascular inflammation and coronary plaque burden, suggesting that psychiatric comorbidities may play an important role in promoting subclinical atherosclerosis beyond traditional cardiovascular risk factors in psoriasis.

Functional Regulation of TIP150-Cortex Interaction with cortactin Mediating Directional Cell Migration. G. Adams, X. Peng, D. Cao, Z. Wang, X. Yao, (C. Waterman); Laboratory of Cell Biology and Tissue Morphodynamics.

Cell migration is fundamental and an essential physiological process for development, morphogenesis, tissue repair, and tumor metastasis. Physical targeting and capturing of microtubules (MTs) plus end with actin cytoskeleton at special cortical regions are necessary for cell migration. Evidence indicates that cell motility is a vital facet of metastatic cancer which is the primary cause of death in cancer patients. Understanding the fact that metastatic cancer accounts for most of cancer-associated deaths, the past several years have increasingly geared focus to secondary tumor formation, or metastasis. Furthermore, cell migration is orchestrated by dynamic interaction of microtubules with plasma membrane cortex. However, the regulatory mechanisms underlying cortical actin cytoskeleton and microtubule dynamics is less characterized.

Cell migration is a highly polarized process in which rapidly changing activities are spatially segregated, principally at the cell front and rear. Cytoskeletal networks comprised of actin and microtubules are required for the coordination of efficient cell migration. Hence, cytoskeletal elements must be cooperatively regulated for the cell to fulfil complex cellular functions, as widespread as cell migration.

TIP150 is a 150 kDa novel characteristic microtubule +TIP with labelling pattern appearing as comet like structures throughout the cell cycle, dependent on End Binding Protein (EB)-1. Expression and modification of +TIPs directly impacts microtubule dynamics and organization, linking them to the cell cortex and to interfaces such as kinetochores and therefore, contribute to mitosis and cell migration which are arbitrated by cytoskeletal components. The functional dynamics of microtubules and actin interactions to mediate cell migration, and together with the molecular interaction of cortactin and TIP150, potentially regulates cell migration. The proposed study to elucidate the functional and molecular role of TIP150 in migrating cells, will lead to the development of novel therapeutic applications, especially in clinical treatment of cancer metastasis.

Virtual Neighborhood-Built-Environment Quality Audits Provide Insights into Neighborhood Walkability: The Washington, DC Cardiovascular Health and Needs Assessment. J. Adu-Brimpong¹, N. Coffey², C. Ayers³, D. Berrigan⁴, L. Yingling¹, S. L. Thomas¹, V. Mitchell¹, T. M. Powell-Wiley¹; ¹Social Determinants of Cardiovascular Risk and Obesity. ²Global and Community Health Department at George Mason University School of Public Health. ³Donald W. Reynolds Cardiovascular Clinical Research Center at University of Texas Southwestern Medical Center. ⁴Division of Cancer Control and Population Sciences at National Cancer Institute.

Little is known about the association between walkability and neighborhood built environment quality measured using novel virtual neighborhood audit methods. This study aims to explore the link between neighborhood walkability measured by Walk Score®, an online, publicly available, validated tool, and neighborhood-built-environment quality measured using virtual audits. Walk scores for 36 home addresses from study participants in a community-based participatory research (CBPR) project in Washington, D.C. (NCT01927783), were retrieved via WalkScore.com. Google Maps Street View imagery and the Active Neighborhood Checklist (the Checklist), consisting of five main sections (89 questions total), were used for virtual audits. Twelve street segments, approximately 4-blocks, adjacent to participants' home addresses were assessed for 1) Land-Use Type, 2) Availability of Public Transportation, 3) Street Characteristics, 4) Quality of Environment and 5) Sidewalks/Related Features for Walking and Biking. Scores ranged from 0-2 points per question (maximum of 87 points per segment) based on their hypothesized influence on physical activity engagement. Scores from the Checklist sections were consolidated and an overall built environment quality score computed for each participant. Pearson correlations were calculated for a) Walk Scores® and overall scores, b) Walk Scores® and section scores. Maximum overall possible score is 1044 points; participants' scores ranged 333-472 with mean(sd) of 384.2(34.3). Participants' Walk Scores® ranged 37-91 with mean(sd) of 61.9(13.8) (maximum Walk Score® is 100 points). Significant

positive correlations were found between overall audit scores and Walk Scores® ($r = .61, p = .001$). Three of the five sections, Land-Use Type ($r = .46, p = .01$), Quality of Environment ($r = .45, p = .01$) and Sidewalks ($r = .55, p = .01$), showed significant correlations with Walk Scores®. Data from this CBPR project demonstrate that neighborhood built environment quality as measured by a virtual audit is associated with neighborhood walkability. Virtual audits may help define the relationship between neighborhood quality and cardiovascular health for developing targeted community interventions where health is most impacted by built environment resources.

Correlation of clinical and mutational markers of disease progression in chronic lymphocytic leukemia treated with ibrutinib. I. Ahn¹, A. Albitar², C. Underbayev³, S. Herman³, S. Soto³, X. Tian⁴, M. Stetler-Stevenson⁵, I. Maric⁶, M. Farooqui³, M. Albitar², A. Wiestner³; ¹Medical Oncology Service, NCI, ²NeoGenomics Laboratories, Irvine, CA, ³Hematology Branch, ⁴Office of Biostatistics Research, ⁵Laboratory of Pathology, Center for Cancer Research, NCI, ⁶Department of Laboratory Medicine, Clinical Center, NIH.

Ibrutinib covalently binds to Bruton's tyrosine kinase, inhibits B-cell receptor signaling, and is active in chronic lymphocytic leukemia (CLL). Progressive disease (PD) on ibrutinib has been reported due to histologic transformation or mutations of *BTk* or *PLCG2*. Here we report integrated analyses of clinical and mutational characteristics of CLL pts who progressed on ibrutinib (PD group).

Under a phase II investigator-initiated trial (ClinicalTrials.gov, NCT01500733) 86 CLL pts with *TP53* aberration (deletion 17p by FISH or *TP53* mutation) or \geq age 65 were treated with ibrutinib 420mg daily. Samples from the PD group were tested for mutations of *BTk* and *PLCG2* by a high-sensitivity assay utilizing branched and locked nucleic acids. In pts with mutations at PD, stored samples from earlier time-points were also sequenced.

13 (15.5%) of 84 pts progressed at a median follow up of 24 months (range 0.4-40). 3 of 4 early PDs (≤ 12 months) were due to histologic transformation, while 8 of 9 late PDs (median 34.9 months) were due to CLL. PFS was inferior in subgroups with *TP53* aberration, unmutated IGHV, advanced Rai stage (III/IV), high β -2 microglobulin ($>4\text{mg/L}$) and relapsed/refractory disease (log-rank $p < 0.05$ for all tests). 8 pts with progressive CLL were subsequently treated with small molecules targeting PI3K or Bcl-2, and 6 were alive to date (longest follow-up 15 months). Two types of non-synonymous mutations at *BTk* exon 15 (C481S, C481R) and five types of non-synonymous mutations at *PLCG2* exon 19, 20 and 24 (R665W, P664S, P664L, S707Y, L845F) were identified in 8 out of 9 pts having progressive CLL. No mutation was found in pts with transformation and in one pt with progressive CLL. Concomitant *BTk* and *PLCG2* mutations were found in 5 out of 8 pts (62.5%). Mutations pre-dating clinical PD were identified in stored samples from 6 pts as early as 13 months before progression (median 5.3 months [1.8-13.0]). The median time to the first detection of mutation was 23.1 months (range 5.4-34.7). Mutational complexity increased over time as reflected by increasing types of mutations ($n=3$) and allele frequencies ($n=3$) at later time-points. In the PD group, best responses to ibrutinib included no response ($n=2$), stable disease ($n=3$), partial response ($n=6$), and complete response ($n=2$).

Both PD and non-PD groups showed equivalent depth of response in peripheral blood (PB) and bone marrow during treatment ($p > 0.05$). At progression, tumor burden increased by 2 to 32-fold from nadir based on PB flow cytometry.

Most pts with progressive CLL on ibrutinib carry *BTk* and/or *PLCG2* mutations. Concurrent mutations of *BTk* and *PLCG2* are common at progression, and either or both of these mutations can be acquired many months before clinical progression. In cases with detectable mutations but without clinical progression, pts can benefit from prolonged treatment with ibrutinib until clinical progression occurs. Upon clinical progression with CLL, pts can still show responses to alternative targeted agents.

Improved Differentiation of Mouse Embryonic Stem Cells into Purkinje Neurons. C. J. Alexander, J. A. Hammer; Laboratory of Cell Biology.

While the use of embryonic mixed primary cerebellar cultures has proven valuable for dissecting structure: function relationships in Purkinje Neurons (PNs), this technique is technically challenging and often yields few cells. Recently, mouse embryonic stem cells (mESCs) have been successfully differentiated into PNs, although the available methods are very challenging as well. The focus of this study was to simplify the differentiation of mESCs into PNs. Using specific extrinsic factors, we successfully differentiated mESCs into PNs without the use of a postnatal feeder-layer. The morphology of mESC-derived PNs is indistinguishable from PNs grown in primary culture in terms of gross morphology, spine length and spine density. Furthermore, mESC-derived PNs express Calbindin D28K, IP3R1, PLC β 4 and myosin IIB-B2, all of which are PN-specific markers. Finally, using poly-L-ornithine, poly-L-lysine and gelatin as the extra cellular matrix allowed us to grow mESC-derived PNs in monolayers, which is crucial for live cell imaging. Current efforts are focused on expressing exogenous DNAs specifically in mESC-derived PNs using the novel PN-specific promoter. If this is successful, we will then attempt gene editing in stem cells using CRISPR, followed by complementation using exogenous DNA. Together, this technology would provide a scalable, high-throughput method for dissecting specific molecular mechanisms in PNs, especially when a KO mouse is not available.

High Throughput Single-cell RNA Sequencing of iPSC-Derived Hematopoietic Stem Cells: One Drop Closer to Treatments of Inherited Bone Marrow Failure Syndromes. L. Alvarado, G. Chen, I. Asokan, K. Johnson, JP. Ruiz, Y. Wakabayashi, J. Zhu, J. Zhou, M. Boehm, A. Laroche; Laboratory of Regenerative Therapies for Inherited Blood Disorders.

Inherited bone marrow failure syndromes (IBMFS) are a diverse set of genetic disorders characterized by pancytopenia and associated life-threatening hematologic complications due to paucity of hematopoietic stem cells (HSCs). Allogeneic HSC transplantation and gene therapy approaches offer a potential cure but limited availability of matched donors and the near absence of autologous HSCs for genetic correction have restricted these treatment options. Induced pluripotent stem cell (iPSC)-based approaches are a tractable alternative for these patients because of their potential to provide an unlimited source of autologous patient-specific HSCs after hematopoietic differentiation of genetically corrected iPSCs. Protocols to derive HSCs

from iPSCs have generated phenotypically-defined HSCs, but they have failed to generate functionally transplantable HSCs. We hypothesized that current iPSC differentiation protocols are unable to recapitulate the normal ontogenic processes resulting in the *ex vivo* generation of cells with various deregulated pathways preventing sustained multilineage reconstitution after transplantation. To address this hypothesis, we have developed a unique monolayer-based, xeno-free protocol that facilitates the scale-up of hematopoietic differentiation from human iPSCs. We compared single-cell transcriptomes of phenotypically-defined *ex vivo*-generated HSCs to their matched primary donor-derived HSCs using Drop-Seq, a novel high-throughput RNA sequencing approach that captures single cells along with sets of uniquely barcoded primer beads in nanoliter droplets. We present preliminary differential gene expression analyses of *bona fide* and iPSC-derived HSCs from healthy donors. These data will facilitate the emergence of transplantable HSCs from iPSCs *in vitro* to exploit their clinical potential in the treatment of IBMFS and other disorders affecting blood-forming stem cells.

Regulatory role of MYB on Fetal Hemoglobin Expression. N. Angelis, X. Wang, L. Mendelsohn, S. L. Thein; Sickie Cell Branch.

Due to the hemoglobin switch, adults have residual levels (<1% total) of fetal hemoglobin (HbF, $\alpha_2\gamma_2$) after 2 years of age. While elevated HbF has no consequences in healthy adults, increased HbF levels clinically benefit patients with β -hemoglobinopathies (sickle cell disease and β -thalassemia). MYB, an important transcription factor in hematopoiesis, has recently been implicated in the control of HbF in adult life; low MYB levels in erythroid progenitor cells are associated with high HbF expression. We have used a human immortalized erythroid cell line, Human Umbilical cord blood-Derived Erythroid Progenitor -2 (HUDEP-2), to investigate HbF expression in a low MYB and absent MYB environment, by knocking down and knocking out MYB respectively. HUDEP-2 cells mimic adult erythropoiesis producing functional adult hemoglobin with expression of erythroid-specific markers and production of enucleated red blood cells following induction of differentiation. MYB was knocked-down using 5 different shRNA constructs in a lentiviral expression system, and knocked-out (KO) using genome editing (Clustered Regularly-Interspaced Short Palindromic Repeats/Cas9 (CRISPR/Cas9)). An LRF-KO HUDEP-2 cell line that expressed elevated HbF levels was used as positive control. Effects of the shRNA constructs on MYB expression will be validated in another human erythroleukemia K562 cell line that has abundant MYB expression, prior to HUDEP-2 transduction. Fetal hemoglobin expression will be monitored by quantitating F cells with FACS analysis and by quantitating fetal hemoglobin by HPLC. Our data should validate if reducing MYB levels lead to increased HbF expression, and if so, it could provide an alternative approach for increasing HbF in the treatment of β -hemoglobinopathies.

Mechanism of Activation of the TRPV1 Channel by a Double-Knot Tarantula Toxin. C. Anselmi¹, C. Bae^{2,3}, A. Jara-Oseguera², J. I. Kim³, K. J. Swartz², J. D. Faraldo-Gómez¹; ¹Theoretical Molecular Biophysics Section NHLBI, ²NINDS, ³Gwangju Institute of Science and Technology, Republic of Korea.

The double-knot toxin DkTx from the Chinese bird spider venom activates the TRPV1 cation channel upon formation of a high-affinity complex. DkTx belongs to a large group of so-called inhibitor cysteine-knot toxins, which consist of two cysteine-rich lobes (K1 and K2) interconnected by a polypeptide linker. Functional studies have indicated that both lobes in DkTx concurrently bind to TRPV1, resulting in an extremely high avidity for its channel target. The recently determined cryo-EM structure of the TRPV1-DkTx complex has provided further insights into this interaction (PDB entry 3J5Q). The structure shows two DkTx molecules bound atop the tetrameric channel, with the two lobes in each toxin molecule pinching the inner pore helices. However, owing to the limited resolution of the cryo-EM map (3.8 Å) and the four-fold symmetrization of the data, the binding configuration of the K1 and K2 lobes is unknown, as is the detailed chemical structure of the channel-toxin interface. Here, we solve the NMR structure of the toxin in solution and we use ROSETTA to obtain a refined atomic-resolution structure of the TRPV1-DkTx complex, on the basis of 4-fold and 2-fold symmetrized cryo-EM maps and existing structural models. Molecular dynamics simulations based on the optimized structures and mutagenesis experiments are carried out to characterize the interface between

DkTx and TRPV1 and clarify the mechanism of activation of the channel by the toxin. Our results show that DkTx binding alters the interaction network of a number of residues, located on the extracellular side of the channel in between helices S5, P and S6, whose mutations are known to disrupt the channel activation by DkTx. We propose that these conformational changes are triggered by the toxin binding at the protein/membrane interface and are key for TRPV1 activation.

Modular LIM domains Mediate Actin Cytoskeletal Strain Recognition. L. Axiotakis, R. Cail, G. Alushin; Cell Biology and Physiology Center.

The ability of cells to probe and respond to the mechanical properties of their microenvironments (“mechanosense”) is critical for fundamental cellular processes including division, migration, differentiation and survival. The contractile actomyosin cytoskeleton connects to the extracellular matrix through focal adhesions (FAs), forming a complex and dynamic protein interaction network implicated as a central player in mechanosensation. Components of this network containing LIM (LIN-11, ISI1, MEC-3) domains have been shown to modulate their relative abundance at FAs in response to myosin contractility, hinting at a role for LIM proteins as “mechanosensors.” One well-studied example is zyxin, whose C-terminal LIM domains have been shown to be necessary and sufficient for localization to sites of mechanical damage in actin stress fibers (SFs), where it recruits repair factors using an N-terminal motif. This mechanism has been linked to maintaining cytoskeletal integrity in response to spontaneous SF ruptures (“strain sites”) due to intrinsic contractility in stiff environments, as well as mediating global SF rearrangement and reinforcement in response to uniaxial cyclic stretch. This lead us to hypothesize that other LIM domains would confer mechanosensitive SF localization in diverse protein contexts. We have thus undertaken a live-cell imaging screen for strain-site localization of 30 GFP-tagged LIM proteins which had been identified as FA components. Of 16 constructs which are successfully expressed and associate with the actin cytoskele-

ton, 6 (40%) demonstrate strain-site localization, consistent with a more general role for LIM domains as mechanosensors. In addition, we see an overlapping pattern of LIM protein association with remodeled, reinforced SFs upon uniaxial substrate elongation. While our work supports widespread mechanosensory activity in LIM domains, underlying molecular mechanisms remain elusive. In future work, we will use mass-spectrometry based proteomics in stretched cells to identify upstream effectors in mechanosensitive LIM domain cytoskeletal recognition.

Pulsatile Contractions are an Intrinsic Property of Myosin-IIa in Adherent Cells. M.A. Baird, R. S. Fischer, A. Wang, R.S. Adelstein, C.M. Waterman; Cell Biology and Physiology Center.

Non-muscle myosin-IIa is vital to many cellular and developmental processes including cell adhesion, migration, cytokinesis, and tissue morphogenesis. Myosin-II activity can be observed in steady contraction events such as during cytokinesis, but may also exhibit pulsatile contraction in other contexts. For example, during embryogenesis in *Drosophila*, myosin-II is recruited to the cell cortex to initiate pulsatile contractions, which directly correlate with cell constriction thereby inducing large structural changes in tissue. Here, we find that myosin-II pulses also occur in a variety of adherent cells in culture, suggesting that this behavior is an intrinsic property of the actomyosin cortex, and is not unique to cells in a tissue. Each pulsatile event displays a consistent duration, while intervals between contraction pulses can vary. Utilizing a photoactivatable myosin-IIa probe, we show that these pulses are the result of local recruitment of new myosin II mini-filaments to sites of contraction pulses, and F-actin is locally concentrated concomitantly with the contraction pulse. Small molecule perturbations of myosin II activators demonstrate that myosin II phosphorylation is required for the pulsatile behavior. The contraction pulses occur independently of integrin activation. Using gadolinium inhibition we find that the pulsatile contractions require the activity of stretch-activated calcium channels. Additionally, we show that this pulsatile behavior is unique to myosin IIA and not IIB. Utilizing myosin-IIA / IIB chimeras, we show that the myosin IIA motor domain is required for the pulsatile behavior. Thus, the contractile pulses are a result of the kinetics of the myosin-IIa motor, whereas the myosin-IIB motor is insufficient to induce this dynamic behavior. We conclude that this pulsatile contraction is an inherent and intrinsic property of myosin-IIA / F-actin networks in adherent cells independent of their assembly into organized tissues.

Identification and Characterization of Novel Members of the Nonsense-Mediated mRNA Decay Pathway. T.D. Baird, J.R. Hogg; Laboratory of Ribonucleoprotein Biochemistry.

Eukaryotic mRNA decay is a highly dynamic process central to the regulation of gene expression and maintenance of cellular homeostasis. A major contributor to this regulation is the nonsense-mediated mRNA decay (NMD) pathway, which degrades diverse mRNAs in all eukaryotes. In addition to serving as a surveillance monitor for aberrant transcripts containing premature termination codons (PTCs) resulting from genetic mutations or errors during mRNA biogenesis, the NMD pathway degrades 5-10% of non-aberrant human mRNAs. Much of our understanding of the core regulation of the NMD pathway was derived from genetic screens performed in yeast and nematodes. To better understand the activities and regulation of the human

NMD pathway, our collaborators (Inglese, Buehler, and Martin groups, NCATS) conducted a genome-wide screen in a human cell line using a siRNA library targeting over 21,000 genes. From this screen, we identified two putative novel members of the NMD pathway that, when depleted, led to increased abundance of canonical NMD targets. RNAseq analysis of cells depleted of one of these factors revealed a strong correlation with the mRNA profile of cells lacking the essential NMD factor UPF1. Furthermore, *co*-immunoprecipitation data indicated these novel members interact with UPF3B and eIF4AIII, core components of the NMD machinery. Future studies will focus on the nature of this biochemical interaction and ultimately how these proteins dictate gene expression.

Structural Insight into Interaction of Fibrin and Very Low Density Lipoprotein Receptor. K. Banerjee¹, S. Yakovlev², L. Medved², N. Tjandra¹; ¹Laboratory of Structural Biophysics, ²University of Maryland School of Medicine.

Fibrin, which is formed by thrombin-mediated cleavage of fibrinogen, is abundantly present in blood. Furthermore, recent study has shown that the β N domains of fibrin interact with Very Low Density Lipoprotein Receptor (VLDLR) of endothelial cells. VLDLR is one of the receptor proteins in the low-density lipoprotein receptor family expressed in various tissues and more importantly in vascular endothelium. VLDLR-fibrin interaction promotes transendothelial migration of leukocytes and triggers inflammation. We are interested in understanding the fibrin-VLDLR interaction and its role in inflammation related atherosclerosis. However, so far there is no structural information of VLDLR and neither of fibrin β N (β N domain of fibrin). The highest affinity of the VLDLR and fibrin β N is when three-domain repeats of VLDLR are present. Solution NMR studies have been done to attain the structural details of fibrin β N, VLDLR, and VLDLR-fibrin β N complex. Preliminary structural studies have shown fibrin β N domain to be unstructured. The three domain repeats of VLDLR comprise of 120 residues including 18 cysteines forming disulfide bonds and thus preserving the functional integrity of VLDLR. Almost all of the cysteines are found to form disulfide bonds based on the chemical shifts assignment. Each of the VLDLR domains bind to Ca²⁺ and it is most stable in the Ca²⁺ bound form. We have mapped the binding sites of fibrin β N on VLDLR. The binding sites seem to coincide with the calcium binding regions, implying Ca²⁺ binding is very crucial for fibrin β N and VLDLR interaction. Comparison of backbone relaxation dynamics of the complex is done with free VLDLR to understand the mode of binding of fibrin β N to different domains of VLDLR. Combination of complete structural information and dynamics of all the domains of VLDLR only and upon binding with fibrin β N would provide better understanding of the biological significance of VLDLR-fibrin interaction and provide a platform for designing better inhibitor of this interaction that can reduce inflammation.

Multiplex Cytokine Profiling as Monitor and Prognosis Tool in Sickle Cell Disease Progression to Crisis. E.A. Barbu, L. Mendelsohn, A. Ikeda, H. Ackerman, S.L. Thein; Sickle Cell Group.

Sickle cell disease (SCD) is a heritable blood disorder caused by a point mutation in the β -haemoglobin gene. Polymerization of the de-oxygenated HbS and formation of "sickled" cells trig-

gers a cascade of events leading to vasculopathy and inflammation, and ultimately systemic organ damage. Levels of various inflammatory markers and cytokines have been shown to be altered in SCD. Here, we investigated if the different phases of SCD have different inflammation profiles for specific cytokines, chemokines and adhesion factors. In a first preliminary experiment, we used a multiplex ELISA assay to determine titers for 21 cytokines, chemokines and adhesive factors in serum samples of 12 SCD patients at crisis and recovery, respectively, 2 patients at steady state, crisis and recovery, 3 patients at steady state only, and 6 healthy controls. Analytes were chosen for their inflammatory activity, as well as their known or potential contribution to SCD. Preliminary data showed that increased IL-1ra titers at crisis correlated with decreased SDF-1 α and vice-versa. Both these molecules have inflammatory and regulatory function and their relationship might be relevant in the context of SCD crisis environment. Other analytes (IL-4, IL-18, ICAM-1) had very mildly elevated titers over the healthy controls across the SCD cohort at crisis, with little or absent decline at recovery. For IL-6, high titers were found at crisis, but returned to healthy levels at recovery. Finally, no changes were found at either crisis or recovery for several analytes (IL-23, Eotaxin) compared with the healthy controls. Additionally, we correlated abnormally high crisis titers of several products including IL-6 and E-selectin, with highly divergent CBC test results. The relevance of additional inflammation molecules will be addressed in further studies.

Conformational Heterogeneity of Inactive Bax? A. Barnes, P. Shukla, J.L. Baber, M.-P. Strub, N. Tjandra; Laboratory of Molecular Biophysics.

The Bcl-2 family member Bax is known for its pro-apoptotic role within the mitochondrial pathway of apoptosis. Upon receipt of a death signal, monomeric Bax, which exists predominantly in the cytosol of healthy cells, undergoes a conformational change and translocates to the mitochondria where it oligomerizes and fragments the outer mitochondrial membrane to release cytochrome c and other apoptogenic factors, thereby, initiating the irreversible process of programmed cell death. However, despite extensive studies on Bax, the conformational selection mechanism responsible for its transition from an inactive to active form as well as the possible existence and regulatory role of the minor (or “invisible”) states of this protein with respect to its pro-apoptotic function remain uncertain. In this regards, there are divergent reports about the conformational ensemble of Bax prior to apoptosis. Recently, it has been suggested that inactive Bax exists in equilibrium with a lowly populated conformer that is different from its NMR structure. To resolve these discrepancies, we revisited the structural analysis of Bax in solution using techniques geared to probe for its invisible states, specifically, nuclear magnetic resonance (NMR) paramagnetic relaxation enhancement (PRE), NMR relaxation dispersion, and electron paramagnetic resonance (EPR) double electron-electron resonance (DEER). Based on our relaxation data, we observed unreported conformational fluctuations in Bax. We are combining our EPR and NMR data to describe the nature of these fluctuations and whether they are strictly attributable to local exchange or global domain reorientations of Bax that are crucial for its role in apoptosis.

Cholesterol crystals in atherogenesis and beyond? Y. Baumer, S. McCurdy, T. Weatherby-Carvalho, S. Halherr, P. Halbherr, N. Yamazaki, N. Mehta, W. Boisvert; Section of Inflammation and Cardiometabolic Diseases, University of Hawaii, John A Burns School of Medicine, Center for Cardiovascular Research.

Endothelial cells (EC) play a key role in atherosclerosis by providing a critical barrier between blood and vessel wall. Although the current paradigm is that low density lipoproteins (LDL) transcytose through the endothelium, whether EC metabolize the LDL directly, and how this would affect atherogenesis, is unclear. Thus, our objective was to assess whether EC process LDL under hyperlipidemic conditions and whether this contributes to atherogenesis. Our results indicate that EC not only robustly take up and process LDL, but that when overburdened with intracellular cholesterol, EC generate cholesterol crystals (CC) that involve autophagosomes and lysosomes and deposits them on the basolateral side of the EC. As cAMP plays an important role in EC function, and because EC treated with LDL have diminished cAMP levels, we employed forskolin/rolipram (F/R) as cAMP-enhancing agent to mitigate the effects of LDL on EC CC production. F/R was incorporated into liposomes designed to target inflamed endothelium, and when administered to apoE^{-/-} mice it significantly attenuated atherosclerosis in an eNOS-dependent manner compared to controls. In conclusion, hyperlipidemic conditions induce EC to actively process LDL and generate CC thereby promoting atherogenesis. The CC production and the resulting atherosclerosis can be inhibited by administering cAMP-enhancing agents.

Actin Dynamics and Non-Muscle Myosin 2 Monomer Availability Drive Localized Filament Expansion. J. R. Beach, K. Bruun, K. Remmert, D. Li, L. Shao, E. Betzig, J. A. Hammer; Cell Biology and Physiology Center.

The ability for non-muscle myosin 2 (NM2) to function is entirely dependent on its ability to rapidly and transiently assemble into filaments in precise subcellular locales to produce forces on the actin cytoskeleton. Despite decades of *in vitro* studies and cellular analyses that have produced a thorough understanding of both the domains of NM2 and the upstream regulators of NM2 required for bulk NM2 assembly and function, the mechanism by which individual NM2 monomers are recruited to precise spatio-temporal locales remains lacking. Here, we use a variety of super-resolution imaging approaches to analyze NM2 filament nucleation and growth in the lamella of primary fibroblasts. We describe a novel mechanism by which NM2 filaments rapidly proliferate in a nucleation-limited manner, whereby a filament from a single nucleation event splits to form two filaments. This process continues, eventually propagating dozens of filaments from a single nucleation. We label this process of **grouped expansion of myosin later than initial nucleation** as GrEMLIN. Multi-color imaging reveals GrEMLIN events frequently coincide with the movements of actin fibers or bundles and small-molecule inhibitors that stall actin dynamics inhibit this process, suggesting NM2 filaments bound to multiple actin bundles can be pulled apart to produce two daughter filaments, which can then grow and continue the process. Interestingly, inhibition of Rho kinase (ROCK), which is proposed to be responsible for NM2 assembly in central stress fibers, dramatically increases the rate of NM2 growth and GrEMLINing in the lamella. Con-

versely, myosin light chain kinase (MLCK) inhibition abrogates filament growth and GrEMLINing and rescues the effects of ROCK inhibition. We hypothesized that ROCK inhibition releases a surplus of sequestered NM2 monomer that is then utilized by MLCK, a model that would suggest NM2 monomer is limiting in the cell and RLC kinases are competing over it. To test this hypothesis, we artificially altered NM2 levels using over-expression or moderate shRNA. Increasing NM2 expression resulted in an increase in filament growth and GrEMLINing while reducing NM2 expression resulted in a decrease in filament growth and GrEMLINing. Together, our data suggest a nucleation-limited process in which a single nucleated-NM2 filament can rapidly expand to produce many filaments depending on actin dynamics and NM2 monomer availability, providing a mechanism for rapid assembly of many NM2 filaments with precise spatio-temporal control.

Microfluidic Models of the Microvasculature for Red Blood Cell Metrology in Sickle Cell Disease. J. Betz, H. Ackerman; Sickle Cell Branch. J. Betz, D. LaVan; NIST.

The microvasculature plays an important role in the pathology of sickle cell disease. As erythrocytes deliver oxygen while traversing the arterial and capillary networks, deoxygenated sickle hemoglobin begins to polymerize into fibers, causing changes in erythrocyte mechanical and adhesive properties that contribute to the obstruction of capillaries and postcapillary venules. Recently, microfluidic devices have been introduced that are capable of providing realistic shear rates but employ channels that are much larger than those of human capillaries. We used lithographic techniques to fabricate microfluidic devices from (poly)dimethylsiloxane that recapitulate the internal dimensions of human capillaries. The physical constraints imposed by these channels allow us to measure the dynamics of deformation and how quickly a red cell recovers its shape upon exit from a channel. In our devices, the inlet channel bifurcates five times, resulting in 32 capillaries that are 4 μm wide and 1 mm long. The channels are 2.5 μm tall, which orients the erythrocytes flat, keeping them within the focal plane of a microscope objective lens. We used high speed video microscopy to record and analyze the cells at 1% hematocrit. We measured the differences in erythrocyte elongation and circularity, as well as characterizing the time to return from the constrained shape in the capillaries to the more relaxed discoid shape, in sickle cell patients and healthy controls under both oxygenated and deoxygenated conditions. These measurements provide quantitative assessment of erythrocyte deformability and shape recovery that we will use to study vascular occlusion that occurs in sickle cell disease.

Apolipoprotein C-III Nanodiscs Studied by Site-Specific Tryptophan Fluorescence. C. Brisbois, J. Lee; Laboratory of Molecular Biophysics.

Over the past twenty years, there has been a large body of research on the so-called “membrane scaffold protein” (MSP) and its ability to remodel phospholipid membranes *in vitro* to produce “nanodiscs” which are structurally similar to high-density lipoprotein (HDL) particles. Though nanodiscs hold tremendous potential to enable future biotechnologies, little characterization of nanodiscs beyond the MSP model has been accomplished. Apolipoprotein C-III (ApoC-III) is a protein component of HDL and can remodel both unilamellar and mul-

tilamellar membranes composed of 1,2-dimyristoyl-*sn*-glycero-3-phosphocholine (DMPC) into nanodiscs through spontaneous self-assembly. They are monodisperse as characterized by dynamic light scattering and have a diameter of 13 ± 2 nm as visualized electron microscopy. Using three single-Trp-containing variants of ApoC-III, specific lipid-interactions in nanodiscs were studied at positions 42, 54, and 65. Steady-state fluorescence reveals distinct spectral differences for ApoC-III nanodiscs compared to micelle- or bilayer-bound states. Time-resolved fluorescence measurements show W54 experiencing the fastest anisotropy decay, which is similar to that observed for unilamellar vesicles. Using circular dichroism spectroscopy (CD), it was confirmed ApoC-III adopts a highly helical conformation upon formation of nanodiscs. CD temperature scans of preheated solutions of ApoC-III mutants and DMPC reveal differences in thermal stability of helix folding. Our data would suggest that nanodiscs produced from ApoC-III mutants are comparable near the transition temperature of DMPC at 28 °C but assembly is greatly altered at physiological temperatures. The W42 mutant is nearly indistinguishable from wild-type protein and may be the most important region for promoting lipid-protein interaction.

Circumventing trogocytosis through a complement based retargeting strategy in lymphoid malignancy. E.J. Carstens¹, M. Skarzynski¹, V. Butera¹, M.A. Lindorfer², I. Ahn¹, I. Maric¹, M. Stetler-Stevenson¹, E.M. Cook², B. Vire¹, J. Valdez¹, Susan Soto¹, M.Z.H. Farooqui¹, C. Rader^{3,4}, R.P. Taylor², A. Wiestner¹; ¹Laboratory of Lymphoid Malignancies, ²University of Virginia School of Medicine, ³Scipps Res. Inst., ⁴NCI

Treatment of lymphoid malignancies with anti-CD20 antibodies (mAbs) is frustrated by the loss of cell surface CD20 through trogocytosis, creating “escape variants” that are no longer sensitive to the anti-CD20 mAb. In patients with chronic lymphocytic leukemia (CLL) treated with the anti-CD20 mAb ofatumumab, we observed that these escape variants carried covalently bound C3d complement fragments. Therefore, we hypothesized that C3d is a neoantigen that could be exploited to re-target cells that have escaped from anti-CD20 mAb therapy.

We generated a human IgG1 mouse chimera mAb specific to C3d that is not competed by full length C3 in serum. We collected blood samples from CLL patients before (day 1) and 24 hours (day 2) after administration of ofatumumab and found that while the anti-C3d mAb did not bind CLL cells obtained pre-treatment but it killed day 2 CLL effectively through CDC, NK cell mediated ADCC, and phagocytosis.

We also tested the efficacy of the anti-C3d mAb in two mouse models. First, in NSG mice injected with PBMCs obtained from CLL patients on day 2 (containing the C3d opsonized CD20 escape variants), one injection of anti-C3d mAb effectively reduced tumor burden in both peripheral blood and spleen compared to isotype. Second, in SCID mice subcutaneously xenografted with HBL2 cells, a CD20+ mantle cell lymphoma line, the combination of the anti-C3d mAb with ofatumumab extended time to tumor development and prolonged overall survival compared to ofatumumab alone (median survival 48 days vs 34 days, respectively, $p < 0.001$).

Elucidating the Properties of Prenylated Ras Isoforms in Biological Membranes. M. Chakrabarti, R. W. Pastor; Laboratory of Computational Biology.

Ras is a central component of receptor tyrosine kinase-mediated signaling, modulating cellular growth, survival, proliferation, and differentiation. Humans express three proto-oncogenes encoding four Ras protein isoforms: H-Ras, N-Ras, K-Ras4A, and K-Ras4B, the latter two resulting from alternative splicing of the KRAS gene. Ras mutations are involved in nearly 30% of all cancers, and K-Ras is implicated in nearly 86% of these Ras-mediated cancers. As such, it represents an important therapeutic target. Ras proteins can be uniquely identified through their C-terminal hypervariable region (HVR). All Ras proteins have a farnesylated C-terminal cysteine that targets Ras to the plasma membrane. However, several Ras isoforms have additional upstream cysteine residues that can be reversibly palmitoylated, acting as secondary localization signals. Each Ras isoform is known to partition into spatially distinct nanoclusters on the plasma membrane, a behavior dependent on membrane lipid composition. Significantly, the partitioning behavior of K-Ras4A is currently unknown. In this study, we employ all-atom molecular dynamics simulations to elucidate the partitioning behavior and free energy profile of K-Ras4A HVR insertion into membranes comprised of DOPC, DPPC, and cholesterol, and having a mixed liquid-ordered/liquid-disordered composition. As a basis of comparison, the free energy of K-Ras4A insertion into a uniform hexadecane phase is being computed. Early results indicate that K-Ras4A insertion into hexadecane can occur through unrestrained dynamics, but that biasing potentials are needed for K-Ras4A insertion into biological membranes. Studies are currently underway to determine the membrane partitioning behavior of the prenylated K-Ras4A HVR.

RNA-seq Reveals Markers for the Two Major Cell Types in the Mouse Renal Collecting Duct. L.H. Chen, J.W. Lee, C.L. Chou, S.M. Wall, D. Brown, M.A. Knepper; Epithelial Systems Biology Laboratory.

The renal collecting duct contains two major cell types, principal cells and intercalated cells, which bear different molecular signatures and regulate sodium/water and acid/base excretion, respectively. To better understand these cells, a reliable, high-yield isolation technique and a systematic transcriptomic profiling of these cells is needed. Here we show that FACS with cell-type specific surface markers enables direct isolation of the two major cell types. Initially, we used transgenic mice that express GFP-driven by the *Alp6v1b1* promoter to label intercalated cells. Transcriptomic analysis of these cells identified c-kit as being selectively expressed in these cells (confirmed by immunofluorescence microscopy). Additionally, others have identified that *Dolichos biflorus* agglutinin (DBA) preferentially binds to mouse collecting duct principal cells. We hypothesized that c-kit and DBA could be used as cell surface markers for flow sorting. Indeed, we found that with these markers, the two cell populations could be efficiently isolated from mouse kidneys (confirmed by RT-PCR). We used FACS sorted DBA positive cells and C-kit positive cells from normal mice for RNA-seq analysis. The profiling results confirmed that they are distinct cell types and identified additional unique makers for principal cells and intercalated cells. The analysis identified several genes in both cell types with likely roles in the functions of the two cell types. These studies provide groundwork for future single-cell RNA-seq studies of collecting duct cell types.

CD16A Based Universal Chimeric Antigen Receptors Enhanced ADCC Mediated by NK Cells. L. Chen, D. Chin-nasamy, R. Childs; Laboratory of Transplantation Immunotherapy.

Chimeric Antigen Receptors (CARs) are engineered receptors composed of the extracellular binding domain, intramembrane anchoring and intracellular signal transduction domain. CARs can be efficiently expressed in T cells as well as natural killer (NK) cells, and the efficacy of the CD19 and CD20 CARs-modified T cells has already been demonstrated in the treatment of patients with lymphoma. In NK cells, CD16A plays an important role through antibody-dependent cell-mediated cytotoxicity (ADCC). Previous studies have demonstrated that CARs based on CD16A enhanced the cytotoxicity of T cells. We hypothesize that expression CD16A based CARs in NK cells could enhance the ADCC effects and also improve their expansion and survival. We designed three CARs, which contained the extracellular part of CD16A V158 high affinity mutant and intracellular signal (4-1 BB and CD3 ζ) but differed in signal peptides and transmembrane domain. When transduced into the Jurkat (human leukaemic T cell line) and the embryonic cell line 293T (human embryonic kidney cell line), all CARs showed comparable level of expression to that of the CD16A V158 and assembled correctly as confirmed by WB. Future studies are planned to transduce these CARs into primary human NK cells and NK cell lines and evaluate their expression and ability to enhance the ADCC of NK cells against tumor cells *in vitro* and *in vivo* in mouse models.

CoSync: an R package for Co-Synchronization Network Analysis of Pseudo-temporally Ordered Single Cell Data. Y. Chen, S. Gao, N. Wolanyk, X. Wang; Systems Biology Core.

Here we report a new R package CoSync that takes pseudo-temporally ordered single cell data, apply several dynamic systems and signal processing techniques that include phase synchronization, Granger causality, and coherence analysis, to evaluate infer gene interactions and construct co-synchronization networks. It connects smoothly with a number of single-cell pseudo-temporal ordering tools on its upstream, and the co-expression network tool WGCNA to construct co-synchronization networks on the downstream. Its functionalities and potential has tested with two real data sets. CoSync can be used as a module in a regulatory network modeling pipeline of single cell studies.

Intercellular transmission of enteroviral populations with vesicles. Y.H. Chen¹, P.M. Takvorian², A. Cali², E.S. Stempinski³, G. Altan-Bonnet⁴, N. Altan-Bonnet¹; ¹Laboratory of Host-Pathogen Dynamics, ²Rutgers University, ³Electron Microscopy Core Facility, ⁴NCI

During cell-to-cell transmission, viruses are largely thought to behave as discrete infectious units. Upending this view, we recently discovered that enteroviruses could travel between cells, not only as independent viral particles but also as clusters of viral particles. We reported that members of the enterovirus family of positive-strand RNA viruses, including poliovirus, coxsackievirus, and rhinovirus, all are released non-lytically from cells in culture within large vesicles that contained up to several hundred viral particles. We discovered that the vesicle membrane surrounding the enterovirus particles was enriched in phosphatidylserine (PS)

lipids. We show that vesicular PS lipids are co-factors to the relevant enterovirus receptors in mediating subsequent infectivity and transmission, in particular to primary human macrophages. These vesicles then facilitated virus spread to other susceptible cells by collectively transferring multiple viral genomes into the cytoplasm. We found that the enterovirus containing extracellular vesicles were highly infectious. Surprisingly, we observed significantly higher infection efficiencies when cells were infected with viral particles within vesicles as opposed to equivalent titers of free viral particles. Additionally, viral particles within vesicles are capable of suppressing the production of antiviral mRNAs of primary human macrophages rather than free single viral particles. This study reveals a novel mode of viral transmission, where enteroviral genomes are transmitted from cell-to-cell en bloc in membrane-bound PS vesicles instead of as single independent genomes. This has implications for facilitating genetic cooperativity among viral quasispecies, enhancing viral replication as well as regulating innate immune responses.

A New Mechanism of Selective mtDNA Inheritance Regulated by TFAM. Z. Chen, H. Xu; Laboratory of Molecular Genetics.

Mitochondria are under dual genetic control of both nuclear DNA and mitochondrial genome. Different from nuclear genome, mitochondrial genome contains thousands of copies of circular mitochondrial DNA (mtDNA) and is exclusively inherited down the maternal line. Recent studies show that the inheritance of deleterious mtDNA mutations was restricted by strong selection, but the mechanisms remain largely unknown. Understanding the mechanisms governing mtDNA transmission is essential if we are to understand the mitochondrial etiology of complex diseases, as well as seeking effective treatment. Recently I found the mtDNA binding protein mitochondrial transcription factor A (TFAM), a histone-like protein for mtDNA, played a role in the selective mtDNA inheritance. In a heteroplasmic *Drosophila* that contains both wild type and mutant mtDNA, knockdown of TFAM in the female germline led to a wider genotypic variance among progeny, and further resulted in faster selection of mtDNA over generations. Knockdown of TFAM in culture cells caused the aggregation of nucleoids and their asymmetric partition between dividing daughter cells. TFAM knockdown does not affect the mtDNA replication, but segregation of newly synthesized mtDNA is impaired. Thus TFAM may regulate symmetric mtDNA partition and control effective segregation unit number during cell division in germ line development, which further regulates mtDNA inheritance. The specific stages that TFAM affect the mtDNA transmission during oogenesis will be defined in future studies.

The Thrombopoietin Receptor Agonist Eltrombopag Has DNA Repair Activity in Human Hematopoietic Stem and Progenitor Cells. P.S. Cheruku, A. Cash, A. Larochelle; Regenerative Therapies for Inherited Blood Disorders.

Thrombopoietin (TPO) is the primary regulator of megakaryocytes and is also vital for the maintenance of hematopoietic stem and progenitor cells (HSPCs) in part by stimulating DNA repair. However, recombinant TPO is no longer supported for clinical applications due to the development of neutralizing antibodies. The alternative non-immunogenic TPO receptor agonist, eltrombopag, was developed and received FDA approval

for the treatment of acquired severe aplastic anemia, although, its mode of action is incompletely understood and a role in HSPC DNA repair has not yet been investigated. We hypothesized that eltrombopag may stimulate DNA repair activity similar to TPO and be of potential clinical benefit for subjects with Fanconi Anemia (FA), an inherited bone marrow failure disorder characterized by mutations in the FA DNA repair pathway and increased susceptibility to DNA damage. To test this hypothesis, G-CSF mobilized human CD34+ cells from 5 independent healthy donors were cultured in the presence of the cytokines SCF and Flt3-L (SF), SF and TPO (SFT), or SF and eltrombopag (SFE) for 24 hours, exposed to 2Gy γ -irradiation, and cultured for an additional 5 to 24 hours. We found that eltrombopag significantly improves DNA repair and survival of CD34+ cells by quantifying DNA damage, cell death and gene expression after irradiation. Eltrombopag's protective effect was demonstrated in both progenitor cells using in vitro CFU assays and long-term repopulating stem cells after transplantation in NSG mice. These pre-clinical data suggest that eltrombopag may be of benefit in the treatment of patients with FA.

Disruption in Arterial Branching Leads to Defective Hair Follicle Development. J.Y. Choi, W. Li, Y.S. Mukouyama; Laboratory of Stem Cell and Neuro-Vascular Biology.

Proper innervation and vascularization are essential in organ development. We have previously shown that sensory nerves become aligned with arterial branching in mouse embryonic skin. We sought to understand what happens to hair follicle development in disruptive sensory nerve-artery alignment. To address this question, we have developed a high-resolution 3D whole-mount imaging technique of embryonic skin to visualize cellular components and architecture of hair follicles. Our preliminary data demonstrate that arteries, but not veins, branch out adjacent to hair papilla. Mutants, which fail to develop sensory nerve-vessel alignment and arterial branching, exhibit a reduced number of hair follicles. These data suggest that defective hair follicle development is a functional consequence of defective sensory nerve-mediated arterial branching in the developing skin. We are currently investigating what arterial signals influence hair follicle development.

Investigating the Mesoscale Structure and Dynamics of Dense-Core Vesicle Docking Machinery. J. Cierniecki, A. Trexler, K. Sochacki, J. Taraska; Laboratory of Cellular and Molecular Imaging.

Vesicular docking is the process in which vesicles attach to their target membrane, spatially orienting themselves for fusion. In INS-1 rat β -cells, dense-core vesicles (DCVs) contact the plasma membrane, initiating the clustering of trans-SNARE components, thus prolonging their residence time at the plasma membrane. Many other proteins are, however, associated with DCVs, but the exact spatial organization and dynamics of molecules in the docked state are not known. Here, we use a combination of regular and super-resolution total internal reflection fluorescence (TIRF) microscopy, and correlative light and electron microscopy (CLEM), to explore the spatial organization and dynamics of proteins on or around putatively docked vesicles in INS-1 cells. We find that vesicle presence at the plasma membrane is an impermanent state, with an inverse relationship between vesicle diffusion coefficient and residence time. We also

investigate protein dynamics around vesicles in an immobile state by measuring changes in the fluorescence intensity of the proteins around immobile DCVs. We find that Rab27a and Actin fluorescence increases during this transition to immobility, while Tomosyn is transiently recruited during the transition. Concurrently, we are using CLEM to visualize the docking machinery around DCVs of unroofed INS-1 cells. CLEM will allow us to resolve the nanoscale spatial organization of these proteins within the context of electron microscope cell images. Our studies will help to gain a greater understanding of the docking machinery's mesoscale structure and how it helps regulate vesicle presence at the plasma membrane.

Autologous stem cell transplantation in immunoglobulin light chain amyloidosis with factor X deficiency. S. Cordes, M. Gertz, K.K. Buadi, Y. Lin, M.Q. Lacy, P. Kapoor, S.K. Kumar, A. McCurdy, A. Dispenzieri, D. Dingli, S. Hayman, W.J. Hogan, R.K. Pruthi; Department of Hematology, Mayo Clinic, Rochester, MN.

Acquired factor X deficiency and associated hemorrhage can be consequences of immunoglobulin light chain amyloidosis. There are limited data on the safety and efficacy of autologous stem cell transplant (ASCT) on factor X deficiency. We retrospectively reviewed immunoglobulin light chain amyloidosis patients with factor X levels below 50%, not on chronic anticoagulation who underwent ASCT at the Mayo Clinic, Rochester, Minnesota, USA, between April 1995 and December 2011. Twenty-seven of 358 patients (7.5%) met study criteria. Median pre-ASCT factor X was 36% (range: 2–49%). The most frequent and severe bleeding complications occurred in patients with factor X levels below 10%. Peri-procedural prophylaxis included activated recombinant factor VII, fresh frozen plasma and platelet transfusions. Steady-state post-ASCT factor X levels were determined in 12 patients. Post-ASCT factor X levels increased in 100% of patients, with median factor X improvement of +32% (range: +8 to +92%). About 46.2% of patients were no longer factor X deficient after ASCT. The degree of improvement in factor X levels was correlated with an improvement in markers of renal involvement by amyloid. Improvement in factor X correlated with an improvement in the degree of total serum protein ([rho] = 0.54; P = 0.04) and proteinuria ([rho] = -0.54; P = 0.04). Our findings support the decision to offer ASCT to factor X-deficient patients as both appropriate and efficacious.

Ibrutinib acts as a dual B-cell receptor and Toll-like receptor inhibitor in chronic lymphocytic leukemia. E. Dadashian, S.E.M. Herman, E. McAuley, D. Wong, C. Sun, D. Liu, A. Wiestner; Laboratory of Lymphoid Malignancies.

Chronic lymphocytic leukemia (CLL) cells rely on the microenvironment to induce cell activation, proliferation and survival. Microarray analysis of CLL cells harvested from patient-matched lymph node and peripheral blood demonstrated up-regulation of BCR and NF- κ B signaling. As NF- κ B signaling can be regulated downstream of multiple pathways, we sought to determine alternative mechanisms of NF- κ B activation. Utilizing microarrays, we found that Toll-like receptor (TLR) signaling was also up-regulated in lymph nodes compared to circulating cells. Activation of TLR signaling leads to increased NF- κ B transcriptional activity leading to the production of cytokines, such as IL-10 and increased JAK/STAT signaling. We sought to

determine if inhibition of TLR signaling could have therapeutic benefit for the treatment of CLL. CLL cells were stimulated *in vitro* with a CpG oligonucleotide, a TLR9 agonist. Increased IL-10 production, JAK/STAT signaling and up-regulation of activation markers were observed. Using an IRAK1/4 inhibitor, in combination with CpG-stimulation, we found significant inhibition of TLR signaling, resulting in reduced NF- κ B activity and downstream signaling events. This suggests that inhibition of the TLR signaling pathway could be clinically beneficial. We next compared the effect of inhibition of TLR signaling with inhibition of BCR signaling utilizing ibrutinib, a BTK inhibitor. Interestingly, ibrutinib not only inhibited BCR signaling, but also down-regulated TLR signaling; as measured by reduced cytokine production and JAK/STAT signaling. Thus, the TLR signaling pathway is a potential target for the treatment of CLL and can be inhibited by ibrutinib, a treatment option that is already clinically approved to treat CLL.

The Mitochondrial Interactome by Crosslinking Mass Spectrometry: Evidence for Supercomplexes in Intact Mitochondria. B.M. Dancy, R.S. Balaban; Laboratory of Cardiac Energetics.

While genomics, epigenomics, transcriptomics, proteomics, and metabolomics provide valuable insights into the identities of molecules in cells, these methods do not give a global picture of protein 3D structures or protein-protein interactions, both of which are important for protein function and rapid regulation. Protein structures and protein-protein interactions are usually studied individually, not on an "omics" level. Furthermore, for membrane proteins, which make up a large portion of the vital proteins in mitochondria, most biochemical methods are only able to look at protein structures and interactions after detergent solubilization, which may introduce artifacts. Our aim is to characterize the mitochondrial interactome as it exists in intact mitochondria. We therefore chose a strategy in which permeable crosslinking agents are allowed to act on mitochondria while they are still intact, and then the crosslinks are subsequently mapped using mass spectrometry methods. To make this possible in a complex sample, we used a crosslinking agent, DSSO, which is cleaved during collision-induced dissociation in the mass spectrometer, combined with an analysis platform called XlinkX that identifies the crosslinked sites. We present here an analysis of how our data compare with crystallography, for both single protein structures and protein-protein interaction surface mapping. We present experimental evidence to suggest several novel protein-protein binding pairs. We also present the first direct experimental evidence of the presence of interactions, in the absence of detergent, between the electron transport chain complexes I-III, II-III, and III-IV. We present the structural model of the I-III-IV "supercomplex" that is most consistent with our observed crosslinked sites. In conclusion, our work demonstrates the power of this technology to characterize the mitochondrial interactome.

Amoeba Host Model for Evaluation of *Mycobacterium abscessus* Clinical Isolates Virulence. J.L. Da Silva, J. Nguyen, K. Fennelly, A. Zelazny, K. Olivier; Microbiology Service.

Mycobacterium abscessus has become a global challenge with substantive burden of illness, especially in cystic fibrosis patients. Although highly important, virulence of these organisms

still remains poorly understood due to a lack of host models to study *M. abscessus* virulence *in vitro*. Here, we investigated whether *Acanthamoeba castellanii* may be useful to evaluate virulence of *M. abscessus* clinical isolates. *A. castellanii* was infected with *M. abscessus* (MOI 10) isolates previously collected at different disease severity time points from a patient with cystic fibrosis. Infection was carried out in 24-well plates, at 28 °C for 72 h. Samples were collected every 24 h and virulence toward *A. castellanii* evaluated by association assay, intracellular number of mycobacteria and survival of *A. castellanii*. The interaction between *M. abscessus* clinical isolates and *A. castellanii* is beneficial for intracellular mycobacterial growth. The association assay showed that mycobacteria collected from early versus late in the infection course present a different rate of attachment to *A. castellanii*. There is an increase in the number of mycobacteria after 72 h infection followed by a markedly reduction in *A. castellanii* survival. Our data suggests that *A. castellanii* might be a useful *in vitro* host model to study relative virulence of *M. abscessus* clinical isolates to aid in the identification and assessment of putative genomic virulence factors.

Examination of Antigen-Induced Endocytic Structures in B Lymphocytes by Fluorescence Microscopy. T.M. Davenport, A. Dickey, K. Sochacki, J. Taraska; Laboratory of Molecular Biophysics.

B lymphocytes play an essential role in generating protective immunity against pathogens. Activation of naïve B cells and their subsequent affinity maturation depend critically upon the ability of these cells to bind and internalize antigen through their B cell receptors (BCR). The mechanism of antigen internalization by B cells appears to require cooperation between the actomyosin network and clathrin-mediated endocytic processes. While a number of proteins have been identified to be critical for antigen internalization, gaps remain in our understanding of the basic cellular structures responsible for antigen uptake and the mechanism by which these structures form. Here, we used confocal, total-internal reflected fluorescence (TIRF), and correlative super-resolution light and electron microscopy (CLEM) to directly observe endocytic structures in lymphocytes from the human DG-75 B cell line. Cells expressing GFP-tagged BCR and red fluorescent protein-tagged endocytic proteins were stimulated with anti-human IgM Fab'2 to model BCR clustering and internalization. We observed recruitment of early adaptors of clathrin mediated endocytosis – FCHO1, FCHO2, Eps15, Epsin, CALM, and clathrin itself – to Fab'2-induced BCR clusters by TIRF and confocal microscopy. CLEM revealed that BCR clusters are heterogeneous in size and frequently partition with clathrin off of larger endocytic structures. This work expands our understanding of antigen uptake in B cells and reveals novel features of antigen-induced endocytic structures.

Host Cell Pathways Hijacked for Coronavirus Transmission. T.A. Dellibovi-Ragheb, M.C. Hagemeijer, P.M. Takvorian, A. Cali, N. Altan-Bonnet; Laboratory of Host-Pathogen Dynamics. Coronaviruses are a family of enveloped viruses with a large, positive-strand RNA genome. Two members of this virus family have gained notoriety in recent years due to the outbreaks of severe acute respiratory syndrome (SARS) in Asia in 2003, and Middle East respiratory syndrome (MERS) in 2012. Our work focuses on a closely related member of the coronavirus family,

mouse hepatitis virus (MHV). We are investigating how MHV hijacks host cell pathways for viral propagation and transmission. The entire infection cycle of coronaviruses, as with other positive-strand RNA viruses, is closely associated with cellular membranes. This provides several advantages to the virus, including concentrating and scaffolding replication factors to increase replication kinetics, and shielding the virus from host defenses. In the case of MHV, viral RNA replication occurs in double-membrane vesicles derived from the ER, and virus assembly and budding occurs at the ER-Golgi intermediate compartment (ERGIC). It was assumed that MHV then exits the cell through the secretory pathway. However, we have shown that if protein secretion is blocked with Brefeldin A (BFA) at different time points during virus infection, we observe an inhibition of viral replication, but not virus release, suggesting that virus release is independent of the secretory pathway. We are currently defining the molecular mechanisms by which coronavirus is released, and believe that understanding this crucial step in viral transmission will have important medical implications, as there are currently no vaccines or treatments available for any human coronaviruses.

Generating HERV-E envelope antigen-specific CD8+ T cells utilizing overlapping peptide libraries to identify TCRs for the immunotherapy of metastatic clear cell renal cell carcinoma. S. Doh, E. Cherkasova, R.W. Childs; Laboratory of Transplantation Immunotherapy.

Previously our lab discovered a novel human endogenous retrovirus type-E (HERV-E) as the target of cytotoxic T lymphocytes (CTLs) in patients with metastatic clear cell renal cell carcinoma (ccRCC) whose tumors regressed after hematopoietic stem cell transplant (HSCT) (1). RCC-reactive T cells from these patients were found to be donor-derived and recognized RCC *in vitro*. The target of these CTLs was a HLA-A*11-restricted 10-aa peptide antigen (named CT-RCC-1) derived from the 5'LTR region of HERV-E spliced transcripts, named CT-RCC-8, CT-RCC-9, and CT-RCC-Env. Importantly, this provirus is selectively expressed in the majority of ccRCC, but not in other tumors or normal tissues as a consequence of VHL inactivation (2). We found that the CT-RCC-Env transcript contains two open reading frames (ORFs) encoding for transmembrane (TM) and surface (SU) partial proteins. Peptides originating from these proteins might be ideal targets for T cell mediated immunotherapy of metastatic ccRCC. Accordingly, we found that HLA-A*0201-restricted peptides predicted to be products of the CT-RCC HERV-E envelope transcript stimulated CD8+ T cells which could recognize HLA-A*0201-positive HERV-E-expressing kidney tumor cells (3). Currently, we are looking for additional peptides originating from this envelope using overlapping peptides libraries designed from HERV-E TM and SU sequences. T cell bulk cultures from healthy donors initially exhibit peptide-reactivity. However, we encountered problems isolating and expanding HERV-E Env specific CTL clones, which raises the possibility that the target may be expressed in activated T cells. Further work is underway to determine whether TM and SU regions are expressed in activated T cells.

Cathepsin L as a Synuclease: Degradation Mechanisms of α -Synuclein Amyloid Fibrils.

G.A. Dominah, R.P. McGlinchey, J.C. Lee; Laboratory of Molecular Biophysics.

α -Synuclein (α -syn) is an intrinsically disordered protein whose cytosolic accumulation and amyloid formation is a major hallmark of Parkinson's disease. This accumulation may be counteracted by mechanisms of protein degradation involving the lysosome. Recently, we reported that lysosomal cysteine proteases including cathepsin L (CtsL) were essential for degrading monomeric α -syn in the lysosome. Interestingly, we also discovered the unique ability of CtsL to proteolyze amyloid fibrils of α -syn, which by definition are highly protease-resistant. To gain mechanistic insights into how CtsL degrades fibrillar α -syn, liquid chromatography mass spectrometry is employed to identify critical cleavage sites that destabilize amyloid structure. Furthermore, we will use N27, a dopaminergic rat cell model, to evaluate whether CtsL is indeed a synuclease and its activity on α -syn fibrils offers a potential therapeutic strategy for making amyloids benign.

A membrane trafficking screen to identify Clathrin-independent endocytosis machinery. D. Dutta, J. Wayt, J. Donaldson; Cell Biology and Physiology Center.

Endocytosis is an important event that cells utilize to internalize cell surface proteins and fluid into the cell. There are two main forms of endocytosis: clathrin-mediated endocytosis (CME) and clathrin-independent endocytosis (CIE), amongst which CME is most studied. While CME is important for the internalization of many surface proteins, bulk trafficking of fluid occurs primarily in a clathrin-independent manner. Our lab has focused on CIE associated with Arf6, although other pathways exist for specific cargoes, and has identified an endosomal sorting system in HeLa cells that sorts CIE cargo proteins after endocytosis. We have established the trafficking itinerary of classical cargoes like MHCI, CD59, CD147 and CD98 but little is known about the entry mechanisms and the proteins that regulate these initial steps. Therefore, we have designed an siRNA screen using the Dharmacon™ Membrane Trafficking library, containing 140 genes, to identify proteins essential for the internalization of CD59 and MHCI in HeLa cells. Target genes are individually knocked down and cells are allowed to internalize CIE cargo proteins. Following internalization, the proteins are visualized by immunofluorescence, the amount of internalized protein is determined and positive and negative hits are scored. Based on the results of this visual screen we hope to identify components of CIE as well as potential regulators of this process. Positive hits will be followed up by future confirmatory tests.

Development of a Human Circulating Fibrocyte Model to Assess the Effect of the 5A Apolipoprotein A-I Mimetic Peptide in Idiopathic Pulmonary Fibrosis. D.M. Figueroa, S. Levine; Laboratory of Asthma and Lung Inflammation.

Idiopathic Pulmonary Fibrosis (IPF) is a chronic progressive lung disease of aging that has a median survival of 3 years following diagnosis. New treatments are needed to halt and ideally reverse disease progression in IPF. Apolipoprotein A-I (apoA-I), the major protein component of high-density lipoprotein (HDL), has anti-oxidant, anti-inflammatory, anti-thrombotic, and anti-fibrotic properties. ApoA-I is reduced in bron-

choalveolar lavage fluid from patients with IPF while treatment with apoA-I decreases disease severity in bleomycin- and silica-induced murine models of experimental pulmonary fibrosis. Collectively, these results suggest that apoA-I might be developed into a novel treatment for IPF. Fibrocytes are circulating CD45⁺/Collagen-I⁺/CD14⁻/CD3⁻/CD19⁻ hematopoietic stem cells that are recruited to sites of tissue injury and promote wound healing, as well as contribute to myofibroblast expansion in IPF. Here, we developed an *ex vivo* culture model to assess if the 5A apoA-I mimetic peptide can suppress the differentiation of circulating fibrocytes from healthy volunteers and IPF subjects into α -smooth muscle actin-expressing (α SMA⁺) myofibrocytes. Fibrocytes are isolated from peripheral blood, cultured with DMEM containing 20% FBS and TGF- β 1, with or without 5A. The cells are then collected, counted, and the number of CD45⁺/Col-I⁺/ α SMA⁺ myofibrocytes are quantified by flow cytometry. Preliminary results show a 54.8% decrease in fibrocyte differentiation in the presence of 5A and TGF- β 1, as compared to TGF- β 1 alone. This *ex vivo* differentiation and culture system of circulating human fibrocytes will provide a platform to assess if apoA-I mimetic peptides might attenuate fibrocyte differentiation in IPF and thereby suppress progressive lung fibrosis.

Substrate Topology Regulates Actomyosin Morphodynamics. R.S. Fischer, X. Sun, J. Fourkas, W. Losert, C.M. Waterman; Laboratory of Cell and Tissue Morphodynamics.

Cell shape is critical to many cellular functions, and is regulated by the actomyosin cytoskeleton and cell adhesions. Previous research has shown that non-muscle myosin II (myoII) can sense local curvature, whereas adhesions and actin polymerization have been shown to be guided by local nanofiber topographies (Petrie et al, 2009). However, it remains unclear whether the ability to "sense" local curvature by the actomyosin cytoskeleton is dependent on localized assembly dynamics of actin or myoII at preferred topologies. Furthermore, the limits of local curvature allow actin and myosin assembly are also unknown. Here, we approached these questions by culturing cells on nanofabricated substrate topographies with a range of local curvatures and observing actin and myoII dynamics by live cell microscopy. On substrates with aligned or curved ridges, cells migrate to orient themselves long axis along the axis of lowest curvature, but on substrates where the mean curvature in orthogonal lateral (X-Y) directions is near equal, cell orientations are randomized. At the molecular level, myoII mini-filaments are aligned along the axis of minimal local curvature. On substrates which expose the cell to defined positive and negative curvatures, MyoII mini-filament arrays assembled at low positive curvatures (0.1- μ m to 0.4- μ m), but contracted to stably associate with low negative curvatures (-0.1- μ m to -0.4- μ m). While these contractile arrays were reminiscent of actomyosin arcs that form in the lamella of cells migrating on planar surfaces, they occurred in the middle of the cell, parallel to the long axis of the cell, rather than at a leading edge. Conversely, F-actin dynamically associated with a wider range of curvatures, and was enriched on the highest curvature topologies where myosin was excluded, with sites of highest curvature associated with filopodia and lamellipodia induction and actin assembly. We conclude that local surface topology can organize and regulate the dynamic assembly of

actomyosin networks, which can then organize global cell shape accordingly.

Structural Features of α -Synuclein Revealed by Raman Spectroscopy. J.D. Flynn, J. C. Lee; Laboratory of Molecular Biophysics.

Parkinson's disease (PD) is a prevalent age-related neurodegenerative disease associated with the aggregation of the neuronal protein α -synuclein (α -syn) into β -sheet-rich fibrils, called amyloid. Several missense mutations of α -syn are linked to familial early-onset PD and have been shown to affect the rate of α -syn aggregation and fibril formation *in vitro*. Previous studies have used electron microscopy to show differences in the morphology of fibrils formed from different α -syn mutants, but a structural understanding of the relationship between protein mutation and resulting fibril polymorph has not yet been achieved. Here, we have used Raman spectroscopy to characterize fibrillar aggregates of five disease-related mutants of α -syn. Additionally, we perform kinetic studies of *in vitro* aggregation, at acidic and neutral pH under various salt concentrations, and electron microscopy experiments to gain a better understanding of how fibril polymorphism may relate to the pathology of α -syn mutants. While it is generally accepted that α -syn fibrils are polymorphic, our work is the first to characterize molecular structure differences using vibrational spectroscopy. Specifically, we observe clear spectral differences in the fingerprint region of the spectrum, suggesting differences in the C-H deformation stretches of the fibril sidechains, which has not been previously reported. Additionally, we observe differences in the maxima position and peak width of the amide-I peak, which suggests slight differences in secondary structure across the mutants. Our results suggest Raman microscopy is a highly sensitive technique useful for characterizing fibril polymorphs and could potentially shed light on how structural differences are linked to disease.

Mechanism of LCAT Activation by Compound A. L. Freeman, S. Demosky, M. Konaklieva, R. Kuskovsky, S. Gordon, A. Ossoli, R. Shamburek, A. Aponte, M. Gucek, J. Tesmer, R. Levine, A. Remaley; Lipoprotein Metabolism Section.

Lecithin:cholesterol acyltransferase (LCAT) catalyzes cholesteryl ester (CE) production from free cholesterol (FC) and phosphatidylcholine (lecithin), promoting HDL formation. Our aim was to investigate activation of LCAT by Compound A (Amgen), a previously described small-molecule activator of LCAT, with the ultimate goal of developing novel LCAT activators for therapeutic use. Compound A was found to increase LCAT activity for a subset of Familial LCAT Deficiency (FLD) mutations to a level above which renal disease may occur. HEK293 cells were then transiently transfected with plasmids containing wild-type (WT) or mutant LCAT cDNA. Cell media was then incubated with either vehicle or Compound A and LCAT activity was quantitated using a novel plate assay utilizing Methylumbelliferyl Palmitate as a substrate. Mutations of Cys31 *in vitro* strongly affected basal LCAT activity as well as activation by Compound A. Charged residues at position 31 profoundly decreased activity whereas bulky hydrophobic groups increased LCAT activity up to 3-fold ($p < 0.005$, all). Mass spectrometry of WT LCAT incubated with Compound A revealed a +103.017 m/z adduct to the tryptic peptide containing Cys31, indicative of a cyanopyrazine adduct to LCAT Cys31. Molecular

modeling identified potential binding sites of Compound A to LCAT. Our findings yield important mechanistic insight into LCAT activation that can be used to design novel LCAT activators for therapeutic use.

Maturation of Induced Pluripotent Stem Cell Derived Cardiomyocytes via Co-Culture with Supporting Cells of the Developing Heart. I.H. Garcia-Pak¹, W. Li¹, H. Uosaki², E. Tampakakis², J. Zou³, Y. Lin³, C. Kwon², Y. Mukoyama¹;

¹Laboratory of Stem Cell and Neuro-Vascular Biology, ²Division of Cardiology, The Johns Hopkins University School of Medicine, ³iPSC Core Facility.

The successful derivation of cardiomyocytes from human pluripotent stem cells, both embryonic and induced pluripotent stem cells (hiPSC), has opened up exciting possibilities for clinical applications such as tissue engineering, disease modeling, and drug toxicity testing. The hurdle in implementing such applications is that these cardiomyocytes are immature; they appear and behave like fetal cardiomyocytes. It has been shown that many cell types including endothelial cells, sympathetic neurons, and epicardium-derived fibroblasts and vascular smooth muscle cells associate with and provide signals to cardiomyocytes in the developing heart. In this study, we aim to overcome this limitation using co-culture of iPSC-derived cardiomyocytes (iPSC-CMs) to mimic the complex cell signaling found in the developing heart. We co-cultured epicardial cells and sympathetic ganglia isolated from mouse embryos with human umbilical vein endothelial cells and immature iPSC-CMs for 30 days. We examined whether these long-termed co-cultured iPSC-CMs exhibit a more mature morphology and up-regulation of cardiac genes highly expressed in the human adult cardiomyocytes. We hope this co-culture system will benefit the field by providing a step forward in mature cardiomyocyte application and therapies.

Standard 3D printed phantom used for calibration in Micro stereo radiography and far-field phase contrast imaging. A. George, P. Chen, H. Wen; Laboratory of Imaging Physics.

In medicine, as well as biological research, x-ray imaging modalities are increasingly used to non-invasively characterize tissues and diseases. The growing applications have propelled rapid development of new imaging techniques in recent years, such as tomosynthesis and phase-contrast imaging. To obtain reliable image resolution and accurate information, it is imperative that a standard phantom be developed such that the transformation between detector-plane and sample-plane coordinates may be resolved. The IPL/BBC laboratory developed micro stereo radiography and phase-contrast imaging prototypes. We designed and constructed 3D printed calibration phantoms to map out the relationship between the points in the imaged object and locations on the acquired images precisely. The phantoms include cavities for highly dense micro beads and retain straight edges. During scanning procedures these object trace out characteristic trajectories in the images. Combining information obtained from the calibration images with known geometric parameters of the phantoms, we are developing algorithms and software to track the position of the beads and edges in the images to estimate the geometric relationship amongst key components of the imaging system, for example: the altitude/position of the sample rotation axis and the tilt/rotation of the x-ray camera. Furthermore, initial calibration scans indicate

geometric distortions within an in-house developed high-efficiency x-ray camera, which spurs the development of generalized calibration algorithms to cover the new type of image warping.

Fluorescent Cell Barcoding: Optimization and Troubleshooting for Multiplexing Flow Cytometry Phenotyping and Signaling Profiling. V. Giudice, X. Feng, S. Kajigaya, N. Young, A. Biancotto; Hematology Branch.

Fluorescent cell barcoding (FCB) is a cell-based multiplexing technique for high-throughput flow cytometric analysis. Individual samples are labeled using different concentrations of FCB marker(s), the reactive form of a fluorophore. Barcoded samples can be mixed, stained, and acquired together, because each specimen has a unique fluorescent signature, minimizing staining variability and antibody consumption, while decreasing required sample volumes. FCB technique has been developed for phosphoflow assay and drug screening, although it can be also applied to immunophenotyping and intracellular cytokine detection. However, several technical issues are to be considered prior to using FCB as a research tool. Indeed, barcoding efficiency is dependent on FCB dye working concentrations, the number of cells required for combined samples, and a higher purity of deconvolution (>95%). In addition, the choice of dyes is dependent on cytometer configuration, the number of samples to acquire, and the panel of specific antibodies used for staining. Using DyLight 350, DyLight 800, Pacific Orange, CBD450, and CBD500, we successfully barcoded six, nine, and 36 human peripheral blood specimens. FCB dyes concentrations ranged from 0 to 125 µg/ml were used to barcode 7.5×10^5 cells, and viability dye staining was also optimized to increase data robustness by excluding dead cells from analysis. Furthermore, a 6-color staining was also optimized using DyLight 350 versus DyLight 800, and DyLight 350 versus Pacific Orange barcoding combinations. Our methods provide validation of FCB technique that would be useful for multiplex drug screening and efficiency, and lymphocytes characterization and changes during disease and treatments.

Defining Roles for Apolipoprotein A-1 and Apolipoprotein E in Modifying Asthmatic Airway Inflammation. E.M. Gordon, H. Xu, S.J. Levine; Laboratory of Asthma and Lung Inflammation.

Apolipoprotein A-1 (apoA-1) and apolipoprotein E (apoE) have protective roles in experimental murine models of asthma. Furthermore, serum apoA-1 levels are positively correlated with less severe airflow obstruction in asthmatics. Here, we hypothesized that apoA-1 and apoE attenuate airway inflammation in human subjects. Alveolar macrophages (AMs) and airway epithelial cells (AECs) were obtained from asthmatics and healthy volunteers by bronchoscopy. First, we found that house dust mite (HDM), but not other pro-inflammatory mediators, such as IL-13, IL-17, IFN- γ , TNF- α , or the TLR agonists, LPS or poly I:C, induced significant increases in apoE secretion by AMs, whereas AMs did not secrete apoA-I. HDM-induced increases in AM apoE secretion were preferentially attenuated by the serine protease inhibitor, AEBSF, as compared to the cysteine protease inhibitor, E64. Antagonists of protease-activated receptors (PAR) 1 and 2 had minimal effects on HDM-induced apoE secretion by AMs, which suggests a role for PAR-independent

pathways. Second, we investigated whether apolipoproteins modify AEC responses to inflammatory mediators. Human AECs were cultured in an air-liquid interface culture system and differentiated into a pseudo-stratified columnar epithelium prior to stimulation with Th2 (IL-13) and Th17 (IL-17) cytokines. Preliminary results suggest that neither apoA-1 nor apoE suppress IL-17-induced IL-8 secretion from AECs. Future studies will assess the effects of apoA-1 and apoE on IL-13- and IL-17-mediated inflammatory pathways in AECs. These investigations will help define the roles of apoA-1 and apoE in modifying airway inflammation in asthma and generate data to support their potential development into new treatments.

A High Density Lipoprotein Proteome Index Correlates with Atherosclerosis Severity in Humans. S.M. Gordon, X. Wang, D. Sviridov, M. Chen, A.T. Remaley. Lipoprotein Metabolism Section.

The cholesterol content of High Density Lipoprotein (HDL-C) has been the traditional biomarker for estimating cardiovascular protection derived from HDL; however, several recent studies have made it clear that the HDL-C metric does not represent a direct measure of the protective capacity of HDL. The diverse protein and lipid content of HDL is becoming increasingly recognized as the basis for the protective capacity derived these particles. Proteomics studies have identified 95 consensus proteins consistently found to associate with HDL. For the majority of these proteins, the functional importance of their association with HDL has not yet been determined. In this study, we tested the hypothesis that the protein composition of HDL is related to the severity of atherosclerosis in human subjects. A total of 101 subjects were selected and divided into 6 groups based on atherosclerosis severity as determined by CT-angiography. HDL was isolated from each patient and analyzed by electrospray ionization tandem mass spectrometry and a spectral index value (derived from normalized spectrum counts and the number of subjects in which the protein was detected) was calculated for each identified protein. We then developed a novel metric for the analysis of HDL proteome data, which takes into account all identified proteins as a single proteomic index. This HDL Proteome Index displays a significant correlation with atherosclerosis severity even after correction for other known risk factors and may represent a novel biomarker for cardiovascular risk with greater predictive power than the current measure of HDL-C.

A New Strategy for Fetal Hemoglobin Induction with Lentiviral-Mediated Knockdown of *POGZ*; evidence in a human erythroleukemia cell line. B. Gudmundsdottir, N. Uchida, J.F. Tisdale; Molecular and Clinical Hematology Branch.

Targeting repressors of fetal hemoglobin has the potential to become a novel therapeutic strategy in sickle cell disease and β -thalassemia. It has previously been demonstrated, using a conditional mouse knockout model, that the C2H2 zinc finger protein POGZ plays an important role in erythroid differentiation during embryonic development and in embryonic hemoglobin repression. To determine if *POGZ* regulates fetal hemoglobin expression in human cells, we knocked down *POGZ* expression in a human erythroleukemia cell line (K562), using 3 *POGZ*-specific lentiviral short hairpin RNA (shRNA) constructs: sh07 and sh09. We found that the shRNA constructs significantly

differed in the ability to knock down *POGZ* expression as measured by RT-qPCR and Western blot analysis. *POGZ* knockdown did not appear to have significant adverse effects on the growth of the K562 cells. RT-qPCR analysis demonstrated an increase in embryonic hemoglobin (HBE) and fetal hemoglobin (HBG) expression upon *POGZ* knockdown, suggesting that *POGZ* has a role in repressing embryonic and fetal hemoglobin expression in human erythroid cells. However, since K562 cells are a leukemic cell line and already express significant levels of fetal hemoglobin, *POGZ* knockdown may only have limited effects in this model. Therefore, our future experiments aim at analyzing the consequences of *POGZ* knockdown on fetal hemoglobin expression in primary human CD34⁺ cells induced for erythroid differentiation.

The Role of Actin Structural Plasticity in Mechanosensation. P.S. Gurel, Y. Takagi, J. E. Bird, J.R. Sellers, G.M. Alushin; Cell Biology and Physiology Center.

The ability of a cell to respond to the mechanical properties of its environment (mechanosensation) influences almost all core cellular processes, including division, migration, differentiation, and survival. Misregulation of mechanosensory pathways has recently been implicated in malignant transformation, tumorigenesis, and metastasis, highlighting this process as a key component of cancer progression. At the foundation of this behavior lies an intricately coordinated contractile network consisting of the actin cytoskeleton, myosin motor proteins, and their myriad binding partners; however, we currently lack a basic understanding of the underlying molecular mechanisms connecting actin to cellular mechanosensation. Actin filaments are flexible polymers that can adopt multiple conformational states, and recent evidence shows that forces can influence interactions with binding partners. Here, we explore how mechanical stimuli alter the actin filament structural landscape and how this may influence downstream interactions, potentially serving as an initial signal in mechanosensation. We have developed a novel reconstitution system to place actin filaments under tension suitable for high-resolution structural studies with cryo-EM. We immobilize active myosinV (barbed-end directed motor) and myosinVI (pointed-end directed motor) onto the carbon substrate of holey EM grids, suspending motor-engaged actin filaments over holes. Using a modified gliding assay, we find that the opposing activity of the two myosins induces mechanical strain in filaments, evidenced by increased severing in the presence of ATP. In contrast, either myosin alone produces processive gliding of filaments. Low-resolution cryo-EM reveals a novel, persistent actin structural state found in the presence of force generation. High-resolution studies are currently underway to investigate the conformational changes produced in actin in detail. Resolving these structures will provide unprecedented insight into the molecular mechanisms of mechanosensation, and ultimately advance the development of targeted therapeutics against specific actin conformational states.

Effects of Ion and Local Lipid Composition on the Physicochemical Properties of PIP₂-Monolayers. K. Han, R.M. Venable, R.W. Pastor; Laboratory of Computational Biology.

Phosphatidylinositol (4,5)-bisphosphate (PIP₂), a phosphorylated derivative of phosphatidylinositol, is among the most important component of eukaryotic cell-membranes. It plays indis-

pensable roles in the regulation of ion channels, autophagy, endocytosis, and exocytosis, and is also the precursor of the essential second messengers for the cellular signal transduction such as inositol (1,4,5)-trisphosphate (IP₃) and diacylglycerol (DAG). The ever-increasing connections of PIP₂ with human diseases have brought forth a number of cellular and molecular-level studies on PIP₂ in the last decade. In the present study, we have performed all-atom molecular dynamics simulations to discover the underlying principle of PIP₂-cluster formation and the context-dependent nature of its biological functions. Special attention has been paid to the effects of counter-ions/co-ions such as K⁺, Mg²⁺, and Ca²⁺ and the roles of local lipid compositions in clustering. Furthermore, the simulation results are applied to the interpretation of target biological experiments such as Langmuir trough experiments on pure and mixed monolayers. This study provides an integrated framework for not only unveiling the underlying principles of physicochemical properties of PIP₂-clusters, but also understanding its biological/ pharmacological effects associated with various human diseases, including cancer, neurodegeneration, metabolic disorder, and inflammation.

Improvement of definitive erythroid cell production from human ES cells using serum-free ES-sac generation. J.J. Haro-Mora, N. Uchida, A. Fujita, J. Tisdale; Molecular & Clinical Hematology Branch.

The *in vitro* erythroid cell generation from human embryonic stem cells (hESCs) could represent an alternative source for red blood cell transfusion. However, in traditional strategies, the yield of hESC-derived erythroid cells is low, and the cells mainly produce embryonic hemoglobin.

We recently developed a protocol to generate definitive erythroid cells mainly expressing gamma- and beta-globin by using ES-sacs, which are endothelial structure containing hematopoietic-like cells. The original protocol includes the use of fetal bovine serum (FBS), which confers high variability for ES-sac generation. Therefore, in this study, we sought to develop serum-free ES-sac generation system.

We generated ES-sacs during 15-day culture with VEGF on C3H feeder cells, in which FBS was switched to Knockout Serum Replacement (KSR), and the ES-sac-derived hematopoietic-like cells were differentiated into erythroid cells for additional 15 days.

After 15-day ES-sac culture, we obtained 63-fold greater numbers of ES-sacs and 3.5-fold greater amounts of hematopoietic-like cells when KSR was used instead of FBS. Using flow cytometry, 20.5-fold greater amounts of CD34⁺CD45⁺ hematopoietic progenitor cells and 2.6-fold fewer amounts of GPA⁺CD41a⁺ erythroid cells were measured in the KSR-based ES-sac generation. After additional 15-day erythroid differentiation, KSR-based ES-sacs resulted in 3.0-fold greater amounts of GPA⁺ erythroid cells, and equivalent gamma- and beta-globin expression was measured.

In summary, we present preliminary data, demonstrating the replacement of FBS by KSR improves the ES-sac generation, and ES-sac-derived erythroid cell production with beta-globin expression. Our findings should be useful to reduce variability during ES-sac generation.

Sirolimus-induced preservation of bone marrow hematopoietic stem and progenitor cells in immune and nonimmune mediated mouse models of bone marrow failure. M.K. Hollinger; Cell Biology Section.

Aplastic anemia (AA) is a typical disease of bone marrow (BM) failure characterized by pancytopenia, BM destruction, and loss of hematopoietic stem and progenitor cells. Since immune-mediated destruction of BM has been implicated in the pathophysiology of AA, novel immunosuppressants have become attractive therapeutic targets for patients resistant to current immunosuppressive therapies. Sirolimus, an inhibitor of the nutrient sensing mTOR pathway, acts as a suppressor of T-cell activation independent of cyclosporine A and anti-thymocyte globulin, two of the most prevalent immunosuppressant treatments for AA. Here we show in a B6 to CByB6F1 lymphocyte infusion based AA mouse model that, in addition to suppressing effector T cells and stimulating immunosuppressive regulatory T cells, treatment with sirolimus at 2 mg/Kg/day for 10 days preserved hematopoietic stem and progenitor cells. BM cells of sirolimus-treated AA mice had significantly higher colony-forming cell (CFC) frequency than untreated AA mice, as measured by methylcellulose colony assay. In another mouse model of chemically-induced BM failure, injection of 5-fluorouracil (5-FU) at 150 mg/Kg three times at two week intervals induced severe BM failure with significantly reduced CFC frequency in the BM. Treatment with sirolimus in 5-FU-injected mice at 5 mg/Kg/time, three times per week for five weeks, increased CFC frequency significantly, especially in granulocyte/macrophage and erythroid compartments. The protective effect of sirolimus on hematopoietic stem and progenitor cells in immune- and nonimmune-mediated BM failure mouse models provides supportive evidence for the utility of sirolimus in the clinic as a therapeutic agent for AA treatment.

Myosin II Facilitates Ligand Discrimination During T Cell Activation. J. Hong, S. Murugesan, J. Hammer; Molecular Cell Biology Section.

The importance of T cell receptor (TCR) mechano-transduction in T cell signaling is highlighted by recent studies showing that T cells can sense and generate force through the interaction between the TCR and peptide-bound major histocompatibility complex (pMHC) on antigen presenting cells (APCs). In this study, we investigate the multifaceted role of non-muscle myosin II in TCR mechano-transduction, focusing on ligand discrimination. Using structure illumination microscopy (SIM), we analyze actomyosin arc structures at the immunological synapse with surfaces coated with either strong agonist OVA:H-2K^b or weak agonist G4:H-2K^b for OT1 T cells. We find that stimulation of T cells with weak agonist resulted disorganized actomyosin arcs, while strong agonist coated stimulation resulted in highly organized actomyosin arcs. As expected, this ligand-dependent actomyosin arc organization is disrupted upon inhibition of myosin II using para-nitro-blebbistatin. Consistent with previous studies, the frequencies of T-APC conjugation as well as the phosphorylation level of early signaling molecules like Lck, Zap-70, and LAT are attenuated upon myosin II inhibition. These data highlight the importance of actomyosin activity in T cell activation triggered by a highly potent ligand. Together, our results suggest an important role for myosin II in TCR mechano-transduction in ligand discrimination which highlights the

biophysical connection between intracellular to membrane-associated cellular components.

Brownian Ratchet Mechanism of Plasmid Segregation. L. Hu, J. Liu; Biochemistry and Biophysics Center.

The segregation of DNA before cell division is essential for faithful genetic inheritance. In many bacteria, segregation of low-copy-number plasmids involves an active partition system composed of a nonspecific DNA-binding ATPase, ParA, and its stimulator protein ParB. The ParA/ParB system drives directed and persistent movement of DNA cargo. We develop a computational model to investigate the underlying mechanism of ParA-mediated low-copy-number plasmid movement and partition. We show that the ParA/ParB system can work as a Brownian ratchet, which effectively couples the ATPase-dependent cycle of ParA-nucleoid affinity to the motion of ParB-bound plasmid. By controlling plasmid speed and refill kinetics of ParA depletion zone on the nucleoid surface, the model recapitulates the modes of plasmid motility observed *in vivo*, including the diffusive motion, pole-to-pole oscillation, and the directed segregation movement that positions plasmids at equidistance along the long axis of the cell. Importantly, unlike diffusion and oscillation, directed segregation movement could ensure the fidelity of low-copy-number plasmid segregation, which entails the partition system to operate near the transition regime between directed segregation movement and oscillation.

Novel Role of TRPML2 in the Regulation of the Innate Immune Response. Y. Hua, L. Sun, S. Vergara-Jauregui, H. Diab, R. Puertollano; Laboratory of Cell Biology.

TRPMLs constitute a family of endosomal cation channels with homology to the transient receptor potential (TRP) superfamily. In mammals, the TRPML family includes three members, TRPML1-3. While TRPML1 and TRPML3 have been well characterized, the cellular function of TRPML2 has remained elusive. To address TRPML2 function in a physiologically relevant cell type, we first analyzed TRPML2 expression in different mouse tissues and organs and found that TRPML2 was predominantly expressed in lymphoid organs and kidney. Quantitative RT-PCR revealed tight regulation of TRPML2 at the transcriptional level. While TRPML2 expression was negligible in resting macrophages, TRPML2 mRNA and protein levels dramatically increased in response to toll-like receptor (TLR) activation both *in vitro* and *in vivo*. Conversely, TRPML1 and TRPML3 levels did not change upon TLR activation. Immunofluorescence analysis demonstrated that endogenous TRPML2 primarily localized to recycling endosomes both in culture and primary cells, in contrast with TRPML1 and TRPML3 that distribute to the late and early endosomal pathway, respectively. To better understand the *in vivo* function of TRPML2 we generated a TRPML2 knockout mouse. We found that the production of several chemokines, in particular CCL2, was severely reduced in TRPML2 knockout mice. Furthermore, TRPML2 knockout mice displayed impaired recruitment of peripheral macrophages in response to intraperitoneal injections of either LPS or live bacteria, thus suggesting a potential defect in immune response. Overall, our study reveals interesting differences in the regulation and distribution of the members of the TRPML family and identifies a novel role for TRPML2 in innate immune response.

Use of CRISPR-Phosphoproteomics to Investigate Role of Myosin Light Chain Kinase in Vasopressin Signaling. K. Isobe, V. Raghuram, C.-R. Yang, P. Sandoval, C.L. Chou, M.A. Knepper; Epithelial Systems Biology Laboratory, Systems Biology Center.

Renal water excretion is controlled through the action of vasopressin to regulate aquaporin-2 (AQP2). Vasopressin regulates AQP2 in part through control of trafficking to and from the plasma membrane. We have previously reported that Ca^{2+} -calmodulin and myosin light chain kinase (MLCK) are involved in AQP2 trafficking. However, the detailed mechanism by which MLCK regulates AQP2 is unclear. To address this problem, we generated 'MLCK knock-out' (MLCK-KO) collecting duct cell lines using CRISPR-Cas9. Separate KO lines were generated using four different gRNAs. Successful deletion was confirmed by western blotting and genomic sequencing. The MLCK-KO cells were viable and grew well. However, the MLCK-KO cells were flatter and their nuclei had increased volume relative to control lines. Measurement of AQP2 phosphorylation using phospho-specific antibodies showed no difference versus control cells (western blotting). Measurements of AQP2 internalization with vasopressin withdrawal (immunofluorescence microscopy) were consistent with a decrease in AQP2 endocytosis. To assess the signaling pathways affected, we carried out quantitative phospho-proteomics of the MLCK-KO cells versus control cells (SILAC labeling). As expected, there was substantial decrease in phosphorylation of many phosphorylation sites. The decrease in myosin regulatory light chain phosphorylation was only ~40%, indicating that other kinases may substitute for MLCK. Interestingly, many phosphorylation sites showed increases in the MLCK-KO cells, indicating that MYLK may be involved in negative feedback on other kinases. These results indicate that MLCK 1) plays a critical role in AQP2 endocytosis; and 2) is involved in signaling pathways beyond its recognized role phosphorylation of myosin regulatory light chain.

$\alpha\text{M}\beta 2$ integrins mediate the formation of a focal adhesion-like cytoskeleton and signaling platform during phagocytosis. V. Jaumouillé, T.-L. Liu, E. Betzig, C.M. Waterman; Laboratory of Cell and Tissue Morphodynamics.

Professional phagocytes, such as macrophages and dendritic cells, form the first line of defense of the immune system. They constantly survey their environment and engulf unwanted material: infiltrated microbes, apoptotic cells and debris. Highly expressed in macrophages, $\alpha\text{M}\beta 2$ integrins are very promiscuous receptors, which bind the complement molecule iC3b, bacteria LSP, fungi β -glucan, fibrinogen, Factor X and ICAM-1, for instance. Consistently, $\alpha\text{M}\beta 2$ has been reported as the main entry route for many pathogens and participate in the clearance of the billions of cells that are turned over every day. However, the regulation of actin dynamics during $\alpha\text{M}\beta 2$ dependent phagocytosis remains largely unknown. Using live cell imaging, we observed that engagement of complement-coated particles lead to a very dynamic reorganization of the actin cytoskeleton, accompanied by ruffle formation and followed by contraction of the cortex. Moreover, phagosome formation leads to tyrosine phosphorylation of Paxillin, FAK and Syk, and the assembly of focal adhesion-like signaling platforms at the phagocytic cup, characterized by the recruitment of Vinculin, α -Actinin, Zyxin, Cortactin, Arp2/3 and Myosin II. In addition, contrary to previous

reports, we found that particle engulfment requires Src family kinases, Syk and FAK activities, as well as the Arp2/3 complex. Our observations suggest that engagement of $\alpha\text{M}\beta 2$ integrins leads to the formation of small focal adhesion-like molecular complexes that elicit polymerization of a highly dynamic branched actin network via a tyrosine kinase-Arp2/3 signaling pathway.

Having fun with shapes: α -Synuclein lipid tubules, ribbons and discs. Z. Jiang, J.C. Lee; Laboratory of Molecular Biophysics.

α -Synuclein (α -syn) is an abundant protein of ill-defined function enriched in the presynaptic terminals of neurons. However, its membrane binding property has been suggested in its function and dysfunction relating to Parkinson's disease. Recent studies have found that α -syn induces membrane tubulation in both anionic and zwitterionic lipids, such as POPG (1-palmitoyl-2-oleoyl-*sn*-glycero-3-phospho-(1'-rac-glycerol)) and POPC (1-palmitoyl-2-stearoyl-*sn*-glycero-3-phosphocholine). In this work, we investigated the effect of membrane fluidity on the membrane binding and remodeling by α -syn by using zwitterionic vesicles made with DMPC (1,2-dimyristoyl-*sn*-glycero-3-phosphocholine) and DPPC (1,2-dipalmitoyl-*sn*-glycero-3-phosphocholine). Since both lipids have high phase transition temperatures (T_m), they exist in a gel phase at RT. In contrast to anionic lipids, we found that α -syn binds to both DMPC and DPPC in their gel states, forming α -helix structure. While membrane binding is abolished upon raising the temperature above T_m , membrane remodeling occurs. As visualized by transmission electron microscopy, multilamellar DMPC vesicles are transformed by α -syn into various curved structures, including tubes, ribbons, vesicles, and nanodiscs. This process is dependent on lipid-to-protein ratio. We are extending this work to DPPC to study the effect of acyl chain length. Overall, these results further substantiate the ability for α -syn to bend membranes.

Genome-wide Detection of DNase I Hypersensitive Sites in Single Cells and FFPE Tissue Samples. W. Jin, Q. Tang, M. Wan, K. Cui, Y. Zhang, G. Ren, B. Ni, J. Sklar, T.M. Przytycka, R. Childs, D. Levens, K. Zhao; Laboratory of Epigenome Biology.

DNase I hypersensitive sites (DHSs) provide important information on the presence of transcriptional regulatory elements and the state of chromatin in mammalian cells. Conventional DNase-Seq for genome-wide DHSs profiling is limited by the requirement of millions of cells. Here we report an ultrasensitive strategy, called Pico-Seq, for detection of genome-wide DHSs in single cells. We show that DHS patterns at the single cell level are highly reproducible among individual cells. Among different single cells, highly expressed gene promoters and the enhancers associated with multiple active histone modifications display constitutive DHS while chromatin regions with fewer histone modifications exhibit high variation of DHS. Furthermore, the single-cell DHSs predict enhancers that regulate cell-specific gene expression programs and the cell-to-cell variations of DHS are predictive of gene expression. Finally, we apply Pico-Seq to pools of tumor cells and pools of normal cells, dissected from formalin-fixed paraffin-embedded (FFPE) tissue slides from thyroid cancer patients, and detect thousands of tumor-specific DHSs. Many of these DHSs are associated with pro-

motors and enhancers critically involved in cancer development. Analysis of the DHS sequences uncovers one single-nucleotide variant (*chr18:52417839 G>C*) in the tumor cells of a follicular thyroid carcinoma patient, which affects the binding of the tumor suppressor protein p53 and correlates with decreased expression of its target gene *TXNL1*. In conclusion, Pico-Seq can reliably detect DHSs in single cells, greatly extending the range of applications of DHS analysis for both basic and translational research and may provide critical information for personalized medicine.

Macrophage Deposition of Cholesterol into the Extracellular Matrix. X.T. Jin¹, D. Sviridov², Y. Liu¹, B. Vaisman², L. Addadi³, A.T. Remaley², H.S. Kruth¹; ¹Experimental Atherosclerosis Section, ²Lipoprotein Metabolism Section, ³Department of Structural Biology, Weizmann Institute of Science, Israel.

Atherosclerotic plaques develop as a result of an imbalance between cholesterol accumulation and cholesterol removal. How macrophages eliminate excess cholesterol has been of great interest, and is important for understanding the cholesterol accumulation process in developing atherosclerotic plaques. Our previous research has identified a novel macrophage cholesterol processing pathway, in which macrophages deposit excess cholesterol into the extracellular matrix where it can accumulate unless mobilized by HDL. Apolipoprotein A-I (ApoA-I) is the major protein component of HDL. In this study, we examined the function of ATP-binding cassette transporter A1 (ABCA1) in ApoA-I mobilization of cholesterol deposited into the extracellular matrix by cholesterol-enriched macrophages. We have also determined whether an ApoA-I mimetic peptide, 5A, can mobilize macrophage deposited cholesterol. Method: Human monocyte-derived macrophages and mouse bone marrow-derived macrophages with and without ABCA1 were cultured and cholesterol enriched. Extracellular cholesterol deposited by cholesterol-enriched macrophages was detected with a monoclonal antibody. Conclusions: Our findings show that extracellular cholesterol deposited by macrophages can be mobilized by both ApoA-I and 5A, but that mobilization depends on macrophage ABCA1. Importantly, ApoA-I mimetic peptide already complexed with phospholipid can mobilize the extracellular cholesterol even in the absence of ABCA1, suggesting that this cholesterol acceptor could have efficacy even when ABCA1 activity in atherosclerotic plaques is limited.

Rab22 and Arf6 Control T Cell Conjugate Formation through Regulation of the Clathrin-Independent Endosomal System. D. Johnson^{1,2}, J. Wilson², J. Donaldson¹; ¹Cell Biology and Physiology Center, ²Cellular and Molecular Medicine, University of Arizona.

The clathrin independent endosomal system is required for cellular homeostasis and specialized modifications of the plasma membrane like cell spreading and polarization. We have characterized Arf6-associated clathrin-independent endocytosis (CIE) in the human T cell line Jurkat. Our findings indicate that the CIE pathway is similar in this cell type including rates of internalization, recycling, and cargo sorting.

Two GTPases, Arf6 and Rab22, have been shown to regulate CIE and to play a role in cell spreading. We found that wild type and constitutively active Arf6 co-localized with CIE cargo in resting T cells. Rab22 also co-localized with CIE cargo at the

endocytic-recycling compartment. Expression of the dominant negative Rab22 mutant reduced internalization of MHC1 indicating it plays a direct role in CIE cargo internalization.

We then examined the role of Arf6 and Rab22 in T cell/antigen presenting cell conjugate formation. Expression of dominant negative Arf6 or Rab22 reduced T cell conjugate formation. Rab22 knockout cells were also incapable of forming conjugates. Cells expressing the dominant negative mutants of Arf6 and Rab22 were not able to spread on antibody-coated coverslips that normally cause T cell activation. This indicates that CIE is required for proper conjugate formation and T cell spreading during activation.

Our results confirm that CIE is a highly conserved process. The Arf6-associated clathrin-independent endosomal system is used by T cells to polarize membranes to the immunological synapse. Our findings suggest a requirement for Arf6 and Rab22 in mediating membrane trafficking and signaling events at the immunological synapse.

Recognition of a bacterial alarmone through long-distance association of two riboswitch domains. C.P. Jones, A.R. Ferré-D'Amaré; Laboratory of Ribonucleoprotein Biochemistry.

Purine biosynthesis is a nearly universal metabolic pathway culminating in the production of adenosine and guanosine. A purine biosynthesis intermediate that accumulates during purine or folate starvation, ZTP was proposed to act as an “alarmone” for folate stress more than 30 years ago. However, its cellular targets were a mystery until the recent discovery of ZTP riboswitches in bacteria. Often found in the 5′ untranslated regions of bacterial mRNAs, riboswitches are highly structured RNA motifs that regulate gene expression by adopting an alternative conformation when bound to a specific ligand. To understand how ZTP riboswitches achieve specificity to ZTP despite higher cellular concentrations of ATP or GTP, we have solved the structure of the *Fusobacterium ulcerans* ZTP riboswitch. Discrimination against purines occurs via interactions between ZTP and a Mg²⁺ ion, which sterically hinders purine binding. The overall structure of the ZTP riboswitch is composed of two domains connected by a flexible linker associating around ZTP at the domain-domain junction. Through isothermal calorimetric measurements of ZTP riboswitches with linker sequences lengthened by 5-100 nucleotides, we show that linker length modulates the apparent dissociation constant (*K_D*) of the *F. ulcerans* ZTP riboswitch by ~25-fold. Additionally, the two separately synthesized domains can also function *in trans* to bind ZTP with a *K_D* similar to that of the longest linker variants. These experiments suggest that the natural linker length variation in ZTP riboswitches tunes their affinity and that the longest linker variants are functionally equivalent to riboswitches operating *in trans*.

Novel Role of TFEB and TFE3 in Cellular Response to ER Stress. J.A. Martina, H.I. Diab, O.A. Brady, R. Puertollano; Protein Trafficking and Organelle Biology Group.

To reestablish homeostasis and mitigate stress, cells must activate a series of adaptive intracellular signaling pathways. The participation of the transcription factors TFEB and TFE3 in cellular adaptation to starvation is well established. In the present study we identify a novel role of TFEB and TFE3 in cellular response to endoplasmic reticulum (ER) stress. Treatment with ER stressors causes translocation of TFEB and TFE3 to the

nucleus in a process that is mTORC1-independent but requires PERK and calcineurin. Following activation, TFEB and TFE3 enhance cellular response to stress by inducing direct transcriptional up-regulation of ATF4, the master regulator of the Integrated Stress Response. Furthermore, TFEB and TFE3 target additional critical regulators of the Unfolded Protein Response (UPR), including genes implicated in ER function, redox homeostasis, and apoptosis. Unexpectedly, we found that TFEB and TFE3 promote cell death under conditions of prolonged ER-stress. This suggests that the duration of the stress shifts the role of these transcription factors from cell survival to apoptosis. Considering their extraordinary therapeutic potential, this novel role of TFEB and TFE3 in the control of cell fate is of critical importance. Overall, our work reveals a broader role for TFEB and TFE3 in cellular response to stress than previously recognized. The unique ability of these transcription factors to respond to changes in the activity of either mTORC1 or PERK makes them ideal modulators of the cross-talk between lysosomes and ER. Moreover, our study opens new venues for understanding the integrated cooperation between different cellular stress pathways.

Curvature Preference in Professional Phagocytes: A Mechanochemical Modeling Approach. S. Kale, J. Liu; Theoretical Cellular Physics.

Phagocytes rely on surface curvature information in order to decide on whether to internalize an external agent, or merely spread on the surface. This strategy is hard-coded in the mechanochemical machinery responsible for initiating and evolving the phagocytic cup; yet little is known about the precise spatiotemporal regulation of the process and how it is coupled to curvature sensing. We approach this challenge from a modular point of view where we regard engulfment as the result of a crosstalk between phosphoinositide (PI) chemistry and actin polymerization. In immunoglobulin receptor mediated phagocytosis, the PI 'module' regulates actin recruitment, which in turn applies the intricate forces needed to remodel the cell membrane. We hypothesize that PI chemistry itself is curvature-controlled as, e.g., a more exposed PIP2 head is more susceptible to dephosphorylation. At the heart of the model lies an energetically faithful and numerically stable representation of the phagocytic cell membrane, which has been the initial focus of present work.

Automated tracking and analysis of sleep-like behavior in *Drosophila* larvae. C. Kim¹, Q. Gaudry², S.T. Harbison¹; ¹Laboratory of System Genetics, ²Dept. of Biology, University of Maryland, College Park, MD.

Sleep is universally conserved among animals and invertebrates, but its purpose remains elusive. Although many studies have provided insights into the genetic architecture of sleep in adult flies, little is known about this behavior in the early developmental stages of the fly. Here we introduce a method based on machine vision to continuously measure kinematic parameters in third instar larvae during the first 4 hours of the dark cycle. We are measuring larvae from the *Drosophila* Genetic Reference Panel (DGRP) in order to associate genetic polymorphisms with rest and activity correlates. Preliminary results indicate that significant genetic variation among the lines is present for activity and rest measurements. This powerful approach enables the

construction of behavioral profiles of individual larvae using high-throughput behavioral screening.

High-resolution structural insight into the myosin VI-F-actin interface. L.Y. Kim^{*1}, P.S. Gurel^{*1}, T. Omabegho², Z. Bryant^{2,3}, G.M. Alushin¹; ¹Cell Biology and Physiology Center, ²Department of Bioengineering and ³Department of Structural Biology, Stanford University. ^{*}Equal contribution

The large superfamily of myosin motor proteins is responsible for movement and force generation at multiple scales of biology, ranging from muscle contraction to intracellular transport. While the mechanism of actomyosin has been subject to extensive biophysical, biochemical, and structural characterization, to our knowledge no experimental high-resolution structure has been obtained of a myosin-F-actin interface, a major gap in the complete mechanistic characterization of myosins. Making use of recent methodological developments in cryo-EM, here we present a 4.5 Å resolution reconstruction of an engineered myosin VI, an unconventional minus-end directed motor, in a nucleotide-free state bound to F-actin. We observe rearrangements in both the myosin motor domain and actin relative to structures of these components in isolation, suggesting a reciprocal relationship between actin and myosin conformation during force generation. In addition to providing mechanistic insights specific to myosin VI, this study paves the way for high-resolution structural analysis of diverse actomyosin complexes.

Dramatic Radiation Dose Reduction over 7 Years of Experience for Coronary CT. A. Knab, D. Melo, J. Yu, D.W. Groves, E.A. Nelson, K. Bronson, M. Stagliano, S. Rollison, A.D. Choi, S.M. Shanbhag, M.Y. Chen; Advanced Cardiovascular Imaging Group.

Cardiac computed tomographic angiography (CCTA) is a well-established diagnostic modality in the risk stratification of coronary artery disease. However, CT still represents a major source of ionizing radiation. Constant efforts to obtain as low as reasonably achievable radiation doses have included aggressive heart rate control, patient specific tube voltage and tube current selection, prospective gating, and the utilization of iterative reconstruction and other post-processing techniques. The purpose of this study was to analyze radiation dose trends in cardiac CT over the last 7 years in the context of these efforts. 3,140 ECG-gated coronary CT exams were performed on a 320-detector row scanner between January 2009 and September 2015. The median radiation dose progressively decreased over time and represented a 71% reduction over 7 years from 5.8 mSv (IQR 4.2-11.3) in the first 6 months to 1.7 mSv (IQR 0.9-3.0) in the last 6 months. During this observation period, the patient body mass index did not change over time. The use of lower kVp settings increased during the seven year time period where 100 kVp was utilized 9.8% of the time within the first year and increased to 69.3% in the seventh year. Additionally, x-ray exposure time decreased over time: 0.6 seconds (IQR 0.44-1.13) within the first year and 0.29 seconds (IQR 0.28-0.34) in the last year. Progressive reduction in radiation exposure at a single center is achievable by utilizing radiation dose saving measures such as meticulous patient preparation, lower tube potential, shorter x-ray exposure times and iterative reconstruction techniques.

A New Energy Potential for Solvent Paramagnetic Relaxation Enhancements (sPRE) in XPLOR-NIH. H. Kooshapur¹, N. Tjandra¹, C. Schwieters²; ¹Laboratory of Molecular Biophysics, ²Division of Computational Bioscience, Center for Information Technology, NIH.

Nuclear Magnetic resonance (NMR) is a powerful method for characterizing the three-dimensional structure and dynamics of biological macromolecules in solution. However, a major bottleneck in structure determination by NMR is that the number of available distance restraints is limited. One source of additional distance restraint is paramagnetic relaxation enhancement (PRE) obtained from soluble paramagnetic probes, generally known as solvent PRE (sPRE). sPRE data can provide important information about the solvent accessibility, structure and dynamics of macromolecules. Currently, however, the application of sPRE data is limited due to lack of a practical computational framework for using sPREs in NMR structure calculation. Here, we have implemented a new energy potential for sPRE in the structure calculation program XPLOR-NIH and tested it on several experimental sPRE datasets obtained from proteins and protein complexes. This new energy potential for sPRE will be applicable to NMR protein structure refinement and validation as well as docking of macromolecular complexes.

Genome-wide identification of H2A.Z-interacting proteins by bPPI-seq. W. Ku, Y. Zhang, K. Cui, W. Jin, Q. Tang, W. Lv, B. Ni, K. Zhao; Laboratory of Epigenome Biology.

Histone variant H2A.Z is a critical player in setting up the chromatin environment that mediates transcription and other activities on chromatin. However, how H2A.Z is incorporated to specific chromatin regions is not clear. To examine the potential role of sequence-specific transcription factors in targeting H2A.Z, we screened for genome-wide H2A.Z-interacting proteins *in vivo* using a novel technique called bait Protein-Protein Interaction-sequencing (bPPI-seq). Among the hundreds of H2A.Z-interacting proteins identified by bPPI-seq, we show that a zinc-finger transcription factor, Osr1, interacts with H2A.Z both *in vitro* and *in vivo* and co-localizes with H2A.Z on chromatin. Knockdown of Osr1 compromised H2A.Z deposition to hundreds of chromatin sites enriched with Osr1 binding motifs. Furthermore, Osr1 and H2A.Z co-regulate the expression of numerous target genes. These results indicate that Osr1 directly interacts with H2A.Z, mediates its incorporation to a large number of target sites and regulates gene expression. Our data indicate that bPPI-seq can be widely applied to identify unbiasedly interacting proteins under physiologic conditions.

Global Organization of a Protein Binding Site Network. J. Lee, J. Konc, D. Janežič, B.R. Brooks; Laboratory of Computational Biology.

The global organization of all known protein binding sites is analyzed by constructing a weighted network of binding sites based on their structural similarities and detecting communities of structurally similar binding sites based on the minimum description length principle. The analysis reveals that all binding sites are categorized into about 300 communities. The largest community consists mainly of metal binding sites, particularly Zn²⁺ binding sites, and plays the role of the structural hub of other sites. We found that the sizes of communities follow a power-law distribution, which means that a few dominantly large

and many small communities co-exist. The power-law distribution implies that the binding sites included in the largest communities may be the most ancient binding sites in existence. We also found that larger binding site communities tend to bind to more diverse ligands and be embedded in more diverse backbone structures.

Nonmuscle Myosin II-A Plays a Role in Spermatid Elongation. C.B. Lerma Cervantes¹, M.A. Conti¹, K. Tokuhito², Y. Zhang¹, M.J. Kelley³, R.S. Adelstein¹; ¹Laboratory of Molecular Cardiology, NHLBI, ²Laboratory of Cellular and Developmental Biology, NIDDK, ³Division of Medical Oncology, Duke University.

During spermiogenesis, male mice undergo a complex nuclear-cytoplasmic remodeling process where round spermatids must: elongate their nuclei, eliminate their cytoplasm, and develop the acrosome and tail structures necessary for fertilization. During this process, the spermatid develops an F-actin containing cytoskeletal plate, the acroplaxome. Furthermore, the acroplaxome anchors the acrosomal vesicle to the nuclear lamina. Although it is also thought the acroplaxome may play a role in sperm head shaping, the mechanism whereby this is achieved is poorly understood. Herein we describe a mouse line with a mutation in nonmuscle myosin II-A (NM II-A), E1841K, found in human MYH9-related disease. In addition to modeling MYH9-related disease male mice homozygous for the mutation (A^{E1841K}/A^{E1841K}) are sterile. Histological analyses and transmission electron microscopy of the A^{E1841K}/A^{E1841K} mouse testes show severely impaired spermatid elongation. In the aberrant spermatids, the acroplaxome fails to correctly extend the developing acrosome. In addition, there is also failure in coupling of the tail to the spermatid head. Moreover, immunofluorescence confocal microscopy of both wild type and mutant developing round spermatids shows localization NM II-A to the acroplaxome. However, the mutant NM II-A acroplaxome often shows an irregular wave-like appearance not seen in the wild type. These observations suggest wild type NM II-A is required for proper spermatid nuclear-cytoplasmic remodeling and male fertility, both previously unknown functions for NM II-A.

Improvement in psoriasis skin disease severity is associated with reduction of coronary plaque burden. J.B. Lerman, A.A. Joshi, J. Rodante, T. Aberra, M.T. Kabbany, T. Salahuddin, Q. Ng, J. Silverman, M.Y. Chen, D.A. Bluemke, N.N. Mehta; Section of Inflammation and Cardiometabolic Diseases.

Psoriasis (PSO), a chronic inflammatory disease associated with increased cardiovascular (CV) risk, provides a clinical human model to study inflammatory atherogenesis. While PSO severity is associated with *in vivo* vascular disease and future CV risk, the longitudinal impact of PSO severity on coronary disease progression is unknown. We hypothesized that an improvement in PSO severity may lead to a reduction in coronary plaque burden by coronary CT angiography (CCTA).

Consecutively recruited PSO patients (N=50) underwent CCTA (320 detector row, Toshiba) and cardiometabolic profiling at baseline and 1-year follow-up. Total (TB) and non-calcified (NCB) coronary plaque burden were quantified using QAngio (Medis, Netherlands). PSO severity was measured by PSO area severity index (PASI). The longitudinal change in cor-

onary plaque burden was analyzed with unadjusted and adjusted regression.

The cohort had a low Framingham Risk Score and mild to moderate PSO. Patients whose PASI improved (Δ PASI -27%; $p < 0.001$) (N=33) had significant improvement in TB ($\beta = 0.40$, $p = 0.003$) and NCB ($\beta = 0.49$, $p < 0.001$) (Table 1) beyond adjustment for traditional CV risk factors, BMI, statins, & systemic/biologic PSO therapy.

Improvement in PSO severity was associated with improvement in coronary plaque burden by CCTA. Our study suggests that a reduction in skin inflammation may reduce progression of early, non-calcified plaque. Larger studies are needed to confirm these findings.

Local hypoxia controls neuro-vascular patterning through CXCL12 and VEGF-A in the developing skin. W. Li, Y. Mukouyama; Laboratory of Stem Cell and Neuro-Vascular Biology.

The vascular system and peripheral nervous system share several anatomical characteristics and are often patterned similarly. We have previously demonstrated that sensory nerves determine the arterial branching pattern in the developing skin. At the molecular level, nerve-derived CXCL12 functions as a patterning factor to control vessel branching and alignment with nerves, and nerve-derived VEGF-A functions as a differentiation factor to control arterial differentiation. In this study, we seek to understand what specifies the correct timing of these angiogenic signals in order to form the stereotypical branching pattern of the neuro-vascular network. Consistent with the previous observation that *Cxcl12* and *Vegf-a* are hypoxia-induced genes, local hypoxia is detectable in/around the nerves prior to the establishment of the nerve-artery alignment in the skin and the oxygen-starved dorsal root ganglia (DRG) containing sensory neurons and glia enhance the expression of *Cxcl12* and *Vegf-a* in culture. Interestingly, hypoxia inducible factors (HIFs) appear not to enhance the *Cxcl12* and *Vegf-a* expression in response to hypoxia in the DRG culture. Rather, NF-kappaB signaling enhances CXCL12 expression and cAMP-response Element-Binding Protein (CREB) signaling activates VEGF expression in the hypoxic DRG culture. In order to examine whether these signaling pathways control the nerve-vessel alignment and arterial differentiation in the skin, we are currently generating mutant mice carrying sensory nerve-specific inactivation of NF-kappaB and CREB signaling pathways. These experiments will open up new areas of research about the regulation of vascular branching morphogenesis and patterning by the metabolic microenvironment.

Rapamycin stimulates regulatory T cells in a mouse model of immune-mediated bone marrow Failure. Z. Lin, W. Sun, M. Hollinger, J. Chen, X. Feng, N.S. Young; Hematology Branch.

Decreased number of CD4⁺CD25⁺Foxp3⁺ regulatory T (Treg) cells is associated with impaired immune homeostasis leading to the development of autoimmune diseases such as aplastic anemia (AA). In the current study, we tested therapeutic efficacy of two immunosuppressive agents, rapamycin (Rapa) and cyclosporine A (CsA), for the treatment of AA using an immune-mediated AA mouse model we previously developed. Infusion of lymph node (LN) cells from C57BL6-DsRed donors to sub-lethally-irradiated C.B10 recipients induced AA with se-

vere pancytopenia and bone marrow (BM) hypoplasia at 14 days following LN cell infusion. Treatment with 2 mg/kg/day of Rapa through intraperitoneal injection for 11 days significantly increased red blood cells, blood platelets and total BM cells, with an efficacy much higher than treatment with 50 mg/kg/day CsA ($P < 0.05$). In defining cellular mechanisms responsible for Rapa's superior therapeutic effect, we examined cellular composition in the BM and found a significantly higher percentage of Treg cells in CD4⁺ T cells and in total CD3⁺ T cells in Rapa-treated than in CsA-treated AA mice ($P < 0.01$). AA mice treated with Rapa also had higher CD4/CD8 T cell ratio ($P < 0.01$) than untreated AA mice or the mice treated with CsA. We conclude that Rapa is a superior therapeutic agent relative to CsA for the treatment of AA, as it selectively stimulates immunosuppressive Treg cells.

MICU1 Serves as a Molecular Gatekeeper to Prevent *in vivo* Mitochondrial Calcium Overload. J.C. Liu, J. Liu, K.M. Holmström, S. Menazza, R.J. Parks, M.M. Fergusson, Z.X. Yu, D.A. Springer, C.H. Halsey, C. Liu, E. Murphy, T. Finkel; Laboratory of Molecular Biology.

MICU1 is a component of the mitochondrial calcium uniporter, a multiprotein complex that regulates entry of mitochondrial calcium. Patients lacking MICU1 develop severe neurological symptoms, along with a proximal myopathy. Here, we describe a mouse model of MICU1 deficiency. Mitochondria or cells isolated from MICU1^{-/-} mice demonstrate altered calcium handling with increased uptake rates at low calcium concentrations and reduced uptake rates at high calcium concentrations. In mice, the absence of MICU1 expression results in significant perinatal mortality with less than one in six MICU1^{-/-} animals surviving into adulthood. Similar to afflicted patients, surviving MICU1^{-/-} mice exhibit marked ataxia and muscle weakness. These animals also exhibit increased levels of mitochondrial calcium, altered mitochondrial morphology, elevated tissue lactate levels, reduced ATP, and increased levels of mitochondrial reactive oxygen species. In an effort to confirm the role of calcium overload in these phenotypes, we generated additional mice with a targeted deletion in EMRE, another essential component of the uniporter. Remarkably, the absence of one allele of EMRE rescued the marked perinatal mortality observed in MICU1^{-/-} mice. Furthermore, EMRE haploinsufficiency restored gatekeeping function to MICU1^{-/-} mitochondria, lowered mitochondrial calcium levels and significantly improved the biochemical, neurological and myopathic features observed in MICU1^{-/-} mice. These results demonstrate that the primary function of MICU1 is to prevent *in vivo* mitochondrial calcium overload. It further suggests that manipulating calcium uniporter activity might provide a strategy to treat patients lacking MICU1, as well as for the growing number of other conditions characterized by mitochondrial calcium overload.

Generation of Rhesus Monkey iPSC-derived Endothelial Cells. Y. Liu¹, Z. Yu¹, Y. Huang¹, H. Liu¹, Y. Lin², J. Zou², H. San³, C. Dunbar⁴, G. Chen¹, M. Boehm¹; ¹Laboratory of Cardiovascular Regenerative Medicine, ²IPS Core, ³Animal Program, ⁴Hematology Branch.

Endothelial cells form a monolayer covering the luminal surface of all vessels, and play a significant role in angiogenesis, modulation of smooth muscle cell function, and regulation of vascular responses to hemodynamic forces. Endothelial cell dys-

function contributes to cardiovascular diseases, including coronary heart disease, myocardial infarction, and other ischemic processes. Embryonic-derived or induced-pluripotent stem cell-derived endothelial cells are a promising regenerative medicine tool to study cardiovascular disease phenotypes. In contrast to rodent models, the nonhuman primate Rhesus monkey is an excellent preclinical transplantation model for modeling human disease. We developed a protocol for the generation of endothelial cells from Rhesus monkey induced pluripotent stem cells (RiPSCs). These Rhesus monkey iPSC-derived endothelial cells (RiECs) display phenotypic endothelial cell markers, possess a similar capacity for tube-like structure formation, and uptake acetylated low density lipoprotein (acLDL), as compared to primary endothelial cells. In a xenograft assay, co-injection of RiECs and tumor cells increased tumor burden, suggesting that the RiECs promote tumor angiogenesis. Histological analysis of xenograft tumors is ongoing. To investigate the potential role of our RiECs as a therapy for ischemic diseases, we injected RiECs in a hind limb ischemia mouse model and found that RiECs can partially rescue the ischemic area. Taken together, we have successfully developed a method to generate RiECs from RiPSCs that are readily expandable, possess characteristic endothelial cell phenotypes, and display similar *in vitro* and *in vivo* functional capabilities compared to HUVEC controls. Future studies will assess the ability of RiECs to promote RiPSC-derived cardiomyocytes proliferation and maintenance *in vitro* and *in vivo*.

Erk regulation of actin capping and bundling by Eps8 promotes cortex tension and leader bleb-based migration.

J.S. Logue^{1,2}, A.X. Cartagena-Rivera², M.A. Baird¹, M.W. Davidson³, R.S. Chadwick², C.M. Waterman¹; ¹Laboratory of Cell and Tissue Morphodynamics, ²NIDCD, ³National High Magnetic Field Laboratory and Department of Biological Science, The Florida State University.

Within the confines of tissues, cancer cells can use blebs to migrate. Eps8 is an actin bundling and capping protein whose capping activity is inhibited by Erk, a key MAP kinase that is activated by oncogenic signaling. We tested the hypothesis that Eps8 acts as an Erk effector to modulate actin cortex mechanics and thereby mediate bleb-based migration of cancer cells. Cells confined in a non-adhesive environment migrate in the direction of a very large 'leader bleb.' Eps8 bundling activity promotes cortex tension and intracellular pressure to drive leader bleb formation. Eps8 capping and bundling activities act antagonistically to organize actin within leader blebs, and Erk mediates this effect. An Erk biosensor reveals concentrated kinase activity within leader blebs. Bleb contents are trapped by the narrow neck that separates the leader bleb from the cell body. Thus, Erk activity promotes actin bundling by Eps8 to enhance cortex tension and drive the bleb-based migration of cancer cells under non-adhesive confinement.

Artificial actin-binding proteins with novel multifunctional properties.

A. Lopata, C. Tiede, D.C. Tomlinson, J.R. Sellers, P.J. Knight, M. Peckham; Laboratory of Molecular Physiology.

Actin filaments are traditionally labelled with antibodies, phalloidin, or directly functionalized to bind dyes or biotin. We have developed a new approach, which uses Adhirons, small (~12kDa), non-antibody proteins that have specific and tight binding to the protein of interest (Tiede et al., 2014). The ad-

vantage of using Adhirons is that these proteins are small, and once isolated by screening, can be expressed and purified using *E. coli*, or expressed as GFP-tagged constructs in mammalian cells for functional studies.

We isolated four actin binding Adhirons (Adh2, 6, 14 and 24) by phage display assay. Measurements of their binding affinity to F-actin, using actin spin-down assays, showed a tight binding (K_d less than 0.5 μ M) for three of the Adhirons (Adh6, 14 and 24). These three Adhirons seem to bind to distinct binding sites on F-actin, however myosin-5 subfragment 1 (S1) competes all of them off F-actin. They also inhibit myosin-5 actin-activated ATPase activity, which might be a consequence of reduced binding sites available on F-actin due to actin bundling. GFP-tagged versions of Adh6, 14 and 24 stain actin and localize to distinct cellular structures, when expressed in live cells.

As these proteins are small, easy to express and are already proven to bind to actin effectively, they are likely to be useful as a new approach to label actin, not only in fluorescence microscopy, but in *in vitro* assays, such as attaching actin filaments to glass slides for *in vitro* motility assays, or to plastic beads for optical trapping assays.

Biophysical assays to detect the interaction between alpha globin and eNOS.

D. Ma, H. Ackerman; Sickie Cell Branch.

Alpha globin, a subunit of red blood cell hemoglobin, is also expressed in human and mouse resistance artery endothelial cells. Qualitative protein-protein interaction methods have been used to identify a macromolecular complex that forms between alpha globin and endothelial nitric oxide synthase (eNOS). The purpose of this work is to characterize the interaction between alpha globin and eNOS quantitatively using biophysical methods. To this end, alpha globin was purified from whole hemoglobin using ion exchange chromatography and the purity was assessed by Mass spectrometry. The oxygenase of eNOS was expressed in PGEX vector and UT5600 *E. Coli* system. Ultracentrifugation and two-step ammonium sulfate fractionation were performed to purify the eNOS oxygenase. Further, the ForteBio Octet system was used to identify the binding characterization of purified alpha globin with eNOS. The results showed that alpha globin binds with the eNOS oxygenase domain with lower affinity compared to the interaction between alpha globin and its molecular chaperon α -Hemoglobin stabilizing protein. Detailed binding characterization is being investigated to calculate the kinetics and will improve our understanding of endothelial alpha globin function.

Using Whole-Exome Sequencing to Identify Genetic Variants in Patients Diagnosed with Pentalogy of Cantrell.

B. MacTaggart, C. Bowen, M. Markowitz, J. Chong, M.J. Bamshad, X. Ma, R.S. Adelstein; Laboratory of Molecular Cardiology, University of Washington Centers for Mendelian Genomics.

Pentalogy of Cantrell (POC) is a developmental disorder estimated to occur in 1-5.5 per 1 million live births with a 61% survival rate. The syndrome includes five features: 1) a defect in sternal fusion, often resulting in *ectopia cordis*, 2) a diaphragmatic hernia, allowing the abdominal organs to protrude into the thoracic cavity, 3) a weakened abdominal wall, often resulting in an omphalocele, 4) a missing pericardium, and 5) structural and valvular defects in the heart. Our laboratory has generated mice with a point mutation (R709C) in the non-muscle myosin IIB

heavy chain (encoded by the gene *Myb10*) which phenocopy the human POC. Generation of the mouse model prompted us to initiate a clinical study in humans in which we conducted whole-exome sequencing of POC patients and their parents to determine a possible genetic etiology for POC. The twenty-four probands in our study to date range from 1 day to 31 years of age at time of enrollment and exhibit different subsets of the five characteristic features of the disorder. We filtered for rare variants in the exome data that segregated with POC in each family. To date, we have identified one rare variant in the teneurin-4 gene (*TENM4*), which appears to exhibit incomplete penetrance for POC. We are also currently investigating a number of *de novo* variants identified in POC patients born to unaffected parents. To interpret the results, we are developing genetic and protein-interaction networks in order to understand the mechanism(s) underlying POC.

Imaging adipose tissue across scales of resolution: from two-photon to super-resolution microscopy. D. Malide; Light Microscopy Facility.

Adipocyte cell size, shape, and number have a modulating effect on their metabolism and hormone actions and, therefore, morphological approaches that allow probing adipose cells in their native environment became highly desirable. As a step toward this goal, we developed imaging approaches using two-photon microscopy, which enable simultaneous high resolution assessment of specifically fluorescently marked cells in conjunction with structural components of the adipose tissue. We employed a series of strategies based on ex-vivo fluorescent vital-dye labeling, the use of fluorescent proteins genetically expressed and tracking label-free cells via second and third harmonic generation microscopy (SHG, THG). These enabled high resolution depth-resolved imaging of whole mount, intact adipose tissue without the need for physical sectioning. Thus 3D-architecture of adipose cells, extensive blood vasculature and collagen fibers networks were visually dissected over large areas. Quantitative analysis of adipose cell size and relationship to blood vessels in intact tissue indicated differential distribution of smaller cells near the blood vessels and outlining the periphery of clusters of internally-located larger adipose cells. Furthermore, THG interface signals, outlining cell membranes and tissue inhomogeneities, revealed clearly demarcated lipid droplets, blood vessels and cells, and myelinated peripheral nerves. In another scale, we imaged using super-resolution STED microscopy freshly excised adipose tissue for a detailed assessment of subcellular compartments including mitochondria, endoplasmic reticulum, lysosomes, using vital-dyes or genetically-expressed fluorescent proteins. Together these techniques bring new possibilities for a comprehensive examination of the adipose tissue at different scales of resolution.

Molecular mechanisms of coupled transport in secondary transporters: lessons from a $\text{Na}^+/\text{Ca}^{2+}$ exchanger. F. Marinelli, J. Liao, C. Lee, Y. Huang, Y. Jiang, J. D. Faraldo-Gómez; Theoretical Molecular Biophysics Section.

Secondary-active transporters catalyze the uptake and efflux of substances across biological membranes, driven by the electrochemical potential gradient of one of the transported species, typically Na^+ or H^+ . The mechanism of these transporters has been widely rationalized in terms of the alternating-access model,

i.e. their inherent ability to undergo a conformational cycle that exposes one or more substrate binding sites within the protein to one or the other side of the membrane (or none), but not both simultaneously. In contrast to other membrane proteins whose conformation is dependent on transmembrane potentials, e.g. voltage-gated ion-channels, secondary transporters do not require a driving force to interconvert between different conformational states; an electrochemical gradient is however required to drive their conformational cycle in one specific direction. Instead, the energizing of transport relies on a seemingly simple principle - that is, the interconversion between outward and inward facing states requires that the appropriate type of substrates be recognized, in uniquely defined stoichiometries. The physical basis of this mechanism of conformational control, however, remains to be established. Here, we address this central question for a prokaryotic homolog of the cardiac $\text{Na}^+/\text{Ca}^{2+}$ exchanger, NCX_Mj, which transports either three Na^+ or one Ca^{2+} across the membrane, in either direction. Specifically, we focus on the step of the ion-exchange cycle leading to inward $\text{Na}^+/\text{Ca}^{2+}$ translocation, and determine how $\text{Na}^+/\text{Ca}^{2+}$ recognition by the outward-facing state of the transporter reshapes its conformational free-energy landscape, which we examine via enhanced-sampling molecular-dynamics simulations and crystallographic titration experiments. Our results demonstrate that only upon binding of three Na^+ or one Ca^{2+} can the protein adopt a state occluded to both sides of the membrane, which necessarily precedes the transition to the inward-facing conformation. Partial or complete depletion of the binding sites (e.g. 2 Na^+ , or no ion at all) and/or H^+ binding, by contrast, eradicates the population of the occluded state, and induces the opening of hydrated access pathways connecting these sites to the surrounding solution. This study provides clear evidence that it is by inducing or precluding the formation of occluded, dehydrated states that substrate recognition controls the alternating-access transition in secondary transporters.

Cysteine Cathepsins Are Essential in Lysosomal Degradation of α -Synuclein. R.P. McGlinchey, J.C. Lee; Laboratory of Molecular Biophysics.

A cellular feature of Parkinson's disease is cytosolic accumulation and amyloid formation of α -synuclein (α -syn), implicating a misregulation or impairment of protein degradation pathways that involve the proteasome and lysosome. Within lysosomes, the aspartyl protease, Cathepsin D (CtsD) is thought to be the only lysosomal protease implicated in α -syn proteolysis. However, *in vitro* experiments only generate amyloid-forming truncated C-terminal species suggesting that other proteases are likely involved in this process. Here, we show that in addition to CtsD activity purified mouse brain and liver lysosomes harbor cysteine cathepsin activity identified as CtsB and L by using liquid chromatography mass spectrometry. For the first time, the complete degradation process of α -syn in lysosomal extracts has been peptide mapped. Selective protease inhibition experiments show that CtsL activity is essential for generating short peptides that are not aggregation prone. Unexpectedly, we discovered that CtsL is efficient in degrading α -syn amyloid fibrils, which by definition are resistant to broad spectrum proteases. More recently, we have focused our efforts on assessing how α -syn binding partners e.g. the lysosomal hydrolase glucocerebrosidase affects α -syn degradation.

Bayesian Analysis of E3 Ubiquitin Ligase/AQP2 Interactions in the Renal Collecting Duct. B. Medvar^{1,2}, A. Sarkar², M. A. Knepper¹; ¹Epithelial Systems Biology Laboratory, ²Vitreous State Laboratory, The Catholic University of America.

Aquaporin-2 (AQP2) is regulated in part via vasopressin-mediated changes in protein half-life that are in turn dependent on AQP2 ubiquitination. Here we addressed the question, “What E3 ubiquitin ligase is responsible for AQP2 ubiquitination?” using large-scale data integration based on Bayes’ Rule. The first step was to bioinformatically identify all E3 ligase genes coded by the human genome. The 377 E3 ubiquitin ligases identified in the human genome, consisting predominantly of HECT, RING, and U-box proteins, have been used to create a publicly accessible and downloadable online database. We also curated a second database of E3 ligase accessory proteins that included BTB domain, proteins, cullins, SOCS-box proteins, and F-box proteins. Using Bayes’ Theorem to integrate information from multiple large scale proteomic and transcriptomic datasets, we ranked these 377 E3 ligases with respect to their probability of interaction with AQP2. Application of Bayes’ Rule identified the E3 ligases most likely to interact with AQP2 as in order of probability: NEDD4 and NEDD4L (tied for first), AMFR, STUB1, ITCH, ZFPL1. Significantly, the two E3 ligases tied for top rank have also been studied extensively in the reductionist literature as regulatory proteins in renal tubule epithelia. The concordance of conclusions from reductionist and systems-level data provides strong motivation for further studies of the roles of NEDD4 and NEDD4L in the regulation of AQP2 protein turnover.

Spectrum of Cardiovascular Involvement in Erdheim-Chester Disease Evaluated by Cardiac Computed Tomography. D. Melo, A. Knab, S.M. Shanbhag, W.A. Gahl, J.I. Estrada-Veras, M.Y. Chen; Advanced Cardiovascular Imaging Group.

Erdheim Chester Disease (ECD) is a rare type of non-Langerhans cell histiocytosis characterized by accumulation of foamy macrophages and fibrosis. Clinical manifestations vary depending on the organs involved and include bone pain, exophthalmos, interstitial lung disease, renal failure and diabetes insipidus. Patients with multisystem manifestations and organ failure carry a poor prognosis with more than half of patients dying from cardiac complications. Since cardiac manifestations are often silent, advanced imaging techniques are required to elucidate involvement. The purpose of this study was to characterize the prevalence and spectrum of cardiac CT findings in ECD patients. A total of 58 consecutive patients (75% male, age 52±11 years, range 19-72 years) with biopsy proven Erdheim-Chester Disease underwent contrast enhanced cardiac CT on a 320-detector row scanner. Images were evaluated for cardiovascular involvement. Overall, 40% (23/58) of the patients had cardiovascular involvement. The most common manifestation was “pseudo-tumor” or a homogenous soft tissue density involving the right atrioventricular groove (91%; 21/23, Figure 1). Other locations include the right atrium (87%; 20/23), interatrial septum (26%; 6/23), right ventricle (9%; 2/23), left atrium (4%; 1/23), and pericardium (4%; 1/23). Three patients (5%; 3/58) had a pericardial effusion. Six patients examined (10%; 6/58) had circumferential periaortic thickening or a “coated aorta” in visualized portions of the descending aorta (Figure 1). Cardiovascular involvement of Erdheim Chester Disease is not infre-

quent (40%) and the most common feature is pseudo-tumor involvement of the right atrioventricular groove enveloping the right coronary artery; however, there is a spectrum of other manifestations.

Low Concentration Xyloside Treatment Alters GAG Profile and Morphology in Neural Cells. C. Mencia, C. Agbaegbu, H. Katagiri, H. Geller; Developmental Neurobiology Group.

Proteoglycans play an important role in development and injury in the nervous system. Xylosides are small molecules consisting of a xylose residue linked to an aglycone which serve as competitors for the biosynthetic enzymes in the Golgi which construct the glycosaminoglycan (GAG) side chains found on proteoglycans. At high concentrations (>100uM), xylosides inhibit the formation of GAGs on the core protein and have been shown to alter several aspects of cellular function. The most commonly used concentrations in research are in excess of 1mM, however few studies have examined how lower concentrations affect cells. Using the 4-methyl-umbelliferyl-β-D-xylopyranoside, we compared 1μM xyloside treatment with the traditionally used 1mM treatment in Neuro2A, primary astrocytes and neuron cultures. These cultures were assessed after 72h of treatment. We found that all concentrations of xyloside compete and induce protein-free GAG chain formation. In addition to known GAG inhibition by high concentration, changes in the endogenous sugars can be observed after low concentration treatment. Neuronal morphology is also altered by low concentration treatment. Hippocampal neurons treated *in vitro* resulted in exaggerated growth cones and altered cytoskeletal elements in neurites. It remains unclear if these morphological changes are the result of altered sugar structure or a secondary target of xylosides exists that is revealed when using lower concentrations. These results emphasize the importance of how sugars contribute to neural development, function and repair as well as highlight our need to better understand the possible targets and functions of xylosides in modulating GAG biosynthesis and cellular proteoglycan production.

Single Molecule Measurements of DNA Decatenation by the Topoisomerase III-RecQ Helicase Complex. M. Mills, K.C. Neuman; Laboratory of Single Molecule Biophysics.

Topoisomerase III (Topo III) is an ATP-independent enzyme that cleaves a single strand of duplex DNA to relieve torsional strain. Topo III is able to unlink DNA catenanes if one strand contains a single stranded region, but not if both strands are intact. Topo III, however, can decatenate intact DNA when RecQ helicase is present. *In vivo* this complex is involved in resolution of late replication intermediate linkages and double Holliday junctions. The unique functions of the Topo III-RecQ complex have been shown to be important for preserving genome stability.

We directly measured the effect of RecQ on Topo III’s decatenase activity using a magnetic tweezer assay in which two strands of DNA attached to a single bead are interwound to produce a DNA braid. These DNA braids topologically mimic catenated DNA and thus provide an ideal substrate for measuring unlinking at the single molecule level. We tested the effect of RecQ on the rate of Topo III decatenation and unwinding activity. In addition we measured decatenation of intact DNA by the RecQ-Topo III complex. We compared these results to the ef-

fect of RecQ on two other topoisomerases that decatenate DNA but are not known to interact with RecQ: topoisomerase I, which acts on DNA with a single stranded region, and topoisomerase IV, which acts on intact DNA. We also probed the effect of crossover geometry on the decatenation activity of the Topo III–RecQ complex. Our results provide insight into the nature of the functional interaction between Topo III and RecQ.

Receptor Associated Protein (RAP) Abrogates House Dust Mite-induced Experimental Asthma by Attenuating Dendritic Cell Function. A. Mishra¹, P.K. Dagur², J.P. McCoy², K.J. Keeran³, G.Z. Nugent³, K.R. Jeffries³, X. Qu⁴, Z.X. Yu⁴, S.J. Levine¹; ¹Laboratory of Asthma and Lung Inflammation, ²Flow Cytometry Core Facility, ³Animal Surgery and Resources Core Facility, ⁴Pathology Core Facility.

The endocytic and cell signaling receptor, LDL-receptor related protein 1 (LRP-1), is a member of the low density lipoprotein receptor (LDLr) family and plays important roles in a number of physiological and pathological processes. Receptor-associated Protein (RAP), a 39 kDa molecular chaperone, binds and efficiently delivers LRP-1 and other LDLr family members to the cell surface. Furthermore, RAP inhibits binding of all ligands to LRP-1. However, there is limited information regarding the role of LRP-1 in adaptive immunity mediated by dendritic cells (DCs), which are the primary antigen-presenting cell in allergic asthma. In LRP-1 expressing DCs, proinflammatory mediator expression is regulated by LRP-1 ligands in a ligand-specific manner. Here, we show in a DC-driven murine allergic asthma model that adoptive transfer of RAP-treated DCs to the lung suppresses house dust mite (HDM)-induced airway inflammation. Recipients of adoptively transferred HDM-pulsed DCs that were treated with RAP had significant reductions in BALF eosinophils (47%), alveolar macrophages (48.5 %), and lymphocytes (67.8 %) as compared with recipients of HDM-pulsed medium alone. Also, bone marrow-derived DCs treated with RAP had 32%, 28.6%, and 45% lower cell surface expression of CD86, CD40L, and MHCII, respectively, which indicates that RAP impaired DC activation and maturation. These data support the concept that using RAP to block ligand binding to LRP-1 on airway DCs might be developed into a new treatment approach for allergic asthma.

The Combination of ACP-196 and ACP-319 Leads to Increased Survival in the TCL1-192 CLL Mouse Model. H. Mora-Jensen¹, C.U. Niemann^{1,3}, M. Gulrajani², F. Krantz², T. Covey², B.J. Lannutti², A. Wiestner¹, S.E.M. Herman¹; ¹Laboratory of Lymphoid Malignancies, ²Acerta Pharma, Redwood City, CA, ³Department of Hematology, Copenhagen University Hospital, Denmark.

Recent advances in the treatment of CLL focus on targeting the B-cell receptor (BCR) pathway, which is strongly upregulated in CLL. The BTK inhibitor ibrutinib and the PI3K δ inhibitor idelalisib, both targeting the BCR pathway, are approved for clinical use based on significant survival benefit in clinical trials. *In vitro* studies have shown synergy for combined PI3K δ and BTK inhibition. As CLL propagation relies on the microenvironment, *in vivo* models are needed for better testing of new drug combinations. We tested two new inhibitors of BCR, the BTK inhibitor ACP-196 and the PI3K δ inhibitor ACP-319 as single

agents and in combination using the murine TCL1-192 allograft model of aggressive, BCR driven CLL. TCL1-192 cells were injected into SCID mice and vehicle, ACP-196, ACP-319 or ACP-196+319 were administered through the drinking water. Blood was analyzed weekly by flow cytometry and at the end of the study spleens were weighed and analyzed by flow cytometry. We show that combining ACP-196 and ACP-319 is superior to single agent treatment in the TCL1-192 model in: Reducing tumor burden, increased median survival, and decreased phosphorylation of the BCR factors PLC γ 2 and NF κ B. Thus, evaluation of combination treatment with ACP-196 and ACP-319 in clinical trials is merited.

Micro-CT scouting for transmission electron microscopy of human tissue specimens. A.G. Morales, E.S. Stempinski, X. Xiao, A. Patel, A. Panna, K.N. Olivier, P.J. Mcshane, C. Obinson, A.J. George, D.R. Donahue, P. Chen, H. Wen; Laboratory of Imaging Physics.

Transmission electron microscopy (TEM) provides sub-nanometre-scale details in volumetric samples. Samples such as pathology tissue specimens are often stained with a metal element to enhance contrast, which makes them opaque to optical microscopes. As a result, it can be a lengthy procedure to find the region of interest inside a sample through sectioning. We describe micro-CT scouting for TEM that allows noninvasive identification of regions of interest within a block sample to guide the sectioning step. In a tissue pathology study, a benchtop micro-CT scanner with 10 μ m resolution was used to determine the location of patches of the mucous membrane in osmium-stained human nasal scraping samples. Once the regions of interest were located, the sample block was sectioned to expose that location, followed by ultra-thin sectioning and TEM to inspect the internal structure of the cilia of the membrane epithelial cells with nanometre resolution. This method substantially reduced the time and labour of the search process from typically 20 sections for light microscopy to three sections with no added sample preparation.

Comprehensive residual disease assessment improves AML relapse risk stratification in autologous hematopoietic cell transplantation. M.P. Mulé¹, G.N. Mannis², B.L. Wood³, J.P. Radich³, J. Hwang², N.R. Ramos¹, C. Andreadis², L. Damon², A.C. Logan², T.G. Martin², C.S. Hourigan¹; ¹Myeloid Malignancies Section, ²Department of Medicine, Division of Hematology and Blood and Marrow Transplantation, University of California, San Francisco, ³Fred Hutchinson Cancer Research Center, Seattle, WA.

While commonly used in other hematological malignancies, high dose chemotherapy followed by autologous hematopoietic cell transplantation (Auto-HCT) has not been widely adopted in acute myeloid leukemia (AML) due to concerns regarding high post-transplant relapse rates. It is possible that these higher relapse rates are due to contamination of the autograft with residual leukemia cells not eliminated by induction chemotherapy. High sensitivity methods to detect residual AML have demonstrated the ability to correctly identify patients who are in morphological complete remission (CR), but are at increased risk of relapse due to the presence residual disease after treatment. We report here the largest retrospective study to date of adult Auto-HCT AML patients tested for measurable residual disease (MRD)

in the autograft by both molecular methods (RQ-PCR) and multi-parameter flow cytometry (MPFC). Neither WT1 RQ-PCR or flow cytometry testing of the autograft could reliably predict post Auto-HCT relapse. We demonstrated the mechanism of failure for these biomarkers includes the effect of GCSF on gene expression and peripheral blood composition observed in both AML patients and in healthy donors. Autograft WT1 expression was detectable in only a minority of those who relapsed post-transplant. In summary, no one single AML MRD test on autograft samples could reliably predict post Auto-HCT relapse. However, residual disease detection using multiple complementary molecular assays overcame these limitations allowing for identification of a cohort of patients with poor post-transplantation outcomes.

Formin-generated actomyosin arcs propel T cell receptor microcluster movement at the immunological synapse. S. Murugesan, J. Hong, J. Yi, D. Li, J. Beach, L. Shao, E. Betzig, X. Wu, J.A. Hammer; Cell Biology and Physiology Center.

Upon antigen recognition, actin assembly and inward flow in the plane of the radially symmetric immunological synapse (IS) drives the centralization of T cell receptor microclusters (TCR MCs) and the integrin LFA-1. Using two forms of structured-illumination microscopy (SIM), we show here that actin arcs populating the medial, lamella-like region of the IS arise from linear actin filaments generated by one or more formins present at the distal edge of the IS. After traversing the outer, Arp2/3-generated, lamellopodia-like region of the IS, these linear filaments are organized by myosin II into concentric arcs that should possess the anti-parallel organization required for contraction. Quantitative, fixed-cell 3D SIM shows that open, active LFA-1 often aligns with arcs while TCR MCs commonly reside between arcs, and live-cell TIRF-SIM shows TCR MCs being swept inward by arcs. Consistently, disrupting actin arc formation via formin inhibition results in less centralized TCR MCs, miss-segregated integrin clusters, decreased T: B cell adhesion frequency, and diminished proximal TCR signaling. Together, our results define the origin, organization and functional significance of a major actomyosin contractile structure at the IS that directly propels TCR MC transport.

Optimization of Detection of Chondroitin Sulfate on Western Blots with Antibody CS-56. H. Nagase, Y. Katagiri, C.A. Mencia, C. Agbaegbu, H.M. Geller; Developmental Neurobiology Group.

Chondroitin sulfate proteoglycans (CSPGs) are a diverse family of ECM molecules. Each member consists of a protein core and a varying number of long sulfated unbranched negatively charged glycosaminoglycan (GAG) chains. During CNS development, CSPGs are expressed in specific locations and are thought to serve as molecular barriers. Additionally, injuries to the CNS as well as the sites of neurogenesis in the adult mammalian brain are spatially defined and isolated from surrounding structures by abundant CSPGs. These inhibitory/repulsive properties are mediated largely through the CS GAG chains tethered to the CSPG core proteins.

CS-56 is a monoclonal antibody (IgM) against CS GAG chains that has been widely used for tissue staining to analyze the localization of CSPGs. In contrast, very few good western blot

data exist in the literature due to a lack of sensitivity and proper controls, even though western blot is an established method for protein analysis, leaving a big gap between staining data and western blot data. Our aim is to create a new protocol to have reproducible western blot data using CS-56 with greater sensitivity and quality. Every step for western blot analysis, including sample preparation, blocking of the membrane, and reagents for antibody dilution was re-examined. Most prominently, we have improved the sensitivity and signal-to-noise ratio and shortened the entire procedure of the CS-56 western blot by using an immunoreaction enhancing technology. Thus, our new protocol will bridge the gap between tissue staining data and western blot analysis with CS-56.

Characterization of a Murine Model of Psoriasis and its Association to Cardiometabolic Dysfunction. Q. Ng, A. Sorokin, Y. Baumer, M. Playford, H. Teague, A. Noguchi, M. Winge, P. Marinkovich, N. Mehta; Section of Inflammation and Cardiometabolic Disease.

The K14-Rac1 murine model of psoriasis has been previously phenotyped by a group at Stanford University (Marinkovich) who demonstrated that this model is a viable animal model of psoriasis. However this model has not yet been cardiometabolically phenotyped to show the prevalent comorbidities as seen in human psoriasis. Herein we describe the characterization of the K14-Rac1 mouse model of psoriasis based on studies done with our human cohort to fill in the needed gap for a pre-clinical model of human psoriasis. Given the strong similarity in the immune cell and skin characteristics of human psoriasis and the K14-Rac1 mouse model, we sought to show that chronic skin inflammation predisposes the model to vascular inflammation and metabolic dysregulation, as seen with our human cohort. Preliminary data revealed elevated levels of pro-atherogenic serum biomarkers in K14-Rac1 positive mice, therefore we hypothesized that the K14-Rac1 mouse model of psoriasis is predisposed to future adverse cardiovascular events and metabolic dysfunction similarly to human psoriasis. We determined that the skin inflammation in K14-Rac1 mice was associated with increased immune cell infiltration and endothelial cell activation in the aortas of Rac1 positive mice, and signs of metabolic dysregulation such as decreased cholesterol efflux and decreased LDLR gene expression. Our findings suggest that the K14-Rac1 mouse model provides a reliable preclinical model of psoriasis along with its comorbidities.

Regulation of the permeability transition pore is altered in mice lacking the mitochondrial calcium uniporter. R.J. Parks, S. Menazza, A.M. Aponte, T. Finkel, E. Murphy; Laboratory of Cardiac Physiology.

Global knockout (KO) of the mitochondrial Ca^{2+} uniporter (MCU) abrogates rapid mitochondrial Ca^{2+} uptake and permeability transition pore (PTP) opening, but does not protect from ischemic injury. This study investigates the hypothesis that the lack of protection in MCU-KO may be explained by alterations in PTP opening. To investigate whether PTP opens in MCU-KO, Ca^{2+} uptake and swelling were measured in isolated mitochondria in the presence of the Ca^{2+} ionophore ETH129 to permit Ca^{2+} entry. ETH129 enabled MCU-KO mitochondria to take up Ca^{2+} and undergo pore opening. When matrix Ca^{2+} was set to the same level in the two groups, KO underwent PTP

opening at lower Ca^{2+} than WT, suggesting that PTP Ca^{2+} sensitivity is altered. To test whether PTP contributes to ischemic injury, hearts were Langendorff-perfused in the presence of a cyclophilin D-independent pore inhibitor. Preliminary data suggest that PTP inhibition decreases infarct size by ~30% in both WT and MCU-KO hearts, suggesting that pore opening does occur in MCU-KO. To better understand ischemic cell death mechanisms in MCU-KO hearts, the proteome of whole heart homogenates was compared to WT using tandem mass tags. Interestingly, two proteins of F_1F_0 -ATP synthase, proposed to be a component of PTP, were altered. Subunit s and F1-complex assembly factor were 2.2- and 1.6-fold lower in MCU-KO. Interestingly, native PAGE revealed that the ratio of ATP synthase dimers to monomers was reduced in MCU-KO by ~20%. These results suggest that absence of MCU may alter PTP regulation, which might involve changes in ATP synthase.

Microtubule affinity-regulating kinase, MARK2 regulates directed cell migration through modulation of Myosin activity. A. Pasapera, R.N. Fischer, C.M. Waterman; Laboratory of Cell and Tissue Morphodynamics.

Directed cell migration requires establishment of cell polarity to spatially coordinate adhesion formation, the actomyosin cytoskeleton and microtubules organization to drive cell movement. MARK2 (Microtubule affinity-regulating kinase, also known as PAR1b) is well known to regulate front-back cell polarity and the microtubule cytoskeleton. However, the role of MARK2 in polarization of actin, myosin and focal adhesions (FAs) remains less clear. A previous study from our lab using mass spectrometry identified MARK2 as a component of FA. Thus, we hypothesized that in addition to regulating microtubules, MARK2 may promote polarity in cell migration by regulating FAs and their associated actomyosin cytoskeleton. To test this, we analyzed GFP-MARK2 localization and tested its role in regulating FA and actomyosin in cell migration in U2OS cells. We found that besides microtubules and cell protrusions, MARK2 localized at FAs and actin stress fibers. Use of SiRNA or Crispr technology showed that MARK2 depletion abolished cell polarization, slowed cell migration, and decreased FA size. Conversely, over-expression of MARK2 resulted in focal adhesion growth, reduced cell migration and myosin displacement from the cell edge. We also show that MARK2 induce T696 phosphorylation of MYPT1 a phosphatase in charge of Myosin light chain dephosphorylation. These findings indicate that MARK2 not only regulates microtubule stability through phosphorylation of MAPs as reported, but also influences the actomyosin cytoskeleton and focal adhesions.

The transmission of the proton motive force along I-Band segments of the mitochondrial reticulum. K.D. Patel, B. Glancy, R.S. Balaban; Laboratory of Cardiac Energetics.

In the mitochondrial reticulum of skeletal muscle, I-Band segments (IBS) form a contiguous matrix with the mitochondrial segments at the periphery (PS) of the cell. An electrical coupling via the matrix between the PS and IBS has been demonstrated. It is hypothesized that PS can support the production of ATP in the IBS by maintaining the potential energy available to produce ATP deep in the muscle cell via conduction of the PMF down the IBS.

Two mechanisms were considered to drive ion transport along the IBS: the electrical potential and/or concentration gradients between the PS to the end of the IBS. The magnitude of the flux was estimated from the maximum ATP production rate for skeletal muscle. The major transport ions considered were H^+ , Na^+ and K^+ using diffusion coefficients from the literature. Simulations suggest conduction along the IBS via H^+ alone is unlikely requiring unreasonable gradients, while Na^+ or K^+ could carry the current with minor gradients in concentration or electrical potential along the IBS. The majority of conduction down the IBS is likely dependent on $\text{Na}^+\text{-K}^+$ and some anion; however, this requires that H^+ is recycled from the matrix of the IBS to the PS for active extrusion. We propose that the abundant cation-proton antiporter in skeletal muscle mitochondria operates in opposite directions in the IBS and PS to permit local recycling of H^+ at each site driven by cooperative gradients in H^+ and $\text{Na}^+\text{/K}^+$ which favor H^+ entry in the PS and H^+ efflux in the IBS.

Is endothelial alpha-globin predominantly expressed by the Hba-a1 or Hba-a2 locus in mice? L. Pecker, J. Butcher, G. Isakson, H. Ackerman; Sickle Cell Disease Branch.

Alpha-globin deletions are common in humans and until recently were understood only to influence erythrocyte pathophysiology. The discovery that alpha-globin is present in the endothelial cells of resistance blood vessels, where it regulates nitric oxide (NO) signaling and decreases NO bioavailability, raises fundamental questions about the transcriptional regulation of alpha-globin and the physiologic significance of alpha-globin deletions. The relative contribution of the two alpha-globin gene loci to erythrocyte hemoglobin is established; however, relative expression in the vascular endothelium is unknown. To understand the significance of alpha-globin deletions, we are studying C57/Bl6 mice with Hba-1 gene deletion (Hba1^{-/-} mice). We hypothesized that Hba1^{-/-} mice could have decreased alpha-globin expression compared to Hba1^{+/+} control mice. Using RT-PCR, we found that in Hba1^{-/-} mice total alpha-globin expression is decreased in cerebral and mesenteric blood vessels and kidney by 63%, 82% and 83% respectively when normalized to Hba1^{+/+} mice alpha-globin (samples from 3 mice per group, run in triplicate). Beta-globin controls confirmed that blood contamination does not explain our findings. These results suggest that the Hba-1 locus may be predominantly expressed in the vascular endothelium. This may have physiological implications for humans with alpha-globin deletions. We are now refining our assays to distinguish murine Hba-1 and Hba-2 loci to determine the relative contributions of these loci to endothelial alpha-globin expression.

The Disruptive State Of The Membrane Active Antimicrobial Peptide Piscidin 1 Investigated By Multi- μS All-Atom Simulations And Solid-State NMR: Surface Defects Are Favored Over Stable Pores. B.S. Perrin, Jr., R. Fu, M.L. Cotten, R.W. Pastor; Laboratory of Computational Biology.

Antimicrobial peptides (AMPs) that disrupt bacterial membranes are promising therapeutics against the growing number of antibiotic-resistant bacteria. The mechanism of membrane disruption by the AMP piscidin 1 was examined with multi-microsecond all-atom molecular dynamics simulations and solid-state NMR spectroscopy. A 14- μs control simulation of an ar-

chetype barrel-stave alamethicin pore validated the methodology. The primary simulation was initialized with 20 peptides in 4 barrel-stave pores in a fully hydrated POPC/POPG bilayer. The 4 pores relaxed to toroidal by 200 ns, only one pore-like structure containing 2 transmembrane helices remained at 25 μ s, and none of the 18 peptides released to the surface reinserted to form pores. These results imply that the population of toroidal pores is <4% (consistent with ^{15}N NMR). This simulation and a separate 2.5- μ s trajectory of surface-bound peptides show transient distortions of the bilayer/water interface (consistent with ^{31}P NMR), which could be responsible for membrane disruption by piscidin.

Improving free energy calculations with non-Boltzmann Bennett reweighing using QM and MM. F.C. Pickard IV, G. Koenig, B.R. Brooks; Laboratory of Computational Biology.

The correct representation of solute-water interactions is essential for the accurate simulation of most biological phenomena. While many accurate quantum mechanical (QM) methods exist to model such interactions, they typically have difficulty incorporating the effects of entropy beyond the standard harmonic approximation. Conversely, molecular mechanics (MM) forcefields provide an inferior Hamiltonian, yet a vastly superior treatment of solute and solvent entropy. The Non-Boltzmann Bennett (NBB) free energy method can be used to marry the strengths of the two approaches together, by using the ensemble derived from an MM trajectory to properly weight single point energy calculations from various QM methods. We recently participated in the blinded SAMPL5 challenge, using the QM-NBB method to predict distribution coefficients (log D) between water and cyclohexane for 53 drug-like molecules.

Accurate prediction of distribution coefficients is important, because they are commonly used by the pharmaceutical industry as a proxy for bioavailability of a compound. In addition to testing our free energy methodologies, our predictions also required an accurate treatment of pKa, tautomerization and conformational flexibility for each compound. Our best prediction methodology ranked second among over 70 submissions with a RMS error of 2.3 ± 0.3 log D units.

KMT2D controls regulatory T cell development by modulating histone H3 lysine K4 methylation at Foxp3 locus. K. Placek, K. Cui, G. Hu, K. Zhao; Systems Biology Center.

Gene regulatory elements are associated with histone H3 lysine 4 methylation (H3K4me) and H3 acetylation. Changes in histone modification patterns accompany and regulate cell differentiation process. Whilst much is known about changes in histone modifications during T cell differentiation, little is known about the role of histone modifying enzymes in this process. KMT2D is a histone methyltransferase that shapes enhancer landscape by regulating H3K4me. To determine whether KMT2D plays a role in T cell development, we deleted KMT2D specifically in T cells. Our data show that KMT2D deficiency results in reduced number of T cells in periphery. Moreover in the absence of KMT2D, differentiation of regulatory T (Treg) cells *in vitro* and *in vivo* is compromised. We found that KMT2D modulates mono- and di-methylation at regulatory elements of Foxp3 gene, the master regulator of Treg cells. KMT2D-regulated H3K4me peaks are bound by Ets1 transcription factor involved in activation of Foxp3 expression. Furthermore we

found that KMT2D complex interacts with Ets1. Thus, our data suggest that KMT2D controls Treg cell differentiation by modulating H3K4 methylation pattern and interacting with Ets1 at regulatory elements of Foxp3 gene.

Positional Changes of Pericentrin are related to PCM activity at the Centrosome. K. Plevock, B. Galletta, C. Fagerstrom, K. Slep, N. Rusan. Laboratory of Molecular Machines and Tissue Architecture.

Centrosomes, composed of two centrioles surrounded by pericentriolar material (PCM), nucleate and organize the microtubule cytoskeleton and notably the two poles of the mitotic spindle. The amount of PCM correlates with microtubule nucleating capacity of the centrosome. In interphase there is minimal PCM at the centrosome. However, as cells enter mitosis, massive recruitment and reorganization of PCM occurs at the centrosome in a highly regulated manner. A few key proteins have been identified as scaffolds for recruitment of PCM as cells enter mitosis, but how cells regulate PCM incorporation at the centrosome is not well understood. It has been known for 20 years that Pericentrin is a scaffolding protein at the centrosome, but how it performs its scaffolding role is unknown. A compelling hypothesis is that in interphase Pericentrin is auto-inhibited by local fold-backs, whereas in mitosis, Polo kinase permits release of inhibition, to reveal binding sites on Pericentrin responsible for PCM recruitment.

To test the hypothesis that there are positional changes that occur within Pericentrin, we examined the *Drosophila melanogaster* orthologue, Pericentrin-Like-Protein (PLP). SIM measurements reveal that the distance between the N and C-termini of PLP increases by 21 nm in mitosis compared to interphase, concurrent with PCM recruitment. Interestingly, the entire 21 nm shift is due to the N-terminus moving further away from the center of the centrosome. This result is consistent with the hypothesis that PLP opens to reveal sites to recruit/organize PCM. We are now probing the mechanism for this positional regulation.

To further understand how PLP is regulated, we wanted to understand how PLP may be interacting with itself and how those interactions change between interphase and mitosis. Since the N-term of PLP shifts out as cells enter mitosis, there may be a binding site for PLP N-term at PLP-C-term that is released. To address this, we created truncations of the FL molecule to test for interactions in a Y2H screen. This screen revealed an interaction between the N and C-termini. The hypothesis is that interaction between the N and C is specific to interphase, and release of this interaction allows for PLP extension. We have completed a reverse Y2H screen to identify point mutants to disrupt the N and C-term interaction of PLP in order to disrupt this intramolecular interaction.

Another finding that came out of the Y2H screen is a novel self-interaction in central region of PLP. The central region of PLP likely provides a clustering mechanism at the centrosome after PLP N-C inhibition is relieved. Using CD and SEC-MALS, we have shown that the central region of PLP contains alpha helical characteristics and dimerizes. Overall, we have identified a novel positional change that occurs in PLP, identified intramolecular interactions within PLP, and have begun to tease apart the precise mechanism for its regulation. New, exciting questions have arisen regarding the role of a mitotic kinase, Polo, and mi-

croton tubules in regulating Pericentrin, which we are now beginning to address.

Improving the Lennard-Jones Parameters of Ions in CHARMM. M. Pourmoussa, R.M. Venable, R.W. Pastor; Laboratory of Computational Biology.

The accuracy of molecular dynamics (MD) simulations depends on the accuracy of underlying force field parameters that describe bonding and non-bonding interactions. The parameters of Lennard Jones (LJ) potentials for describing cation-anion pair interactions in additive force fields are usually developed to reproduce experimental data in infinitely dilute solutions, and hence, may be incorrect at finite concentrations. The high ion concentration at water bilayer interfaces is a particular concern. In this study, we revise LJ parameters in the CHARMM C36 force field of several ion pairs that model interactions with lipid head groups. The study shows that the default LJ parameters of calcium in CHARMM, which are based on the free energy of solvation in water, fail at calcium-chloride and calcium-acetate concentrations above 0.1 M. This indicates the need to use explicit non-bond exceptions to adjust the interactions of calcium with chloride and with oxygen atoms of acetate groups.

Myosin 18A localizes with myosin II at cell: cell junctions in epithelial cells and tissues. K. Remmert¹, J. Beach¹, N. Porat-Shliom², R. Weigert², J. Hammer¹; ¹Laboratory of Cell Biology, ²Intracellular Membrane Trafficking Unit; Oral and Pharyngeal Cancer Branch; NIDCR.

Class 18A myosins (M18A) are a poorly understood subclass of myosins that is most closely related to conventional class-2 nonmuscle myosins (NM2). The two major splice variants of the MYO18A gene, M18A α and β , have domain architectures similar to that of NM2, with a myosin motor-like domain, a pair of light chain-binding IQ motifs, and a long coiled-coil domain ending in a non-helical tailpiece. In addition, M18A α and M18A β have extra domains at their N- and C-termini. In detail, both contain a C-terminal PDZ domain-binding motif and M18A α has an N-terminal extension comprised of a KE-rich domain, an ATP-insensitive actin-binding site, and a PDZ domain. Surprisingly, both M18A isoforms lack actin-activated ATPase activity and the ability to translocate actin filaments, suggesting that M18A function *in vivo* does not depend on intrinsic motor activity. Of even more significance though is the fact that M18A and NM2 co-assemble via their extended coiled-coil domains into individual mixed bipolar filaments both *in vitro* and in live cells. Based on these data, we hypothesized that M18A may serve to regulate NM2 filament turnover and/or act as an adaptor to link the filaments to different cellular structures/signaling molecules via its extra N- and C-terminal domains, all without interfering with NM2 motor activity. M18A is ubiquitously expressed across mammalian tissues, with elevated expression and isoform-specific expression in numerous cell types, including epithelia. In this study we determined the subcellular localization of M18A in polarized epithelial cell layers and in cryo-sections of various mouse epithelia using a M18A-specific antibody. We find that M18A is concentrated at cell:cell junctions of polarized MDCK cells, a site where NM2 is known to be critical for maintaining the integrity of adherens junctions. Similarly, M18A is enriched with NM2 in kidney proximal tu-

bules and in the intestinal brush border epithelium specifically at cell:cell junctions. Finally, we established an enteroid culture method from primary mouse intestine to more closely recapitulate intestinal epithelium physiology. Our focus is to analyze the role of NM2 and M18A during two essential processes of epithelial gut biology: apoptotic cell extrusion and interkinetic nuclear migration during cell division.

High-resolution maps of chromatin interaction reveal CTCF as a facilitator of enhancer-promoter interaction to maintain robustness of gene expression. G. Ren, W. Jin, K. Cui, J. Rodriguez, D.R. Larson, K. Zhao; Systems Biology Center.

Recent studies have shown that the mammalian genomes are organized into topologically-associated domains (TADs) and sub-functional domains. The insulator-binding protein, CTCF, is established as a key player for the maintenance of chromatin domain boundaries. However, the vast majority of CTCF binding sites are interwoven with enhancers within chromatin domains and do not display chromatin boundary functions. Here we report a positive correlation between the intra-domain CTCF binding with the activity of their associated enhancers. Using a modified high-resolution Hi-C protocol, termed Super-C, we identify 90,518 and 81,773 high-confidence interactions among promoters, p300-bound enhancers and CTCF-bound insulators in murine ES and CD4 T cells, respectively. Analysis of these unprecedentedly high-resolution interaction maps reveals that CTCF binding sites and enhancers are interspersed and extensively interact with each other, and are positively correlated with enhancer-promoter interactions and enhancer activity. Deletion of CTCF sites using CRISPR/Cas9 severely compromises enhancer-promoter interactions and enhancer function in general, suggesting that one major function of CTCF is to facilitate formation of looping between enhancers and promoters by directly interacting with these regions. We further demonstrate that knockdown of CTCF or deletion of CTCF binding sites results in increased cell-to-cell variation of gene expression, accompanied by decreased enhancer-promoter interaction, indicating that stable promoter-enhancer interaction mediated by CTCF plays an important role in maintaining the robustness of gene expression programs.

Effects of Heterologous Expression of Human Cyclic Nucleotide Phosphodiesterase 3A (hPDE3A) on Redox Regulation in Yeast. D.K. Rhee, J.C. Lim, S.C. Hockman, F. Ahmad, D.H. Woo, Y.W. Chung, S. Liu, A.L. Hockman, V.C. Manganelli; Laboratory of Translational Research.

Oxidative stress plays a pivotal role in pathogenesis of cardiovascular diseases and diabetes, however, the roles of Protein Kinase A (PKA) and human Phosphodiesterase 3A (hPDE3A) remain unknown. Here we show that yeast expressing wild type (WT) hPDE3A or K13R hPDE3A (putative ubiquitinylation site mutant) exhibited resistance or sensitivity to exogenous H₂O₂, respectively. H₂O₂-stimulated ROS production was markedly increased in yeast expressing K13R hPDE3A (OxiS1), compared to yeast expressing WT hPDE3A (OxiR1). In OxiR1, YAP1 and YAP1-dependent anti-oxidant genes were upregulated, accompanied by reduction of thioredoxin peroxidase. In OxiS1, expression of YAP1 and YAP1-dependent genes was impaired, and the thioredoxin system malfunctioned. H₂O₂ increased cAMP-hydrolyzing activity of WT hPDE3A, but not K13R

hPDE3A, through PKA-dependent phosphorylation of hPDE3A, which was correlated with its ubiquitinylation. The changes in anti-oxidant gene expression did not directly correlate with differences in cAMP/PKA signaling. Despite differences in their capacities to hydrolyze cAMP, total cAMP levels among OxiR1, OxiS1, and mock were similar, PKA activity, however, was lower in OxiS1 than in OxiR1 or mock. During exposure to H₂O₂, however, Sch9p activity, a TORC1-regulated rpS6 kinase and negative-regulator of PKA, was rapidly reduced in OxiR1, and Tpk1p, a PKA catalytic subunit, was diffusely spread throughout the cytosol, with PKA activation. In OxiS1, Sch9p activity was unchanged during exposure to H₂O₂, consistent with reduced activation of PKA. These results suggest that, during oxidative stress, TOR-Sch9 signaling might regulate PKA activity, and that post-translational modifications of hPDE3A are critical in its regulation of cellular recovery from oxidative stress.

Regulation of Hepatic Gluconeogenesis by Human Long non-coding RNAs. X. Ruan, P. Li, H. Cao; Laboratory of Obesity and Metabolic Diseases.

We have recently demonstrated that long non-coding RNAs (lncRNAs) are important regulators of glucose and lipid metabolism in mice. However, since lncRNAs are much less conserved between human and mouse than protein coding genes do, the function of lncRNAs in human metabolism and physiology is largely unknown. Hepatic gluconeogenesis is a major pathway that maintains plasma glucose levels during fasting and is also a key contributor to hyperglycemia in diabetes. To identify human lncRNAs that regulate hepatic gluconeogenesis, we systemically screened lncRNAs that are induced by fasting signals in both hepG2 cells and primary human hepatocytes. Among the most induced lncRNAs, knocking down an lncRNA we termed lncGIRG (glucagon-induced repressor of gluconeogenesis) results in increased glucose production in primary human hepatocytes. We further demonstrated that induction of lncGIRG by glucagon is dependent on FOXO1, a key transcriptional regulators of hepatic gluconeogenesis in both mouse and human. Genomewide gene expression analyses revealed that loss-of-function of lncGIRG leads to increased expression of a number of genes in gluconeogenic pathway including G6pc and Pck1. Our results suggest that lncGIRG might serve as a negative regulatory mechanism of hepatic gluconeogenesis in human, and lncRNAs such as lncGIRG could potentially constitute important therapeutic targets for diabetes.

On the Robustness of SAC Silencing in Closed Mitosis. D. Ruth, J. Liu; Theoretical Cellular Physics.

Mitosis equally partitions sister chromatids to two daughter cells. This is achieved by properly attaching these chromatids via their kinetochores to microtubules that emanate from the spindle poles. Once the last kinetochore is properly attached, the spindle microtubules pull the sister chromatids apart. Due to the dynamic nature of microtubules, however, kinetochore-microtubule attachment often goes wrong. When this erroneous attachment occurs, it locally activates an ensemble of proteins, called the spindle assembly checkpoint proteins (SAC), which halts the mitotic progression until all the kinetochores are properly attached by spindle microtubules. The timing of SAC silencing thus determines the fidelity of chromosome segregation. We previously established a spatiotemporal model that addresses

the robustness of SAC silencing in open mitosis for the first time. Here, we focus on closed mitosis by examining yeast mitosis as a model system. Though much experimental work has been done to study the SAC in cells undergoing closed mitosis, the processes responsible are not well understood. We leverage and extend our previous model to study SAC silencing mechanism in closed mitosis. We show that a robust signal of the SAC protein accumulation at the spindle apparatus can be achieved. This signal is a nonlinear increasing function of number of kinetochore-microtubule attachments, and can thus serve as a robust trigger to time the SAC silencing. Together, our mechanism provides a unified framework across species that ensures robust SAC silencing and fidelity of chromosome segregation in mitosis.

Investigations into Rotavirus and Norovirus Replication, Assembly and Exit. M. Santiana, W.L. Du, Y. Mutsafi Ben Halevy, S. Sosnovtsev, J. Patton, K. Green, N. Altan-Bonnet; Laboratory of Host-Pathogen Dynamics.

Rotavirus and norovirus are non-enveloped RNA viruses that are two of the most common causative agents of gastroenteric diseases in humans. Little is known regarding their subcellular replication and assembly sites as well as the pathways by which these viruses are released from host cells. Here using high resolution imaging techniques in combination with proteomics and lipidomics approaches we investigate the rotavirus and norovirus lifecycle in mammalian cells. We demonstrate that both norovirus and rotavirus genomes are translated, replicated and assembled on subcellular membranes, with rotavirus genomes specifically in cytoplasmic domains enclosed by endoplasmic reticulum membranes. Post-assembly both norovirus and rotavirus particles are released from cells non-lytically in vesicles which are subsequently infectious. Our findings with rotavirus, and norovirus extend our previous discoveries with poliovirus, Cocksackievirus and rhinovirus, widening the number of so-called “non-enveloped” viruses being released non-lytically from host cells.

Centrosome-pole cohesion requires Abnormal Spindle and Calmodulin to ensure proper centrosome inheritance in neural stem cells but is dispensable for brain size. T. Schönborg, A. Zajac, C. Fagerstrom, R.X. Guillen, N.M. Rusan; Laboratory of Molecular Machines & Tissue Architecture.

The interaction between microtubule organizing centers (MTOCs) and spindle poles is critical for the establishment and maintenance of the mitotic apparatus in many organisms. However, our understanding of the dynamics of this relationship and the potential implications for tissue homeostasis remains largely unexplored. Here we report that the microcephaly-associated protein, Abnormal Spindle (Asp), plays a key role in maintaining centrosome-pole attachments and pole focusing in *Drosophila* neural stem cells. Complete loss of function mutations in *asp* cause centrosome detachment from poles shortly after metaphase, leading to free-ranging centrosomes that randomly move around the cell until anaphase onset. As a consequence, centrosome inheritance is randomized, with neural stem cells either losing their centrosome or retaining both following asymmetric division. Furthermore, we show that Asp's spindle function is dependent on the calcium-sensing protein Calmodulin (CaM). Both proteins colocalize on spindles and dynamically move towards spindle poles with similar velocities, suggesting that they

form a complex with CaM acting as a regulator of Asp. Our direct binding assay and structure-function analysis of Asp support this hypothesis. However, the Asp-CaM interaction is dispensable for head and brain size, and the aforementioned spindle defects observed in neural stem cells of *asp* mutants does not correlate with microcephaly phenotypes. Instead, the ability of Asp to suppress microcephaly is conferred by an unknown domain in the N-terminus of the protein through a mechanism that has yet to be determined.

Characterization of GB1 using H/D Fractionation. P. Shukla¹, P. Bryan², Y. Chen², J. Orban², N.Tjandra^{1*}; ¹Laboratory of Structural Biophysics, ²Institute for Bioscience and Biotechnology Research, University of Maryland.

Hydrogen bond plays a key important role in determining protein folding and stability. It is also important for modulating substrate-binding specificity in many enzymatic reactions. Due to its importance in protein structure and functions, new methods are required which can estimate H-bond quantitatively. Recently, with the development of NMR experiments to measure J-coupling across H-bonds, one can now quantitate their strengths. Previous studies performed on deuterium fractionation indicated that they might provide information about H-bond as well. Interestingly, upon close inspection these two independent NMR data that were supposed to be sensitive to the same structural feature do not seem to correlate. There are no reports published for proteins which show any direct correlation of H-bond with deuterium fractionation as was observed for small molecules. Therefore, it is still unclear whether deuterium fractionation correlates with hydrogen bond directly or is it a consequence of its dependence on other structural factors.

In view of this, deuterium fractionation studies were performed on GB1. Consistently, we have not observed any good correlation between deuterium fractionation and H-bond scalar coupling⁴. This suggests the possible presence of other contributions in deuterium fractionation on proteins. In order to begin to identify those contributions, we use variation of pH, temperature and mutations on GB1 to characterize changes in fractionation. We observed loss of correlation for deuterium fractionation at different temperature and pH. The fractionation seems to be more sensitive to temperature than to pH or mutations. Furthermore, the changes on fractionation as a function of mutation are not restricted to the local sites of mutation, as seen by comparing wild type GB1 and GB1 with 32Q/L, 37N/K, 38G/T, 40D/E mutations. The changes seem to be global. This also suggests the presence of other contributions such as: electrostatic interactions or changes in folding-unfolding equilibrium.

Exploring the role of Parkin in astrocyte mediated neurotrophic function. K. Singh, M. Sack; Laboratory of Mitochondrial Biology and Metabolism.

Mutations in the PARK2 gene is known to cause early-onset Parkinson's disease (EOPD), where the disease presents itself in the patients as young as in their 20s. PARK2 gene encodes an E3 ubiquitin ligase, Parkin. A growing body of evidence has implicated the glial cells (astrocytes and microglia), which are the support cells in the brain, in the maintenance of neuronal integrity and in PD pathophysiology. This study is aimed at investigating the glia-specific function of Parkin and testing whether the impairment of Parkin function in glia contributes to PD patho-

genesis. Preliminary analysis of the Parkin knockout astrocytes suggests that Parkin impacts both the neurotrophic and immunological functions of astrocytes. Parkin knockout astrocytes had significantly high endoplasmic reticulum (ER) stress, secreted modestly high proinflammatory cytokines, and had significantly impaired dopaminergic neuron protection function when compared to the wild type astrocytes. Additionally, Parkin knockout astrocytes exhibit impaired BDNF signaling. Further analysis showed that Parkin expression positively regulates BDNF transcript and protein expression levels. Current work is focused on testing whether parkin regulates BDNF transcription factors or functions as a direct transcription regulator. Future studies will focus on understanding the molecular mechanism by which Parkin regulates BDNF signaling in astrocytes. We will also explore if Parkin impacts other neurotrophic factors signaling in astrocytes. It is likely that Parkin may be modulating the neurotrophic function of astrocytes and this may be critical for neuron survival.

An FMN2-mediated perinuclear actin/adhesion system protects against DNA damage during confined cell migration. C.T. Skau, P.S. Gurel, H. Racine-Thiam, A. Tubbs, M.A. Baird, M.W. Davidson, M. Piel, G.M. Alushin, A. Nussenzweig, C.M. Waterman. Laboratory of Cell and Tissue Morphodynamics.

Cell migration in tightly confined 3D tissue microenvironments is critical for angiogenesis, extravasation of white blood cells, immune surveillance, and connective tissue maintenance by fibroblasts. Yet how cells squeeze their large and stiff nuclei through such environments is unclear. We discovered an actin cytoskeletal structure that prevents damage to the nucleus and genetic material damage during migration in confined microenvironments. The formin-family actin nucleator FMN2 associates with and generates a perinuclear actin/adhesion system that is compositionally and functionally distinct from previously characterized actin structures. This system controls proper nuclear shape and positioning in fibroblasts migrating on 2D surfaces and promotes cell survival by limiting nuclear envelope damage and DNA double-strand breaks in fibroblasts migrating in confined 3D microenvironments. Collectively our results indicate a critical role for FMN2 in generating an actin/adhesion system that protects the nucleus from damage to promote cell survival during confined migration.

Investigating Protein Dynamics at Sites of Exocytosis in Live Cells. A. Somasundaram, J. W. Taraska; Laboratory of Cellular and Molecular Imaging.

Exocytosis is the cellular process in which cytoplasmic membrane bound vesicles fuse with the plasma membrane and release their contents into the extracellular space. Calcium triggered exocytosis is critical for many physiological functions, including release of neurotransmitters by neurons, and secretion of hormones by endocrine glands. Though the basic steps and the key regulatory proteins involved in this process are known, the temporal and spatial dynamics of these molecules at the sites of exocytosis remain unclear. Here, we use total internal reflection fluorescence microscopy to visualize protein dynamics at individual synaptic-like microvesicles in live PC12 cells. We employ two-color imaging to simultaneously observe vesicles undergoing fusion (using a vesicular neurotransmitter transporter as the

marker), and the dynamics of various exocytic proteins at these sites of fusion, before, during and following fusion. Our experiments reveal that while many exocytic proteins such as the SNAREs, SNARE modulators and Rab proteins are already present at the sites of fusion, the SNARE modulator tomosyn and the Rab proteins, Rab3A and Rab27A, leave these sites soon after fusion. Interestingly, we find that the BAR domain proteins, Amphiphysin1 and Syndapin2, involved in sensing/inducing membrane curvature, are recruited to sites of fusion during exocytosis, suggesting a role for these proteins in regulating fusion pore expansion. Our findings provide insights into the dynamics of key mediators of exocytosis and endocytosis during the moments surrounding fusion in live cells, and advance our understanding of the regulatory roles of these various proteins.

Brg Cancer Mutations Disrupt Direct Interaction with PRC1 to Enhance Polycomb Activity. B.Z. Stanton, C. Hodges, W.L. Ku, K. Zhao, G.R. Crabtree; Systems Biology Center, Stanford School of Medicine.

Genetic alterations of the subunits of the mammalian SWI/SNF (mSWI/SNF or BAF) complex contribute to a range of human diseases, with established roles in early-childhood malignancies and neurologic disorders. We sought to examine defects of the core ATPase Brg (SMARCA4), where heterozygous mutations observed in cancer cluster at conserved regions of the ATPase domain. To examine their mechanistic effects, we generated a library of Brg variants with mutations in three conserved regions of the ATPase domain, and found that heterozygous expression of these ATPase mutants leads to increased occupancy of Polycomb Repressive Complex 1 (PRC1) at bivalent CpG-island promoters, accompanied by increases in H3K27me3 ~2 kbp away. We find that ATPase mutations disrupt a direct interaction between mSWI/SNF and PRC1 that is regulated by ATP in wild-type Brg, revealing that direct remodeling of Polycomb is a previously unknown function of mSWI/SNF complexes, and that PRC1 is a direct target of Brg ATPase activity. As a result, deregulation of Polycomb activity may be a more common feature of mSWI/SNF-mutated cancers than has been previously recognized.

Proteomic Profiling Reveals that 3-dimensional Engineered Heart Tissue Culture Promotes Maturation and Aerobic Respiration of Human Induced Pluripotent Stem Cell-derived Cardiomyocytes. A. Stoeckl¹, B. Ulmer², I. Mannhardt², S. Patel³, M. Gucek³, T. Eschenhagen², A. Hansen², E. Murphy¹
¹Systems Biology Center, ²Dep. of Exp. Pharmacology and Toxicology, CVRC, DZHK, UKE, Hamburg, Germany, ³Proteomics Core Facility.

Human cardiomyocytes differentiated from induced pluripotent stem cells serve as an unlimited source of patient-specific cardiomyocytes and hold a promising future for disease modeling and drug screening. Current limitations include their immature nature when compared to adult human cardiomyocytes. Here, we characterize maturation status of cardiomyocytes when cultured in a physiological format such as engineered heart tissue (EHT). We employed proteomics to identify differences in the status of maturation between 2D and EHT culture using an Orbitrap Fusion system. FACS analysis served to identify MitoTracker-stained mitochondria in 2D and EHT cardiomyocytes. To characterize metabolism blood gas analysis of culture media

and a C¹⁴-oxidation assay were performed. Proteomic profiling identified 256 proteins with significant difference between 2D vs. EHT ($p < 0.05$). ~40% out of these different proteins were mitochondrial, all of these showed increased protein levels in EHT. Cardiomyocytes in EHT exhibited increased protein levels of enzymes involved in fatty acid oxidation such as mitochondrial 3-ketoacyl-CoA thiolase and decreased protein levels of enzymes involved in carbohydrate metabolism such as triosephosphate isomerase ($p < 0.05$). Canonical pathway analysis revealed an increase in oxidative phosphorylation and TCA cycle, and decreased activation of glycolysis and gluconeogenesis in EHT. We compared the mitochondrial proteomic profiles of 2D and EHT to those of non-failing human hearts (NFH) and detected high similarities between EHT and NFH in clustering analysis. MitoTracker-stained cardiomyocytes showed an increase of mitochondrial mass in EHT vs. 2D. EHT-cultured cardiomyocytes consumed less glucose than 2D-cultured cardiomyocytes. In EHT, we measured more mitochondrial oxidative metabolism than in 2D. This study suggests that a physiological 3-dimensional tissue culture promotes human cardiomyocyte maturation. This knowledge might improve future studies in the field of individualized disease modeling in patient-specific cells.

An Addition to the Toolkit of NMR Spectroscopy for Large Proteins and Complexes: Lanthanide-induced Pseudocontact Shifts. M. Strickland, C.D. Schwieters, A.M. Stanley, G. Wang, A.C.L. Opina, S. Buchanan, A. Peterkofsky, O. Vaslatiy, N. Tjandra; Laboratory of Structural Biology.

As protein size increases, NMR structural studies also increase in complexity. Proton-proton distance-based restraints can no longer be used for proteins above 20 kDa due to the need for deuteration. Instead, the static magnetic field produced by the superconducting magnet is exploited to provide long-distance restraints. Residual dipolar couplings (RDCs) provide the relative angles of bonds or domains with respect to the magnetic field (so can essentially provide relative bond angles across infinite distances). Paramagnetic relaxation enhancement (PRE) provides distances from a paramagnetic tag, such as gadolinium or a radical, to the atom of interest, up to distances of around 45 Å. Pseudocontact shifts provide both distances and angles between a paramagnetic tag, usually a lanthanide, and the atom of interest, so provide much richer information than RDCs or PRE. However, until now, lanthanide-containing tags have proven difficult to use, due to their intrinsic flexibility, which lowers spectral quality. Here, we show how a rigidified lanthanide tag can provide high quality information such that we can extract both angular and distance information from the results. We show how this information can be used for structure validation, calculation, and docking. Uniquely, we are provided with distance and angle information that can reach over 100 Å from the lanthanide center, leading to the refinement and docking of a 40 kDa protein complex that could not be solved by traditional methods. In summary, we show that PCS can take its place among the ever-expanding NMR toolkit for large, dynamic, and complex systems.

Rapamycin Augments Regulatory T cell Expansion through Interaction with CD3-CD45R⁻ Cells. W. Sun, K. Keyvanfar, Z. Lin, J. Chen, X. Feng, N. Young; Hematology Branch.

Rapamycin, an immunosuppressive agent, was reported to suppress effector cells directly and expand regulatory T cells (Treg cells) both in vitro and in vivo, which plays important roles in effective therapy of autoimmune diseases such as RA, AIH, UVEitis and in mouse models of autoimmunity (MS, SLE, EOA). It is unclear, though, whether rapamycin's Treg-stimulating effect was achieved by acting on CD4⁺ cells directly or by interacting with other cellular components. We sorted spleen cells from normal C57BL/6 mice into CD3⁺CD4⁺, CD3⁺CD8⁺, CD3-CD45R⁺ and residue CD3-CD45R⁻ cell fractions, and cultured CD3⁺CD4⁺ cells alone or in combination with each of the other three cell components, with or without 50 ng/mL rapamycin. Analyses of cells recovered after 24 -hour culture showed significantly higher proportions of CD3⁺CD4⁺FoxP3⁺ and CD3⁺CD4⁺CD25⁺FoxP3⁺ cells when CD3⁺CD4⁺ cell were co-cultured with rapamycin and CD3-CD45R⁻ cells. Culturing CD3⁺CD4⁺ cells with rapamycin alone, or with rapamycin plus CD3⁺CD8⁺ or CD3-CD45R⁺ cells produced no effect on the proportion of CD3⁺CD4⁺FoxP3⁺ and CD3⁺CD4⁺CD25⁺FoxP3⁺ cells relative to the same cell cultures without rapamycin. In a separate study, we used the same design but extended cell culture to 72 hours. Similar results were observed. Our data suggest that rapamycin expands Treg cells probably by the support of residue cells other than T cells or B cells, the cell components of this population and mechanism of expanding Treg are under investigation.

Actin Retrograde Flow Orients and Aligns Activated Integrins in Focal Adhesions. V. Swaminathan, C.M. Waterman; Laboratory of Cell and Tissue Morphodynamics.

Integrins are transmembrane receptors that bind extracellular matrix and serve as anchors between cells and their environments via linkage to the actin cytoskeleton. Since cytoskeletal forces in migrating cells are organized by a stereotypical "retrograde flow" of actin filaments in the leading edge where focal adhesions form, we hypothesized that cytoskeletal flow should orient and align activated integrins clustered in focal adhesions. We tested this hypothesis using engineered fluorescent protein- α V integrin chimeras and imaging with polarization-sensitive fluorescence microscopy techniques. We show here that α V β 3 integrins are aligned with respect to their neighbors and with respect to the axis of individual FAs in migrating fibroblasts. By manipulating ligand and integrin conformation, we find that adopting the high affinity conformation is not sufficient to induce integrin alignment and orientation, however these functions do require binding to immobilized ligand. Manipulation of actomyosin activity shows that alignment does not require myosin contractility or the mere alignment of the actin cytoskeleton. Finally, by engineering α V integrin with differentially oriented GFP with respect to the integrin heterodimer and Rosetta modeling of the predicted orientations, we suggest that activated α V β 3 integrins are oriented with their β -tail-to- α -tail axes nearly aligned along the FA long axis. These results show for the first time that focal adhesions are built of an anisotropic molecular scaffold that may underlie the ability of cells to sense the direction of force and the alignment of the ECM.

Identification and Characterization of a Novel Gene that Regulates Mitochondrial DNA Replication. J. Tang, Y. Zhang, K. Delaney, H. Xu; Laboratory of Molecular Genetics.

Mitochondrial DNA (mtDNA) replication is essential for mitochondrial function in response to developmental and physiological demand. Impaired mtDNA replication leads to developmental defects, aging and diseases. To identify novel genes involved in the regulation of mtDNA replication, we conducted an in vivo RNAi screen in *Drosophila* and identified a novel gene, CG3862. We found that the protein encoded by CG3862 is associated with the mitochondrial inner membrane. CG3862 mutant has severe developmental delay and is lethal during pupa and adult stages. Genetic analysis indicates that this gene has an essential role in mtDNA replication. Loss of this gene results in impaired mitochondrial oxidative phosphorylation activity. The human homolog, WBSCR16, is one of the genes that flank the Williams-Beuren syndrome (WBS) commonly deleted region. The function of WBSCR16 in human is completely unknown. We expressed WBSCR16 in human tissue culture cells and found it expressed in mitochondria. Knocking down WBSCR16 expression in human tissue culture significantly slows down the mtDNA replication rate. Further characterization of CG3862 mutant and its human homolog may provide insight into the mechanism of regulation of mtDNA replication during development and the pathogenesis of diseases.

***Drosophila* Methionine Sulfoxide Reductase A cannot act as an oxidase.** S. Tarafdar¹, N.M. Rusan², R.L. Levine¹; ¹Laboratory of Biochemistry, ²Cell Biology and Physiology Center.

Methionine sulfoxide reductase A stereospecifically catalyzes the reduction of S-methionine sulfoxide to methionine and is important in defense against oxidative stress. Recently, we reported that mammalian methionine sulfoxide reductase A stereospecifically and selectively oxidizes Met77 in calcium-bound calmodulin and can fully reduce it as well. The control mechanism that prevents futile cycling is hypothesized to be through interaction with a postulated regulatory protein. Thus, cyclic oxidation and reduction of methionines in proteins could function as a redox-based mechanism of cellular regulation. Taking advantage of the powerful genetic tools of *Drosophila*, we set out to assess the physiological significance of methionine sulfoxide reductase A-mediated reversible oxidation of calmodulin Met77. Unexpectedly, our in-vitro assays established that *Drosophila* methionine sulfoxide reductase A was unable to oxidize calmodulin. This led us to explore the mechanistic details of the enzyme. Using a double alkylation approach followed by HPLC-mass spectrometry sequencing, we found that the active site cysteine residue in *Drosophila* methionine sulfoxide reductase A becomes locked in a disulfide bond with the terminal cysteine residue of the protein and thus cannot mediate oxidation of calmodulin.

Spatiotemporal regulation of adhesions disassembly at the G2/M transition of the cell cycle. H.R. Thiam, C.M. Waterman; Laboratory of Cell and Tissue Morphodynamics.

Cell division has two opposite faces: necessary for various physiological processes such as embryogenesis and tissue renewal, it can also lead to death by allowing tumour growth. One hallmark of metazoan cell division is the drastic shape change occurring during mitotic cell rounding. Recent studies have

shown that such shape change is required for proper chromosome segregation as well as spindle positioning, orientation and stability. In order for a dividing cell to round up, it must, reduce its contact area with the extracellular matrix (ECM), and thus loosen its cell-ECM adhesions. The mechanism allowing dividing cells to spatiotemporally regulate their focal adhesion disassembly at the G2-M transition remains unknown. Using TIRF microscopy, we show here that Vinculin, FAK and Paxillin get dissociated from the integrins before nuclear envelope breakdown at mitotic entry leading to focal adhesion disassembly. FAK and milli-calpain have been implicated in focal adhesion disassembly in migrating interphase cells. In order to determine their respective role in focal adhesion disassembly at mitosis; we inhibited FAK and calpain activities using well characterized inhibitors. We found that while FAK inhibition causes a global defect in mitosis (delay in mitotic entry and cytokinesis), inhibition of milli and even micro-calpain leads to a drastic inhibition of focal adhesion disassembly at mitotic entry. Our data suggest that focal adhesion disassembly at mitosis requires calpain proteolysis activity presumably via cleavage of some adaptor proteins such as Talin. The data further suggest that calcium dynamic at mitosis might be a key regulator of focal adhesion disassembly.

Use of Mobile Health (mHealth) Technology to Identify Targets for Improving Cardiovascular (CV) Health For Women in a Resource-limited Community: Observations from the Washington, D.C. CV Health and Needs Assessment. S. Thomas, L. Yingling, G. Wallen, A. Todaro-Brooks, M. Peters-Lawrence, J. Henry, J. Saybe, J. Adu-Brimpong, V. Mitchell, D. Sampson, T. Johnson, K. Wiley, Jr., A. Graham, L. Graham, A. Johnson, T. Powell-Wiley; Social Determinants of Cardiovascular Risk and Obesity Group.

Little is understood about using mHealth technology, particularly wearable devices, to assess CV health factors among women in resource-limited communities. We conducted the Washington, D.C. CV Health and Needs Assessment, community-based participatory research in predominantly African-American, faith-based organizations (NCT01927783) in city wards (5, 7 and 8) with lower socio-economic status. The assessment at each community church measured CV health factors [body mass index, fasting blood glucose and cholesterol, blood pressure, fruit/vegetable intake, physical activity (PA), smoking]. Each participant was trained on using a PA wrist-worn device to monitor PA amount during a 30-day period. PA data was wirelessly uploaded to PA-data collection hubs located at the participating churches. Participants accessed their data on a secure account from a church/home computer. CV health factors were compared across weight classes. Among women ($n=78$; 99% AA; mean age= 59 years), 90% had a BMI categorized as overweight/obese. Across weight classes, PA decreased and self-reported sedentary time (ST) increased ($p \leq 0.05$). Diastolic blood pressure (BP) and glucose increased across weight classes ($p \leq 0.05$); however, cholesterol, glucose, and BP were near intermediate CV health goals. Decreased PA and increased ST are potential community intervention targets for obese women in resource-limited Washington, D.C. areas. mHealth technology can assist in adapting intervention resources to improve CV health for AA women in resource-limited communities.

Fasting regulates NLRP3 inflammasome activation in humans by modulating mitochondrial integrity. J. Traba, S.S. Geiger, M. Kwarteng-Siaw, T.C. Okoli, J. Li, K. Han, M. Pelletier, A.A. Sauve, D. Gius, R.M. Siegel, M.N. Sack; Cardiovascular and Pulmonary Branch.

Fasting confers beneficial effects against inflammation-linked diseases, including vascular disease and diabetes. Activation of the Nod-like receptor family protein 3 (NLRP3) inflammasome, an innate immune surveillance complex involved in the activation of inflammatory cytokines, is implicated in this pathophysiology. It includes cytosolic proteins NLRP3, the adaptor protein ASC and procaspase-1, which assemble on mitochondria, where the extrusion of mitochondrial content (reactive oxygen species, mitochondrial DNA or cardiolipin) mediates its activation. It has been proposed that members of the Sirtuin family of protein deacetylases are involved in mitochondrial homeostasis and are activated by caloric restriction. We hypothesized that fasting blunts the NLRP3 inflammasome via Sirtuin-mediated augmentation of mitochondrial integrity. To test this we performed a clinical study with volunteers. Subjects underwent a 24-hour fast and then were fed a fixed-calorie meal. Blood was drawn during the fasted and fed states and analyzed for inflammasome activation in leukocytes. Individuals showed less NLRP3 inflammasome activation, in parallel with signatures consistent with activation of the mitochondrial-enriched SIRT3, in the fasted state compared with refeed conditions. Pharmacologic SIRT3 activation using Nicotinamide Riboside blunted NLRP3 activity in parallel with enhanced mitochondrial function. We further characterized the role of SIRT3 by studying a downstream effector Superoxide Dismutase 2 (SOD2), which eliminates mitochondrial ROS, a known inflammasome activator. We found that a constitutively active SOD2 mutant strongly inhibited the inflammasome, whereas an inactive mutant did not. SOD2-mediated inhibition of ROS accumulation prevents the localization and assembly of the NLRP3 complex on mitochondria. Together, our data indicate that nutrient levels regulate the inflammasome through SIRT3-SOD2-mediated mitochondrial homeostatic control. This process may be amenable to targeting in disease.

Imaging the lipid landscape at single sites of exocytosis. A.J. Trexler, J.W. Taraska; Laboratory of Molecular and Cellular Imaging.

Lipids play an integral structural and regulatory role in exocytosis. Particular lipids directly bind and regulate the protein components of the exocytic machine, and many lipids directly modulate the biophysical properties of the plasma membrane and affect fusion pore formation and stability. How and when particular lipids are recruited or generated at single sites of exocytosis remains unclear. Here we visualize lipids at single exocytic sites in insulinoma cells using two-color total internal reflection fluorescence microscopy. Lipids species are visualized using lipid-binding protein domains tagged with fluorescent proteins, and exocytic events are identified using a vesicle lumen marker, NPY-GFP. We found the rapid, transient recruitment of a PIP2-sensor to sites of exocytosis around the time of membrane fusion, suggesting either spatial clustering or local synthesis of PIP2. PI4K2A kinase colocalizes with dense-core vesicles and we hypothesize it might locally generate PIP2. Intriguingly, we also observe transient recruitment of a DAG-sensor to sites

of exocytosis, also centered on the time of membrane fusion. We also find that a probe for phosphatidylserine is enriched at exocytic sites prior to membrane fusion and diffuses away after exocytosis. We hypothesize that both PIP2 and DAG may be locally synthesized at sites of exocytosis, where PIP2 helps to recruit a protein complex that modulates cargo release and DAG could directly modulate the nascent fusion pore by changing the biophysical properties of the local lipid membrane. Together this data helps to build a model for the dynamic changes in local lipid environment at sites of exocytosis.

Genomic Sequencing of Cell-free DNA in Sickle Cell Disease. L. Tumburu, L. Li, Y. Wakabayashi, I. Tunc, X. Wang, J. Zhu, S.L. Thein; Sickle Cell Branch.

Cell-free DNA (cfDNA) corresponding to nucleosomes (~147 bp) and chromatosomes (~167 bp), are present at low concentrations in plasma and other bodily fluids. In healthy humans, the source of plasma cfDNA has been primarily attributed to apoptosis of normal cells of the hematopoietic lineage. In contrast, it has been hypothesized that in disease, a considerable proportion of cfDNA is derived from other tissues. Using q-PCR, we have previously shown that cfDNA in patients with sickle cell disease (SCD) increased dramatically during acute painful episodes, suggesting that the cfDNA is derived from necrotic tissues, and might contain evidence of the epigenetic landscapes of the cells giving rise to these fragments. We applied next generation sequencing (NGS) to analyse cfDNA from the plasma of healthy individuals (control), patients with SCD in steady-state, and during painful crises. NGS of conventional, double-stranded cfDNA libraries (average depth < 1 fold) revealed fragment length distributions with a dominant peak at ~170bp, followed by a peak at ~300-400 bp. We hypothesize that the dominant peak at ~170bp is of apoptotic origin, whereas the peak at ~300-400bp is associated with necrosis. No significant difference in the distribution of different sized cfDNA fragments (<100 bp, <115bp, and <150 bp, and >250bp), and genomic distributions of plasma DNA across segments (1kb bins) were observed in each of the control, steady-state, and crisis groups. Recent studies suggest shorter cfDNA fragments (~35-80 bp) which directly footprint the in vivo occupancy of DNA-bound transcription factors, are better recovered by the single-stranded library preparation. We are currently focused on deeper sequencing of the double-stranded, as well as single-stranded libraries, to obtain higher resolution of the genomic and epigenetic footprints of cfDNA in SCD.

A simple CRISPR tool for off-target analysis. I.Tunc, S.Hong, X.Wang, C.E. Dunbar; Systems Biology Core, Hematology Branch.

Rhesus macaques (*Macaca mulatta*) are developmentally and physiologically closely related to humans. Also, most cytokines, antibodies, and other reagents cross-react, making translation to clinical trials more straightforward. Therefore, we believe rhesus macaques are an ideal species to utilize for development of novel gene and cell therapies. However, a limitation has been the lack of robust disease models in macaques. The clustered, regularly interspaced, short palindromic repeat (CRISPR) technology has become a powerful tool for generating RNA-guided nucleases and offers an opportunity to generate macaque disease models to use for investigations of pathophysiology as well as to test new

therapies. Besides improving the specificity of the region of interest, assessment of off-target effects is a crucial step in these studies. Currently, there is an available online tool (<http://crispr.mit.edu>) that helps researchers in analyzing off-target effects for a specified genomic region. However, the current tool does not include genomes of non-human primates. Here, we developed a simple pipeline that helps analyzing rhesus macaque genome and scoring off-target regions by adapting the same formula used in the online tool. Our pipeline has the advantage of being locally installed; therefore it is much faster and can be used for targeting larger regions of interest. It also provides different formats of output results for later downstream analysis. This platform will be of importance to several intramural research groups working in the non-human primate models.

Molecular mechanisms underlying arterio-venous alignment in the skin. Y. Uchida, Y. Mukouyama; Laboratory of Stem Cell and Neuro-Vascular Biology.

In mouse embryonic limb skin, the pattern of sensory nerves provides an anatomical template that controls the arterial patterning, resulting in a congruence of sensory nerve and arterial branching. The observed sensory nerve-artery alignment raised the question of what controls venous branching. Our extensive time-course analysis of venous development in the limb skin vasculature revealed that the venous remodeling of capillary plexus to form large-diameter veins and subsequent vascular smooth muscle coverage begin adjacent to remodeled arteries from E15.5 onwards, suggesting that venous branching is followed by the sensory nerve-artery alignment. By E17.5, the remodeled veins become aligned with the remodeled arteries, albeit no direct association between these two vessels. We have recently found that a chemorepulsive guidance cue Semaphorin3G is preferentially expressed by arteries and its receptor Neuropilin2 is expressed by veins, and these mutants exhibit abnormal arterio-venous alignment such that a very close proximity or association between arteries and veins can be observed. In addition, mutants carrying plexinD1, ephrinB2 and TGFbeta receptor 2 exhibit defective arterio-venous alignment such that veins do not follow arteries. We are currently investigating how these molecules orchestrate venous branching pattern.

Roflumilast Effect on Aquaporin-2 Phosphorylation and Trafficking in Rat Renal Inner Medullary Collecting Duct. E. Umejiego, C-L Chou, M.A. Knepper; Epithelial Systems Biology Laboratory.

Arginine vasopressin (AVP) increases the water permeability in the renal collecting duct through increases in intracellular cyclic AMP. Previous phospho-proteomic studies have shown that AVP increases the phosphorylation of the aquaporin-2 (AQP2) water channel protein at Ser256, Ser264, Ser269 and decreases phosphorylation at Ser261. Proteomic profiling has shown that phosphodiesterase 4 (PDE4) is the predominant isoform of cyclic nucleotide phosphodiesterase in inner medullary collecting duct (IMCD) cells. Roflumilast is a selective phosphodiesterase 4 (PDE4) inhibitor, which is FDA-approved for the treatment of chronic obstructive pulmonary disease. With a view toward treatment of patients with hemizygous mutations in the vasopressin receptor, this study sought to determine the effect of Roflumilast on AQP2 phosphorylation and trafficking in rat IMCD. Neither Roflumilast nor its active metabolic

form Roflumilast N-oxide (RNO) (at 30 nM) had an effect on AQP2 phosphorylation in IMCD suspensions as tested by immunoblotting using phospho-specific antibodies. Furthermore, Roflumilast did not stimulate AQP2 trafficking to the plasma membrane (immunofluorescence) or increased water permeability in freshly microdissected IMCD segments. However, in the presence of the vasopressin analog dDAVP (0.1 nM), both Roflumilast and RNO significantly increased AVP-induced phosphorylation at Ser256, Ser264, Ser269 and decreased phosphorylation at Ser261 in a dose-dependent manner (3-3000 nM). By comparison, another phosphodiesterase inhibitor, IBMX, had effects only at the highest concentration. We conclude that Roflumilast can be used to enhance vasopressin's action on AQP2 activity in the renal collecting duct, but has no effect in the absence of vasopressin.

Mitochondrial Nutrient Sensing, FoxO1 Stability and the Retrograde Control of Gluconeogenesis. L. Wang, I. Scott, L. Zhu, M. Sack. Cardiovascular and Pulmonary Branch.

The nutrient sensing Gcn5-like 1 (Gcn5L1) protein is enriched in liver mitochondria, is found to be differentially regulated in the fasted and fed state, and modulates mitochondrial protein acetylation and function. Gcn5L1 depletion enhances mitochondrial turnover via mitochondrial retrograde signal mediated activation of endosomal-lysosomal trafficking. The molecular characterization of this induction of retrograde signaling and the molecular functioning of Gcn5L1 itself remain poorly defined. To further explore its metabolic role we crossed floxed Gcn5L1 with albumin-cre-recombinase mice to generate Gcn5L1 liver-specific knockout (LKO) mice. The mice were viable and basal metabolic phenotyping showed markedly impaired gluconeogenesis. Given that excessive gluconeogenesis is a sine qua non of type 2 diabetes, we explored the role of Gcn5L1 in regulating gluconeogenesis. Glucose productions under basal conditions and in response to glucagon stimulation were dramatically decreased in Gcn5L1 LKO primary hepatocytes. The expression of key gluconeogenic enzymes, PEPCK and G6Pase, were significantly down-regulated in Gcn5L1 LKO hepatocytes and liver tissues. In parallel, the levels of FoxO1, a critical transactivator of PEPCK and G6Pase expression, were diminished with evidence of FoxO1 ubiquitylation and degradation in the absence of Gcn5L1. The reconstitution with either wildtype or mitochondrial-targeting Gcn5L1 restored FoxO1 levels, gluconeogenic enzyme expression and glucose production. In addition, the depletion of the mitochondrial deacetylase Sirt3 similarly restored the transcript levels of PEPCK and G6Pase in Gcn5L1 LKO hepatocytes. These findings support that mitochondrial acetylation 'nutrient-sensing' modulates the post-translational control of nuclear transcription factor in coordinating the regulation of gluconeogenesis. The retrograde signaling pathways underpinning these findings are actively being explored.

Drosophila Clueless is Involved in Parkin-Dependent Mitophagy by Promoting VCP-Mediated Marf Degradation. Z.H. Wang, C. Clark, E. Geisbrecht; Kansas State University and University of Missouri-Kansas City.

PINK1/Parkin-mediated mitochondrial quality control (MQC) requires valosin-containing protein (VCP)-dependent Mitofusin/Marf degradation to prevent damaged organelles

from fusing with the healthy mitochondrial pool, facilitating mitochondrial clearance by autophagy. *Drosophila clueless (clu)* was found to interact genetically with PINK1 and parkin to regulate mitochondrial clustering in germ cells. However, whether Clu acts in MQC has not been investigated. Here, we show that overexpression of *Drosophila Clu* complements PINK1, but not parkin, mutant muscles. Loss of *clu* leads to the recruitment of Parkin, VCP/p97, p62/Ref(2)P, and Atg8a to depolarized swollen mitochondria. However, clearance of damaged mitochondria is impeded. This paradox is resolved by the findings that excessive mitochondrial fission or inhibition of fusion alleviates mitochondrial defects and impaired mitophagy caused by *clu* depletion. Furthermore, Clu is upstream of and binds to VCP *in vivo* and promotes VCP-dependent Marf degradation *in vitro*. Marf accumulates in whole muscle lysates of *clu*-deficient flies and is destabilized upon Clu overexpression (OE). Thus, Clu is essential for mitochondrial homeostasis and functions in concert with Parkin and VCP for Marf degradation to promote damaged mitochondrial clearance.

Identifying Clusters of Genes Driving Complex Disease Progression. N. Wolanyk, X. Wang, M. Hessner, S. Gao; Systems Biology Core.

The progression of modern medicine has eliminated many diseases and mitigated the effect of others to mere nuisances, but the ones that are still prevalent are complex diseases. Complex diseases are thus named due to the multitude of factors that can play a role in developing the disease. Recent studies have started to paint a picture of a different approach for these diseases. The theory is that there must be a common point among all of the patients of a specific disease where all of the variable factors for the disease combine to begin the process that ends in symptoms and diagnosis. After diagnosis it is difficult if not impossible to return a patient to a healthy state. By targeting the common factor among all patients, a cluster of genes are identified which act in tandem to begin the final push into the disease developing symptoms and diagnosis; this cluster is known as a driving network. I have identified a driving network in Type 1 Diabetes (T1D) and developed a process that is capable of being applied to many other complex diseases without the different stages being known. The data used is affymetrix data from healthy Peripheral Mononuclear Blood Cells exposed to high risk patient's plasma. There are 36 patients with an average of 5 time points spaced half a year apart and roughly half of them progressed into T1D.

Two distinct actin networks mediate traction oscillations to confer mechanosensitivity of focal adhesions. Z. Wu¹, S.V. Plotnikov³, C.M. Waterman², J. Liu¹; ¹Theoretical Cellular Physics Section, LMB, BBC, ²Laboratory of Cell and Tissue Morphodynamics, CBPC, ³Department of Cell and Systems Biology, University of Toronto.

Focal adhesions (FAs) are integrin-based transmembrane assemblies. They serve as mechanosensors through which cells sense the mechanical stiffness of their extracellular matrix (ECM) by exerting actin cytoskeleton-mediated traction force. Interestingly, FA itself is a dynamic structure that adapts its area and composition in response to mechanical force. How the cell manages this FA plasticity to accurately sense ECM stiffness remains an open question. Strikingly, FA-localized traction forces oscil-

late in time and space and govern the cell mechanosensing of ECM stiffness. Precisely how and why the FA traction oscillates is unknown. Combining theory and experiment, we develop a model of FA growth that integrates coordinated contributions of a branched actin network and stress fibers (SF) in the process. We show that the mechanical engagement with retrograde flux of branched actin network contributes to a traction peak near the FA distal tip, while promoting the proximal growth of the FA. This temporally results in a traction gradient within the growing FA that favors SF formation near the FA proximal end. The SF-mediated actomyosin contractility stabilizes the FA and generates a second traction peak near the FA center. Formin-mediated SF elongation negatively feeds back with actomyosin contractility, resulting in the central traction peak oscillation. This underpins the observed FA traction oscillation, and broadens the ECM stiffness range, over which FAs could accurately adapt with traction force generation. We therefore suggest that FA traction oscillation reflects a fundamental mechanism that inherently couples the FA growth with the FA mechanosensing.

Tissue-Resident Macrophage Progenitors Differentiate into Pericytes through TGF- β Signaling in Developing Skin Vasculature. T. Yamazaki¹, A. Nalbandian¹, Y. Uchida¹, W. Li¹, T.D. Arnold², Y. Kubota³, M. Ema⁴, Y. Mukoyama¹; ¹Laboratory of Stem Cell and Neuro-Vascular Biology, ²Department of Pediatrics, Physiology, and Program in Neuroscience, University of California, San Francisco, ³Center for Integrated Medical Research, School of Medicine, Keio University, ⁴Department of Stem Cells and Human Disease Models Research Center for Animal Life Science, Shiga University of Medical Science.

Interactions between endothelial cells and mural cells (pericytes and vascular smooth muscle cells) in blood vessels are essential for the regulation of vascular networks and maintenance of vascular integrity. Despite the significance of pericytes in the vascular function, the origin of pericytes in the developing vasculature has been elusive. Here we show that pericytes are derived from tissue-localized macrophage progenitors in the developing skin vasculature. Whole-mount immunohistochemical analysis revealed that NG2⁺ and platelet derived growth factor receptor (PDGFR) β ⁺ pericytes are distally located from the vascular smooth muscle cell-covered large diameter vessels. To determine their developmental origin in the skin, we conducted a series of *in vivo* fate-mapping experiments using different cell type-specific *Cre* lines. These experiments indicated that tissue macrophage progenitors appear to generate pericytes in the skin. To investigate the requirement of the tissue-macrophage progenitors for the pericyte development *in vivo*, we analyzed *PU.1* mutants lacking myeloid lineage including these progenitors. The mutants fail to develop pericytes in the skin, though their vascular network appears to be normal. Furthermore, FACS-isolated F4/80⁺ tissue-macrophage progenitors from embryonic skins give rise to NG2⁺ and PDGFR β ⁺ pericytes in culture. Interestingly, transforming growth factor- β (TGF- β) signaling is required for pericyte differentiation from tissue macrophage progenitors in culture, and conditional inactivation of type2 TGF- β receptor (*Tgfb β 2*) results in deficient pericyte development in the skin. Combined, these data suggest that tissue macrophage progenitors differentiate into pericytes through TGF- β signaling in the skin vasculature.

Integrative Transcriptome Analyses of Metabolic Responses in Mice Define Pivotal lncRNA Metabolic Regulators. L. Yang, P. Li, W. Yang, X. Ruan, Y. Zhao, K. Kieseewetter, H. Luo, J. Zhu, H. Cao; Laboratory of Obesity and Metabolic Diseases.

The long non-coding RNAs (lncRNAs) are transcripts longer than 200 nucleotides without protein coding potential. Contrary to the longstanding assumption that the mammalian genomes mainly encode protein-coding genes, the number of lncRNA genes exceeds the number of protein-coding genes in human genome. Considering the metabolic function of lncRNAs is largely unknown, we are going to evaluate the significance of lncRNAs, and identify the functional lncRNAs in systemic metabolism in mice. We performed over 100 transcriptome analyses to simultaneously profile mRNAs and lncRNAs in key metabolic organs in mice under pathophysiologically representative metabolic conditions. Similar to mRNAs, lncRNA transcriptome in each tissue forms a metabolic signature reflecting the animal's metabolic or disease condition. Out of 7,608 regulated lncRNAs, function-orientated filters yield 541 tissue-specifically regulated and metabolically sensitive lncRNAs which are predicted by lncRNA-mRNA correlation analyses to function in diverse aspects of energy metabolism. Specific regulations of liver metabolically sensitive lncRNAs (lncLMS) by individual nutrients, metabolic hormones and key transcription factors were further defined in primary hepatocytes connecting these lncRNAs to metabolic signaling pathways. Combining the extensive genome-wide screens, bioinformatics function predictions and cell-based analyses, we have developed an integrative roadmap to identify functional lncRNA metabolic regulators *in vivo*. Mice with liver-specific knockdown of an SREBP1c-inducible lncLMS, predicted to regulate lipid metabolism by our roadmap, exhibit elevated lipogenic gene expressions and circulating levels of triglyceride. Taken together, this study identifies a class of lncRNAs function as important metabolic regulators, and establishes a framework for investigating the role of lncRNAs in physiological homeostasis.

Dietary marine long-chain monounsaturated fatty acid (LCMUFA) attenuates the development of atherosclerosis via PPAR signaling pathway in mouse models. Z.H. Yang¹, M. Bando², H. Miyahara³, J. Takeo³, B. Vaisman¹, M. Pryor¹, H. Sakaue², M. Sata², A. Remaley¹; ¹Lipoprotein Metabolism Section, Cardio-Pulmonary Branch, ²Institute of Biomedical sciences, Tokushima University Graduate School, ³Central Research Laboratory, Nippon Suisan Kaisha.

Cardiovascular disease (CVD) is a major healthcare problem worldwide. Numerous studies have shown cardiovascular benefits of fish oil, and most of these favorable effects have been attributed to omega-3 fatty acids. Fish oils, however, also contain varying amounts of other unusual types of fatty acids not commonly found in other food sources, such as long-chain monounsaturated fatty acids with carbon chain length longer than 18 (LCMUFA). Compared with well-studied omega-3 fatty acids, it remains unclear whether LCMUFA-rich fish oils have beneficial effects on alleviating CVD and its risk factors. We produced an LCMUFA concentrate derived from saury oil, and fed LDLR-KO mice Western diet supplemented with 2% of either LCMUFA concentrate, shorter chain MUFA oleic acid (C18:1)-rich olive oil, or not (control) for 12 wk. LCMUFA, but not olive oil, significantly suppressed the development of athero-

sclerotic lesions and several plasma inflammatory cytokine levels, although there were no major differences in plasma lipids between the three groups. At higher doses 5% LCMUFA supplementation was observed to reduce pro-atherogenic plasma lipoproteins and to also reduce atherosclerosis in ApoE-KO mice fed a Western diet. RNA sequencing and subsequent qPCR analyses revealed that LCMUFA upregulated PPAR signaling pathways in liver. In cell culture studies, apoB-depleted plasma from LDLR-K mice fed LCMUFA showed greater cholesterol efflux from macrophage-like THP-1 cells and ABCA1-overexpressing BHK cells. LCMUFA also promoted PPAR transcriptional activity in hepatic cells. Our research showed for the first time that LCMUFA consumption protects against diet-induced atherosclerosis, possibly by upregulating the PPAR signaling pathway.

Lower Technology Fluency is Not A Barrier to User Adoption of a Mobile Health (mHealth) Wrist-worn Physical Activity (PA) Monitor System: Observations from the Washington, D.C. Cardiovascular (CV) Health and Needs Assessment, L.R. Yingling¹, V. Mitchell¹, C. Ayers², M. Peters-Lawrence³, G.R. Wallen⁴, A.T. Brooks⁴, J. Adu-Brimpong, S. Thomas¹, J.S. Henry⁵, J. Sayge¹, D.M. Sampson⁶, A.A. Johnson⁷, A.P. Graham⁷, L.A. Graham⁷, K.L. Wiley⁸, T.M. Powell-Wiley¹
¹Social Determinants of Cardiovascular Risk and Obesity, ²Donald W. Reynolds Cardiovascular Clinical Research Center at the University of Texas Southwestern Medical Center, Dallas, TX, ³Clinical Center, NIH; ⁴Office of the Clinical Director; ⁵Office of the National Coordinator for Health Information Technology, Washington, D.C.; ⁶Office of Behavioral and Social Sciences Research, Office of the Director, NIH; ⁷College of Nursing and Allied Health Sciences, Howard University, Washington, D.C.; ⁸Division of Genomic Medicine, NHGRI.

Emerging mHealth technologies, like wrist worn PA monitors, offer potential for targeting CV health behaviors among at-risk groups in community-based interventions. It is unknown whether technology fluency impedes user adoption of such mHealth interventions. A CV health evaluation designed using community-based participatory research principles was conducted in African American, faith-based organizations in Washington D.C. wards with the highest obesity rates (NCT01927783). Participants (n=100) underwent a CV health assessment at a community church and were trained on using an mHealth PA monitor for the ensuing 30-day period. Participants wirelessly uploaded PA data weekly to a data collection hub at a participating church then accessed data online. Users were participants with ≥ 1 days of data; non-users had zero days of data. A validated Computer-Email-Web fluency self-report instrument captured technology fluency, with skill levels from 1 (no fluency) to 5 (high fluency). Eighty-one participants were users (mean age=60, 78% female); 19 were non-users (mean age=57, 84% female). Users were more likely than non-users to report a lower household income ($p=0.01$). No differences were noted for computer access (94% vs. 94%, $p=0.2$) or cell phone ownership (88% vs. 89%, $p=0.2$). Technology fluency was similar, with all non-users and 95% of users reporting some level of technology fluency for the 17 surveyed skills. In faith-based communities in at-risk Washington D.C. areas, lower technology fluency does not appear to impede adoption of this mHealth PA-monitoring system, despite lower socioeconomic status among users, a relationship likely explained by similar access to technology among users and

non-users. These findings suggest that an mHealth PA monitoring system incorporating a data collection hub may facilitate a future targeted community-based PA intervention for improved CV health, independent of technology fluency of the targeted group.

The Impact of Aging of Hematopoietic Stem and Progenitor Cells (HSPCs) in Non-Human Primates as Interrogated by Genetic Barcode Clonal Tracking K. Yu, C. Wu, D. Espinoza, I. Yabe, S. Panch, S. Hong, S. Koelle, R. Lu, A. Bonifacio, A. Krouse, M. Metzger, R. E. Donahue, C.E. Dunbar; Molecular Hematopoiesis Section.

Despite advanced age being a strong poor prognostic factor, an increasing number of older patients are receiving hematopoietic stem and progenitor cell (HSPC) transplantation. To quantitatively elucidate the age-related changes that compromise hematopoietic function at a clonal level, we applied a genetic barcoding approach to quantitatively track the clonal behavior of HSPCs in young versus old rhesus macaques following autologous transplantation. There were marked differences in the patterns of clonal lineage relationships between young and old animals, as assessed via pairwise Pearson correlations of all contributing clones as well as clustering algorithms allowing interrogation of patterns of clonal behavior. We discovered a pattern of clonal reconstitution distinct from that in young animals, with persistent unilineage or highly-biased lineage progenitors in the aged animals. In old animals, clones contributing to Gr/Mo versus B or T lineages remained almost completely distinct or markedly biased up to 4m, and B and Gr/Mo became correlated from 5m, B/T/Mo/Gr multilineage clones appeared only by 6.5m, whereas B/T/Mo/Gr multilineage clones appeared by 3-4.5m in young animals. Furthermore, old animals showed the delayed reappearance of CD4⁺ and CD8⁺ naïve T cells in the blood, whereas CD4⁺ and CD8⁺ effector memory T cells showed rapid and abundant recovery compared to young animals. This approach should improve our understanding of the effects of aging on the basic properties of aging HSCs and provide insights important for improving therapies in elderly patients being treated for hematologic diseases.

Effect of Overexpression of LCAT and ApoA-I on Atherosclerosis and Lipoprotein Metabolism in Mice. A. Zarzour, A. Ossoli, B. Vaisman, S. Gordon, M. Amar, L. Calabresi, A. Remaley; Lipoprotein Metabolism Section.

Accumulating evidence is showing reverse cholesterol transport pathway can lead to protection of atherosclerosis formation and progression. Lecithin cholesterol acyl transferase (LCAT) and apolipoprotein A-1 (apoA-1) are key components of this pathway. ApoA-1 is the major protein component of high density lipoprotein (HDL) in plasma; it promotes cholesterol efflux, from tissues to the liver for excretion. It is a cofactor for LCAT which is an enzyme that converts free cholesterol into cholesteryl ester, which is then sequestered into the newly synthesized HDL to mature. We describe a novel mice background overexpressing both apoA-1 and LCAT genes and their effects on HDL metabolism and atherosclerosis formation compared with wild type or apoE KO mice, an established atherosclerosis model. Although the overexpression of both genes has led to increase cholesterol levels, we show that double transgenic mice's HDL have less in vitro cholesterol efflux capacity com-

pared with wild type mice, less neutral lipid uptake compared with ApoE KO mice and decrease in atherosclerosis formation comparing to ApoE KO mice in diet induced atherosclerosis.

A *Drosophila* Model Demonstrates Mitochondrial Regulation of Stem Cell Homeostasis. F. Zhang, K. Zhou, H. Xu; Laboratory of Molecular Genetics.

Stem cells often emphasize on glycolysis for energy production, whereas the mitochondrial activation, switch from glycolysis to oxidative phosphorylation (OXPHOS), is believed to be essential for stem cell differentiation. Mitochondrial inactivation has been considered as an efficient way to facilitate the somatic cell-pluripotent stem cell reprogramming by reversing this metabolic transition. However, the cellular signaling orchestrating the metabolic shift is largely unknown. The link between mitochondrial activity and stem cell differentiation remains to be explored. We took advantage of genetic tools for mtDNA in *Drosophila* to disrupt mitochondrial function in the intestinal stem cells (ISCs). We generated ISCs carrying homoplasmic lethal mtDNA mutation and monitored behaviors of these stem cells and the progenitor cells, enteroblasts (EBs), derived from them. We found that ISCs carrying dysfunctional mitochondria divided much slower to nearly quiescent. Very few progenitors derived from these stem cells failed to differentiate into enterocytes (ECs) or enteroendocrine cells (EEs). This result demonstrates that mitochondrial activity is essential for stem cells proliferation and differentiation, also validates *Drosophila* ISCs as a model to genetically dissect the contribution of mitochondrial activation to stem cell homeostasis.

The mitochondrial outer membrane protein MDI promotes local protein synthesis and mtDNA replication. Y. Zhang, Y. Chen, M. Gucek, H. Xu; Laboratory of Molecular Genetics.

Early embryonic development features rapid nuclear DNA replication cycles, but lacks mtDNA replication. To meet the high-energy demands of embryogenesis, mature oocytes are furnished with vast amounts of mitochondria and mtDNA. However, the cellular machinery driving massive mtDNA replication in ovaries remains unknown. Here we describe a *Drosophila* AKAP protein, MDI that recruits a translation stimulator, Lar-related protein (Larp), to the mitochondrial outer membrane in ovaries. The MDI-Larp complex promotes the synthesis of a subset of nuclear-encoded mitochondrial proteins by cytosolic ribosomes on the mitochondrial surface. MDI-Larp's targets include mtDNA replication factors, mitochondrial ribosomal proteins and electron-transport-chain subunits. Lack of MDI abolishes mtDNA replication in ovaries, which leads to mtDNA deficiency in mature eggs. Targeting Larp to the mitochondrial outer membrane independently of MDI restores local protein synthesis and rescues the phenotypes of *mdi* mutant flies. Our work suggests that a selective translational boost by the MDI-Larp complex on the outer mitochondrial membrane might be essential for mtDNA replication and mitochondrial biogenesis during oogenesis.

Registered Attendants

Tsion Abera
Section of Inflammation and
Cardiometabolic Diseases
Tsion.aberra@nih.gov

Hans Ackerman
Physiology Section, Sickle Cell
Branch
Hans.ackerman@nih.gov

Gregory Adams Jr
Laboratory of Cell and Tissue
Morphodynamics
Gregory.adams2@nih.gov

Robert Adelstein
Laboratory of Molecular
Cardiology
Robert.adelstein@nih.gov

Joel Adu-Brimpong
Social Determinants of
Cardiovascular Risk and Obesity
Joel.abu-brimpong@nih.gov

Chinyere Agbaegbu Iweka
Developmental Neurobiology
Section
Chinyere.agbaegbu@nih.gov

Inhye Ahn
Laboratory of Lymphoid
Malignancies
Inhye.ahn@nih.gov

Clay Albracht
Laboratory of Molecular
Physiology
Clayton.albracht@nih.gov

Christopher Alexander
Laboratory of Cell Biology
chris.alexander@nih.gov

Michele Allen
Murine Phenotyping Core
Allenm@nhlbi.gov

Gregory Alushin
Laboratory of Macromolecular
Interactions
alushing@mail.nih.gov

Luigi Alvarado
Molecular Hematopoiesis Section
Luigi.alvarado@gmail.com

Stasia Anderson
Animal MRI Core
andersos1@nhlbi.nih.gov

Nikolaos Angelis
Sickle Cell Branch
Nikos.angelis@nih.gov

Claudio Anselmi
Theoretical Molecular Biophysics
Section
Claudio.anselmi@nih.gov

Lucas Axiotakis
Laboratory of Macromolecular
Interactions
Lucas.axiotakis@nih.gov

Brian Bailey
Office of Technology Transfer and
Development
bbailey@mail.nih.gov

Michelle Baird
Laboratory of Cell and Tissue
Morphodynamics
Michelle.baird@nih.gov

Thomas Baird
Laboratory of Ribonucleoprotein
Biochemistry
tom.baird@nih.gov

Robert Balaban
Laboratory of Cardiac Energetics
balabanr@nhlbi.nih.gov

Lauren Banaszak
Cell Biology Section
Lauren.banaszak@nih.gov

Koyeli Banerjee
Laboratory of Structural
Biophysics
Koyeli.banerjee@nih.gov

Emilia Alina Barbu
Sickle Cell Branch
Emilia.barbu@nih.gov

Yvonne Baumer
Section of Inflammation and
Cardiometabolic Diseases
Yvonne.baumer@nih.gov

Ashley Barnes
Laboratory of Molecular
Biophysics
Ashley.barnes@nih.gov

Jordan Beach
Cell Biology Section
Jordan.beach@nih.gov

Eric Bennett
Laboratory of Imaging Physics
bennette@mail.nih.gov

Jordan Betz
Sickle Cell Program
Jordan.betz@nih.gov

Neil Billington
Laboratory of Molecular
Physiology
Neil.billington@nih.gov

Burchelle Blackman
Imaging Probe Development
Center
Burchelle.blackman@nih.gov

Christopher Bleck
Electron Microscopy Core
Christopher.bleck@nih.gov

Lynda Bradley
Laboratory of Single Molecule
Biophysics
Lynda.bradley@nih.gov

Owen Brady
Laboratory of Computational
Biology
brb@nih.gov

Chase Brisbois
Laboratory of Protein
Conformation and Dynamics
Chase.brisbois@nih.gov

Xiangning Bu
Translational Research Section
Xiangning.bu@nih.gov

Vicent Butera
Laboratory of Lymphoid
Malignancies
Vicent.butera@nih.gov

Adrienne Campbell-Washburn
Cardiovascular Intervention
Program
adrienne.campbell@nih.gov

Elizabeth Carstens
Laboratory of Lymphoid
Malignancies
Elizabeth.carstens@nih.gov

Ronald Caulder
Blood Diseases & RESCS Lung
Diseases Grant Managme3net
Branch
caulderr@mail.nih.gov

Mayukh Chakrabarti
Laboratory of Computational
Biology
Mayukh.chakrabarti@nih.gov

Ye Chen
Bioinformatics Core
Ye.chen@nih.gov

Lihe Chen
Epithelial Systems Biology
Laboratory
Lihe.chen@nih.gov

Long Chen
Laboratory of Transplantation
Immunotherapy
Long.chen@nih.gov

Zhe Chen
Laboratory of Molecular
Genetics
Long.chen@nih.gov

Ying-Han Chen
Laboratory of Host-Pathogen
Dynamics
Ying-han.chen@nih.gov

Patali Cheruku
Hematopoietic Stem Cell and
Gene Therapy
Patali.cheruku@nih.gov

Jessica Choi
Laboratory of Stem Cell and
Neuro-Vascular Biology
Jessica.choi@nih.gov

Chung-Lin Chou
Epithelial Systems Biology
Laboratory
chouj@nhlbi.nih.gov

John Ciemniecki
Laboratory of Molecular and
Cellular Imaging
John.ciemniecki@nih.gov

Randall Clevenger
Animal Surgery & Resources Core
Rc85n@nih.gov

Christian Combs
Light Microscopy Core
combosc@nih.gov

Stefan Cordes
Hematology Branch
Stefan.cordes@nih.gov

Denise Crooks
Office of Technology Transfer and
Development
crooksd@nhlbi.nih.gov

Eman Dadashian
Laboratory of Lymphoid
Malignancies
Eman.dadashian@nih.gov

Beverley Dancy
Laboratory of Cardiac Energetics
Beverley.dancy@nih.gov

Joas DaSilva
Pulmonary Clinical Medicine
Section
Joas.dasilva@nih.gov

Thaddeus Davenport
Laboratory of Molecular
Biophysics
Thaddeus.davenport@nih.gov

Katherine Delaney
Laboratory of Molecular Genetics
Katherine.delaney@nih.gov

Teegan Dellibovi-Ragheb
Laboratory of Host-Pathogen
Dynamics
Teegan.dellibovi-ragheb@nih.gov

Natalia Demeshkina
Biophysics Core
natalia.demeshkina@nih.gov

Alan Deutch
Office of Technology Transfer and
Development
deutch@nhlbi.nih.gov

Amit Kumar Dey
Section of Inflammation and
Cardiometabolic Diseases
Amit.dey@nih.gov

Heba Diab
Protein Trafficking and Organelle
Biology
diabhi@nhlbi.nih.gov

Andrea Dickey
Laboratory of Molecular
Biophysics
Andrea.dickey@nih.gov

Cory Dixon
Administrative Management
Branch
Cory.dixon@nih.gov

Susan Doh
Laboratory of Transplantation
Immunotherapy
Susan.doh@nih.gov

Gifty Dominah
Laboratory of Protein
Conformation and Dynamics
Gifty.dominah@nih.gov

Venina Dominical
Flow Cytometry Core
Venina.dominical2@nih.gov

Julie Donaldson
Laboratory of Cell Biology
donaldsonj@helix.nih.gov

Dipannita Dutta
Membrane Biology Section
Dipannita.dutta@nih.gov

Hiroko Endo
Translational Research Section
endohiro@mail.nih.gov

Crystal Fagan
RNA Biophysics & Cellular
Physiology
crystal.fagan@nih.gov

Armel Femnou
Laboratory of Cardiac Energetics
armel.femnou@nih.gov

Adrian Ferre-D' Amare
Laboratory of Biochemistry
Adrian.ferre@nih.gov

Emel Ficici
Theoretical Molecular Biophysics
Section
ficicie@nih.gov

Debbie Figueroa
Asthma and Lung Inflammation
Section
Debbie.figueroa@nih.gov

Robert Fischer
Laboratory of Cell and Tissue
Morphodynamics
Fischerr2@nhlbi.nih.gov

Jessica Flynn
Laboratory of Molecular
Biophysics
Jessica.donehue@nih.gov

Lita Freeman
Lipoprotein Metabolism Section
lita@nih.gov

Brian Galletta
Laboratory of Molecular Machines
and Tissue Architecture
Brian.galletta@nih.gov

Iris Garcia-Pak
Laboratory of Stem Cell & Neuro-
Vascular Biology
Iris.pak@nih.gov

Herbert Geller
Developmental Neurobiology
Section
gellerh@nhlbi.nih.gov

Nancy Geller
Office of Biostatistics Research
gellern@nhlbi.nih.gov

Alex George
Laboratory of Imaging Physics
Alex.george@nih.gov

Valentina Giudice
Cell Biology Section
Valentina.giudice@nih.gov

Brian Glancy
Laboratory of Cardiac Energetics
glancybp@nhlbi.nih.gov

Elizabeth Gordon
Laboratory of Asthma and Lung
Inflammation
Elizabeth.gordon@nih.gov

Scott Gordon
Lipoprotein Metabolism Section
scott.gordon@nih.gov

Thirupugal Govindarajan
Laboratory of Molecular
Cardiology
Thirupugal@nih.gov

Marjan Gucek
Proteomics Core
marjan.gucek@nih.gov

Bjorg Gudmundsdottir
Molecular & Clinical Hematology
Branch
Bjorg@mail.nih.gov

Pinar Gurel
Laboratory of Macromolecular
Interactions
Pinar.gurel@nih.gov

Kim Han
Laboratory of Mitochondrial
Biology and Metabolism
Kim.han@nih.gov

Kyungreem Han
Laboratory of Computational
Biology
Kyungreem.han@nih.gov

Susan Harbison
Laboratory of Systems Genetics
susan.harbison@nih.gov

Juan Jesus Haro Mora
Molecular & Clinical Hematology
Branch
Juanjesus.haromona@nih.gov

James Hawkins
Animal Surgery and Resources
Core
hawkinsj@nih.gov

Sara Heissler
Laboratory of Molecular
Physiology
Sarah.heissler@nih.gov

Sarah Herman
Laboratory of Lymphoid
Malignancies
Sarah.herman@nih.gov

Bobby Hogg
Laboratory of Ribonucleoprotein
Biochemistry
j.hogg@nih.gov

Maile Hollinger
Cell Biology Section
Maile.hollinger@nih.gov

Amy Hong
Laboratory of Molecular
Physiology
ahong@nhlbi.nih.gov

Jinsung Hong
Cell Biology Section
jinsung.hong@nih.gov

Kohei Hosokawa
Cell Biology Section
Kohel.hosokawa@nih.gov

Longhua Hu
Theoretical Cellular Physics
longhua.hu@nih.gov

Yinan Hua
Cell Biology Section
Yinan.hua@nih.gov

Zaineb Humayoon
Laboratory of Molecular Genetics
Zaineb.humayoon@nih.gov

Kiyoshi Isobe
Epithelial Systems Biology
Laboratory
Kiyoshi.isobe@nih.gov

Jessica Iyer
Laboratory of Lymphoid
Malignancies
Jessica.iyer@nih.gov

Rebecca Izen
Laboratory of Stem Cell & Neuro-
Vascular Biology
Rebecca.izen@nih.gov

Ji Yong Jang
Laboratory of Molecular Biology
Jiyong.jang@nih.gov

Valentin Jaumouille
Laboratory of Cell and Tissue
Morphodynamics
Valentin.jaumouille@nih.gov

Zhiping Jiang
Laboratory of Protein
Conformation and Dynamics
jiangz2@mail.nih.gov

Wenfei Jin
Laboratory of Epigenome Biology
Wenfei.jin@nih.gov

Xueting Jin
Laboratory of Experimental
Atherosclerosis
tina.jin@nih.gov

Debra Johnson
Laboratory of Cell Biology
debra.johnson@nih.gov

Christopher Jones
RNA Biophysics and Cellular
Physiology
jones.cprice@gmail.com

Aditya Joshi
Advanced Cardiovascular Imaging
Group
Aditya.joshi@nih.gov

Hyun Jun Jung
Epithelial Systems Biology
Laboratory
Hyunjun.jung@nih.gov

Seyit Kale
Theoretical Cellular Physics
Seyit.kale@nih.gov

William Kamp
Laboratory of Cardiovascular &
Cancer Genetics
Matt.kamp@nih.gov

Ju-Gyeong Kang
kangju@mail.nih.gov
Laboratory of Cardiovascular &
Cancer Genetics

Hiro Katagiri
Developmental Neurobiology
Section
katagir@helix.nih.gov

Jiro Kato
Translational Research Section
katoj@nhlbi.nih.gov

Hiroyuki Kawagishi
Laboratory of Molecular Biology
Hiroyuki.kawagishi@nih.gov

Sachiyo Kawamoto
Laboratory of Molecular
Cardiology
kawamots@mail.nih.gov

Camron Keshavarz
Electron Microscopy Core
Camron.keshavarz@nih.gov

Cecilia Kim
Laboratory of Systems Genetics
Cecelia.kim@nih.gov

Dami Kim
Office of Education
Dami.kim@nih.gov

Laura Kim
Cell Biology Section
laura.kim@nih.gov

George Kim
Protein Function in Disease
Section
king@nhlbi.nih.gov

Andrea Knab
Advanced Cardiovascular Biology
Laboratory
knep@helix.nih.gov

Mark Knepper
Epithelial Systems Biology
Laboratory
knep@helix.nih.gov

Hamed Kooshapur
Laboratory of Structural
Biophysics
Hamed.kooshapur@nih.gov

Edward Korn
Laboratory of Cell Biology
edk@nih.gov

Howard Kruth
Laboratory of Experimental
Atherosclerosis
kruthh@nhlbi.nih.gov

Wai Lim Ku
Laboratory of Epigenome Biology
Wailim.ku@nih.gov

Lo Lai
Protein Function in Disease
Section
lo.lai@nih.gov

Kelly Lane
Imaging Probe Development
Center
lanekc@mail.nih.gov

Andre Larochelle
Hematopoietic Stem Cell and
Gene Therapy
larochea@nhlbi.nih.gov

Kang Le
Laboratory of Metabolic
Regulation
lek2@mail.nih.gov

Jackie Lee
Office of Education
Jackie.lee@nih.gov

Juyong Lee
Laboratory of Computational
Biology
juyong.lee@nih.gov

Duck-yeon Lee
Biochemistry Core
leedy@nhlbi.nih.gov

Dorothy Lerit
Laboratory of Molecular Machines
and Tissue Architecture
dorothy.lerit@nih.gov

Connie Lerma Cervantes
Laboratory of Molecular
Cardiology
connie.lerma@nih.gov

Mark Levin
Laboratory of Vascular and Matrix
Genetics
mark.levin@nih.gov

Stewart Levine
Asthma and Lung Inflammation
Section
levines@nhlbi.nih.gov

Huiqing Li
Laboratory of Cell Biology
huiqing.li@nih.gov

Ping Li
Laboratory of obesity & Metabolic
Diseases
Ping.li@nih.gov

Wenling Li
Laboratory of Stem Cell & Neuro-
Vascular Biology
Liw3@mail.nih.gov

Jie Li
Laboratory of Cardiovascular &
Cancer Genetics
Lij19@mail.nih.gov

Jung Mi Lim
Protein Function in Disease
Section
jungmi.lim@nih.gov

Zenghua Li
Cell Biology Section
Zenghua.lin@nih.gov

Jian Liu
Laboratory of Molecular
Biophysics
jian.liu@nih.gov

Chang Liu
Laboratory of Stem Cell & Neuro-
Vascular Biology
Chang.liu@nih.gov

Chengyu Liu
Transgenic Core
Liuc2@mail.nih.gov

Qingguo Liu
Myeloid Malignancies Section
Qingguo.liu@nih.gov

Yangtengyu Liu
Laboratory of Cardiovascular
Regenerative Medicine
Yangtengyu.liu@nih.gov

Jeremy Logue
Laboratory of Cell and Tissue
Morphodynamics
Jeremy.logue@nih.gov

Anna Lopata
Laboratory of Molecular
Physiology
Anna.lopata@nih.gov

Dongying Ma
Sickle Cell Branch
Mad2@nhlbi.nih.gov

Xuefei Ma
Laboratory of Molecular
Cardiology
max@nhlbi.nih.gov

Brittany MacTaggart
Laboratory of Molecular
Cardiology
Brittany.mactaggart@nih.gov

Daniela Malide
Light Microscopy Core
Dmalide@nih.gov

Mery Marimoutou
Protein Function in Disease
Section
Mery.marimoutou@nih.gov

Fabrizio Marinelli
Laboratory of Structural
Biophysics
Fabrizio.marinelli@nih.gov

Jose Martina
Laboratory of Cell Biology
jmartina@nhlbi.nih.gov

Deysi Martinez
Section of Inflammation and
Cardiometabolic Diseases
Deysi.martinez@nih.gov

Philip McCoy
Flow Cytometry Core
mccoyjp@mail.nih.gov

Ryan McGlinchey
Laboratory of Molecular
Biophysics
mcglincheyr@mail.nih.gov

Barbara Medvar
Epithelial Systems Biology
Laboratory
Barbara.medvar@nih.gov

Luca Melli
Laboratory of Molecular
Physiology
Luca.melli@nih.gov

Diana Melo
Advanced Cardiovascular Imaging
Group
Diana.melo@nih.gov

Caitlin Mencia
Developmental Neurobiology
Section
menciocp@nhlbi.nih.gov

Josephine Mgya
Laboratory of Sickle Mortality
Prevention
Josephine.mgya@nih.gov

Kathleen Mills
Laboratory of Single Molecule
Biophysics
millskm@nhlbi.nih.gov

Amarjit Mishra
Asthma and Lung Inflammation
Section
Amarjit.mishra@nih.gov

Helena Mora-Jensen
Laboratory of Lymphoid
Malignancies
Helena.mora-jensen@nih.gov

Alejandro Morales Martinez
Laboratory of Imaging Physics
Alejandro.moralesmartinez@nih.gov

Joel Moss
Translational Research Section
mossj@nhlbi.nih.gov

Yosuke Mukoyama
Laboratory of Stem Cell & Neuro-
Vascular Biology
mukoyamay@mail.nih.gov

Matthew Mulé
Myeloid Malignancies Section
Matthew.mule@nih.gov

Sricharan Murugesan
Laboratory of Cell Biology
sricharan.murugesan@nih.gov

Haruna Nagase
Developmental Neurobiology
Section
Haruna.nagase@nih.gov

Keir Neuman
Laboratory of Molecular
Biophysics
kcneuman@gmail.com

Qimin Ng
Section of Inflammation and
Cardiometabolic Diseases
Qimin.ng@nih.gov

An Nguyen
Laboratory of Mitochondrial
Biology in Cardiometabolic
Syndromes
An.nguyen2@nih.gov

Mitsunori Nomura
Laboratory of Molecular Biology
Mitsunori.nomura@nih.gov

Kenneth Olivier
Pulmonary Clinical Medicine
Section
kenneth.olivier@nih.gov

Jacob Ortega
Laboratory of Molecular Machines
and Tissue Architecture
Jacob.ortega@nih.gov

Haihui Pan
Laboratory of Molecular Biology
Haihui.pan@nih.gov

Ji-Hoon Park
Laboratory of Cardiovascular &
Cancer Genetics
ji-hoon.park@nih.gov

Randi Parks
Laboratory of Cardia Physiology
Randi.parks@nih.gov

Jaya Parulekar
Epithelial Systems Biology
Laboratory
Jaya.parulekar@nih.gov

Ana Pasapera
Laboratory of Cell and Tissue
Morphodynamics
pasaperaam@nhlbi.nih.gov

Richard Pastor
Laboratory of Computational
Biology
pastor@nhlbi.nih.gov

Keval Patel
Laboratory of Cardiac Energetics
Keval.patel@nih.gov

Lydia Pecker
Sickle Cell Branch
peckerlh@nhlbi.nih.gov

Scott Perrin
Laboratory of Computational
Biology
Scott.perrinjr@nih.gov

Frank Pickard
Laboratory of Computational
Biology
frank.pickard@nih.gov

Grzegorz Piszczek
Biophysics Core
piszczeg@nhlbi.nih.gov

Corinne Pittman
Laboratory of Sickle Mortality
Prevention
Corinne.pittman@nih.gov

Martin Playford
Section of Inflammation and
Cardiometabolic Diseases
playfordmp@nhlbi.nih.gov

Karen Plevock
Laboratory of Molecular Machines
and Tissue Architecture
plevockkm@nhlbi.nih.gov

Lisa Postow
Division of Lung Diseases
lisa.postow@nih.gov

Mohsen Pourmousa
Laboratory of Computational
Biology
Pourmousa@gmail.com

Tiffany Powell-Wiley
Social Determinants of
Cardiovascular Risk and Obesity
Tiffany.powell@nih.gov

Magdalena Preciado Lopez
Laboratory of Cell and Tissue
Morphodynamics
Magdalena.preciadolopez@nih.gov

John Ra
Laboratory of Mitochondrial
Biology and Metabolism
Onehyuk.ra@nih.gov

Rajiv Ramasawmy
Cardiovascular Intervention
Program
Rajiv.ramasawmy@nih.gov

Soumya Ranganathan
Laboratory of Ribonucleoprotein
Biochemistry
Soumya.ranganathan@nih.gov

Alan Remaley
Clinical Cardiology Section
Aremaley1@nhlbi.nih.gov

Kirsten Remmert
Molecular Cell Biology Section
remmertk@nhlbi.nih.gov

Gang Ren
Laboratory of Epigenome Biology
Gang.ren@nih.gov

Dong Keun Rhee
Biochemical Physiology Section
Rheed2@mail.nih.gov

Tae-young Roh
Laboratory of Epigenome Biology
tae-young.roh@nih.gov

Tilman Rosales
Optical Spectroscopy Section
rosalest@nhlbi.nih.gov

Ilsa Rovira
NHLBI Safety Committee
rovirai@nih.gov

Xiangbo Ruan
Biochemical Physiology Section
xiangbo.ruan@nih.gov

Donovan Ruth
Theoretical Cellular Physics
Donovan.ruth@nih.gov

Toshihiro Sakurai
Lipoprotein Metabolism Section
Toshihiro.sakurai@nih.gov

Marianita Santiana
Laboratory of Host-Pathogen
Dynamics
Marianita.santiana@nih.gov

Dalton Saunders
Laboratory of Molecular
Cardiology
saundersd@nhlbi.nih.gov

Ankit Saxena
Flow Cytometry Core
Ankit.saxena@nih.gov

Todd Schoborg
Laboratory of Molecular Machines
and Tissue Architecture
todd.schoborg@nih.gov

James Sellers
Laboratory of Molecular
Physiology
sellersj@nhlbi.nih.gov

Yazmin Serrano Negron
Laboratory of Systems Genetics
Yazmin.serranonegron@nih.gov

Yu Shi
Laboratory of Obesity & Metabolic
Diseases
Yu.shi@nih.gov

Yonghong Shi
Cardiovascular Intervention
Program
Yonghong.shi@nih.gov

Bill Shin
Laboratory of Cell and Tissue
Morphodynamics
shinw2@mail.nih.gov

Pushpa Shukla
Laboratory of Structural
Biophysics
Pushpa.mishra@nih.gov

Joanna Silverman
Section of Inflammation and
Cardiometabolic Diseases
Joanna.silverman@nih.gov

Komudi Singh
Laboratory of Mitochondrial
Biology in Cardiometabolic
Syndromes
Komudi.singh@nih.gov

Colleen Skau
Laboratory of Cell and Tissue
Morphodynamics
Colleen.skau@nih.gov

Aleksandr Smirnov
Laboratory of Molecular
Biophysics
smirnovav@helix.nih.gov

Agila Somasundaram
Laboratory of Molecular & Cellular
Imaging
Agila.somasundaram@nih.gov

Alexander Sorokin
Section of Inflammation and
Cardiometabolic Diseases
sorokinav@nhlbi.nih.gov

Sarah Speed
Laboratory of Molecular Machines
and Tissue Architecture
Sarah.speed@nih.gov

Danielle Springer
Murine Phenotyping Core
springerd@nhlbi.nih.gov

Benjamin Stanton
Laboratory of Epigenome Biology
Ben.stanton@nih.gov

Erin Stempinski
Electron Microscopy Core
erin.stempinski@nih.gov

Madeleine Strickland
Laboratory of Structural
Biophysics
Maddy.davison@nih.gov

Nuo Sun
Laboratory of Molecular Biology
nuo.sun@nih.gov

Junhui Sun
Laboratory of Cardiac Physiology
Sun1@mail.nih.gov

Wanling Sun
Cell Biology Section
Wanling.sun@nih.gov

Vinay Shankar Swaminathan
Laboratory of Cell and Tissue
Morphodynamics
swaminathanv@mail.nih.gov

Yasuharu Takagi
Laboratory of Molecular
Physiology
takagi@mail.nih.gov

Jessica Tang
Laboratory of Molecular Genetics
Jessica.tang@nih.gov

Sreya Tarafdar
Protein Function in Disease
Section
Sreya.tarafdar@nih.gov

Joni Taylor
Animal Surgery & Resources Core
Jt100s@nih.gov

Patricia Theard
Laboratory of Asthma and Lung
Inflammation
Patricia.theard@nih.gov

Swee Lay Thein
Sickle Cell Branch
Sweelay.thein@nih.gov

Hawa Racine Thiam
Cell Biology Section
Hawa.racinethiam@nih.gov

Samantha Thomas
Social Determinants of
Cardiovascular Risk and Obesity
Samantha.thomas@nih.gov

Sharada Tilve
Developmental Neurobiology
Section
Sharada.tilve@nih.gov

Florentina Tofoleanu
Laboratory of Computational
Biology
florentina.tofoleanu@nih.gov

Javier Traba Dominguez
Laboratory of Mitochondrial
Biology in Cardiometabolic
Syndromes
javier.trabadominguez@nih.gov

Adam Trexler
Laboratory of Macromolecular
Interactions
Adam.trexler@nih.gov

Laxminath Tumburu
Sickle Cell Branch
Lax.tumburu@nih.gov

Ilker Tunc
Bioinformatics Core
Ilker.tunc@nih.gov

Yutaka Uchida
Laboratory of Stem Cell and
Neuro-Vascular Biology
uchiday@nhlbi.nih.gov

Chingiz Underbayev
Laboratory of Lymphoid
Malignancies
Chingiz.underbayev@nih.gov

Olga Vasalatiy
Imaging Probe Development
Center
Olga.vasalatiy@nih.gov

Phuong Vo
Cell Biology Section
Phuong.vo2@nih.gov

Yoshiyuki Wakabayashi
DNA Sequencing and Genomics
Core Facility
Yoshiyuki.wakabayashi@nih.gov

Xunde Wang
Sickle Cell Branch
Xwang@mail.nih.gov

Zong-Heng Wang
Laboratory of Molecular Genetics
Zong-heng.wang@nih.gov

Lingdi Wang
Laboratory of Mitochondrial
Biology in Cardiometabolic
Syndromes
lingdi.wang@nih.gov

Xujing Wang
Bioinformatics Core
xujing.wang@nih.gov

Kizuku Watanabe
Translational Research Section
Kizuku.watanabe@nih.gov

Jessica Wayt
Membrane Biology Section
Jessica.wayt@nih.gov

Stephanie Webb
Clinical Studies & Training Branch
Webbsl2@mail.nih.gov

Adrian Wiestner
Laboratory of Lymphoid
Malignancies
wiestnera@mail.nih.gov

Rose Willett
Cell Biology Section
Rose.Willett@nih.gov

Delon Wilson
Laboratory of Sickle Mortality
Prevention
Delon.wilson@nih.gov

Nathaniel Wolanyk
Systems Biology Core
Nathaniel.wolanyk@nih.gov

Zhijie Wu
Cell Biology Section
Zhijie.wu@nih.gov

Chuanfeng Wu
Molecular Hematopoiesis Section
wuc3@mail.nih.gov

Zhanghan Wu
Laboratory of Molecular
Biophysics
zhanghan.wu@nih.gov

Jianhua Xiong
Laboratory of Molecular Biology
Jianhua.xiong@nih.gov

Haitao Xu
Laboratory of Asthma and Lung
Inflammation
Haitao.xu@nih.gov

Xihui Xu
Laboratory of Obesity & Aging
Research
Xihui.xu@nih.gov

Ravi Chandra Yada
Hematopoietic Stem Cell and
Gene Therapy
Ravi.yada@nih.gov

Tomoko Yamazaki
Laboratory of Stem Cell & Neuro-
Vascular Biology
tomoko.yamazaki@nih.gov

Ye Yan
Laboratory of Molecular Biology
Ye.yan@nih.gov

Ling Yang
Laboratory of Obesity & Metabolic
Diseases
ling.yang@nih.gov

Zhihong Yang
Lipoprotein Metabolism Section
Zhihong.yang@nih.gov

Leah Yingling
Social Determinants of
Cardiovascular Risk and Obesity
Leah.yingling@nih.gov

Kyung-Rok Yu
Molecular Hematopoiesis Section
Kyung-rok.yu@nih.gov

Zu-Xi Yu
Laboratory of Molecular
Cardiology
yuz@nhlbi.nih.gov

Abdalrahman Zarzour
Lipoprotein Metabolism Section
zarzoura@mail.nih.gov

Fan Zhang
Laboratory of Molecular Genetics
Zhangfan2@mail.nih.gov

Nan Zhang
Molecular & Clinical Hematology
Branch
nan.zhang2@nih.gov

Yi Zhang
Laboratory of Molecular Genetics
Yi.zhang4@nih.gov

Xin Zhao
Cell Biology Section
Xin.zhao@Nih.gov

Yue Zhao
Cell Biology Section
yue.zhao@nih.gov

Wenchang Zhou
Theoretical Molecular Biophysics
Section
Wenchang.zhou@nih.gov

Xuefeng Zhu
Laboratory of Molecular Biology
Xuefeng.zhu@nih.gov

Jun Zhu
DNA Sequencing and Genomics
Core Facility
Zhuj4@nhlbi.nih.gov

Jie Zhuang
Laboratory of Cardiovascular &
Cancer Genetics
jie.zhuang@nih.gov

Jizhong Zou
iPSC Core
Zouj2@mail.nih.gov